Modeling, Simulation, and Optimization of Advanced Air Traffic Procedures to Improve Oceanic Flights

Arman Izadi

Dissertation submitted to the Faculty of the
Virginia Polytechnic Institute and State University
in partial fulfillment of the requirements for the degree of

Doctor of Philosophy
in
Civil Engineering

Antonio A. Trani, Chair
Montasir M. Abbas
Douglas R. Bish
Susan Hotle

May 12, 2020
Blacksburg, Virginia

Keywords: Air Traffic Flow Management, Oceanic Flights, Convective Weather Avoidance, Collaborative Decision Making, In-Trail Procedure

Modeling, Simulation, and Optimization of Advanced Air Traffic Procedures to Improve Oceanic Flights

Arman Izadi

(ABSTRACT)

The Federal Aviation Administration (FAA) has been modernizing the United States' air transportation system within a series of initiatives called the Next Generation Air Transportation System (NextGen). The goal of NextGen is to increase the safety, efficiency, capacity, predictability, and resiliency of American Air Traffic Control (ATC) by implementing satellite-based communication, and navigation systems. Because of the vast oceanic areas controlled by Oakland, New York, and Anchorage air traffic control centers, improving oceanic operations is significant for the United States. According to the FAA, oceanic flights generate 31% of passenger revenue and 40% of cargo revenue in U.S.-controlled airspace. New NextGen procedures offer the opportunity for aircraft to save fuel consumption by allowing oceanic flights to fly at more efficient routes and flight levels. This dissertation investigates three areas to improve flight operations over oceanic airspace.

The first area studies the operational benefits of providing satellite-based meteorological information to aircraft operating in remote and oceanic airspace. This research effort uses two approaches as follows: 1) statistical flight analysis, and 2) simulation-based analysis. The second area provides an optimization technique to improve the current procedures for assigning flights to the Organized Track System (OTS) in the Atlantic Ocean based on the Collaborative Decision Making (CDM) concept. The third area investigates the potential savings of "In-Trail Procedure" (ITP) as one of the advanced surveillance operations in the Pacific and Atlantic oceanic airspace.

To quantify the operational benefits of the proposed procedures, a fast-time simulation tool, the Global Oceanic (GO) model, is developed and employed. The GO Model is a microscopic flight simulation tool that has been developing by the Air Transportation Systems Laboratory at Virginia Tech offering realistic and inexpensive evaluations of novel technologies and procedures to improve flight operations over global oceanic airspace. the results of these studies are analyzed in terms of fuel consumption, travel distance, travel time, level of service, and potential air traffic controllers' workload.

Modeling, Simulation, and Optimization of Advanced Air Traffic Procedures to Improve Oceanic Flights

Arman Izadi

(GENERAL AUDIENCE ABSTRACT)

The economic growth and social connectivity of nations are highly correlated to effective and efficient air transportation systems. The Federal Aviation Administration (FAA) has initiated a program to modernize America's air transportation system and make flight operations safer, and more efficient. This program is called the Next Generation Air Transportation System (NextGen) and its goal is transforming the communication and navigation technologies to satellite-based systems. Improving oceanic flights is one of the main concerns of the NextGen program since the United States controls massive oceanic areas in the Atlantic and the Pacific Ocean. The FAA needs to evaluate the benefits and costs of advanced technologies and procedures to justify the NextGen initiatives. The FAA has employed computer simulation tools to support decisions for future infrastructure investments and encourage airlines to equip their aircraft with more advanced avionics.

The Global Oceanic (GO) model is a microscopic flight simulation tool developed jointly by the Air Transportation Systems Laboratory at Virginia Tech and the FAA providing quick, realistic, and inexpensive evaluations of advanced procedures to improve flight operations over oceans. This dissertation investigates the operational benefit of three advanced procedures using the GO Model. The areas to improve flight operations over oceanic airspace are as follows: 1) operational benefits of providing satellite-based meteorological information to aircraft operating in remote and oceanic airspace, 2) operational benefits of an optimization technique for flight assignments to the Organized Track System (OTS) in the Atlantic Ocean, 3) operational benefits of "In-Trail Procedure" (ITP) as one of the advanced surveillance operations in the Pacific and Atlantic oceanic airspace. These studies quantify the potential savings of these procedures in terms of reducing fuel consumption, travel distance, travel time, greenhouse gas emissions, and potential air traffic controllers' workload.

Dedication

I want to dedicate this dissertation to my parents, and my wife for their unconditional support and continuous encouragement through this journey.

Acknowledgments

I would like to acknowledge those who supported, encouraged me throughout my Ph.D. program at Virginia Tech.

First, I would like to express my sincere gratitude to my advisor, Dr. Antonio Trani, for his invaluable guidance during my program. Truly, Dr. Trani represents the ideal advisor with very practical knowledge and genuine kindness. He has set an example of excellence as a researcher, mentor, instructor, and role model. It was my great honor to work with him in the Air Transportation Systems Laboratory at Virginia Tech.

Special thanks to my committee members: Dr. Montasir Abbas, Dr. Susan Hotle, and Dr. Douglas Bish for their feedback on my dissertation. Some parts of this dissertation were generously supported by the National Center of Excellence for Aviation Operations Research (NEXTOR II) and the Federal Aviation Administration (FAA). Special Thanks to Eldridge Frazier (FAA, ANG-C61), Joseph Post (FAA, the office of NAS systems engineering and integration), Matthias Steiner (NCAR), and Cathy Kessinger (NCAR) for their technical and financial support of the projects.

Finally, I want to express my profound gratitude to my parents, and my wife who has been my source of inspiration and continuous support.

Contents

List of Figures

List of Tables

List of Abbreviations

ADS-B Automatic Dependent Surveillance-Broadcast

ADS-C Automatic Dependent Surveillance-Contract

ANSP Air Navigation Service Provider

ATC Air Traffic Control

ATFM Air Traffic Flow Management

CDM Collaborative Decision Making

CDO Convection Diagnosis Oceanic

CPA Closest Point of Approach

CPDLC Controller-Pilot Data Link Communications

CTH Cloud Top Height

GDP Ground Delay Program

ITP In-Trail Procedure

NAS National Airspace System

NAT North Atlantic

NCAR National Center of Atmospheric Research

NOAA National Oceanic and Atmospheric Administration

OAG Official Airline Guide

OTS Organized Track System

ROMIO Remote Oceanic Meteorology Information Operational

Chapter 1

Introduction

1.1 Background and Motivation

The Federal Aviation Administration (FAA) has been working on the Next Generation Air Transportation System (NextGen) to modernize the National Airspace System (NAS) since 2007. NextGen is a set of initiatives to evolve Air Traffic Control (ATC) and transform the communication, navigation, and surveillance technologies from ground-based systems to satellite-based systems.

Improving flight operations over the oceanic airspace is one of the most significant goals of the NextGen program. According to the United States Department of Transportation, oceanic flights generate 31 percent of air carrier passenger revenue and 40 percent of cargo revenue in the U.S.-controlled airspace. The FAA is upgrading oceanic flight operations with NextGen technologies to give pilots the flexibility to fly at more efficient routes and altitudes. According to EUROCONTROL's aircraft performance model, when a wide-body aircraft deviates as little as 1,000 feet from its optimal altitude, it can consume on average 1.8 kg/min additional fuel. In this study, three challenges for the oceanic air traffic flow management are investigated.

The first challenge is the airspace capacity shortfalls caused by convective weather conditions. Weather influences domestic and oceanic airspace capacity. Weather is uncertain and dynamic, requiring technologies to be quickly updated in the event of new information. As recorded in the OPSNET standard "Delay by Cause" reports, the largest cause of air traffic delay in the NAS is the weather. Figure 1.1 shows that weather caused 69% of delays impacting air transportation systems over six years from 2008 to 2013.

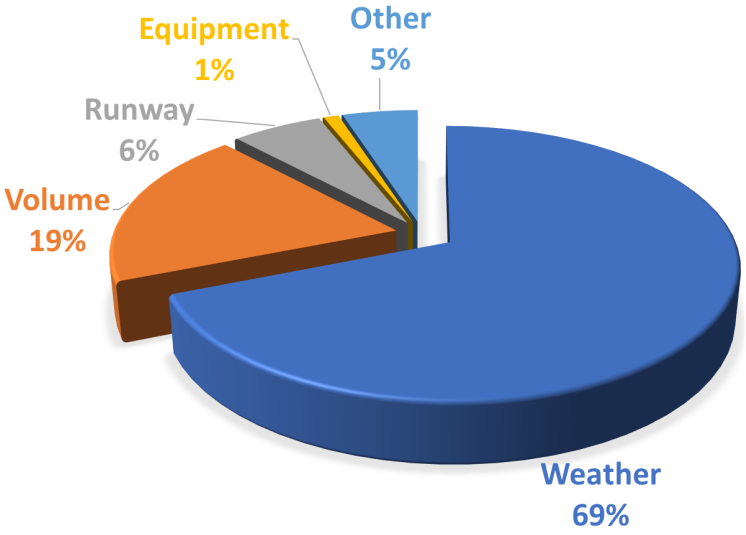

Figure 1.1: Operations network standard reports, delay by cause.

The second challenge is reducing and maintaining separation minima in oceanic regions. In contrary to operations in domestic airspace, flights over the oceanic regions cannot be continuously monitored by radar due to insufficient radar coverage. Consequently, flight operations over the oceans need to follow the oceanic procedure, in which minimum separations are larger than those used in airspace under sufficient radar surveillance. The United States has vast oceanic areas controlled by New York, Oakland, and Anchorage Air Route Traffic Control Centers (ARTCCs). The adoption of reduced oceanic separation standards using technologies such as Space-Based ADS-B (Automatic Dependent Surveillance-Broadcast) promises to save fuel, increase airspace capacity, reduce environmental impacts, and cut costs for aircraft operators.

In-Trail Procedure (ITP) is an advanced ADS-B In application (i.e., the ability to receive, process, and display ADS-B data from surrounding aircraft) that allows ITP-equipped aircraft to move through oceanic flight routes efficiently and improving fuel economy, reducing emissions and avoiding turbulent altitudes. Maintaining optimal cruise altitudes for oceanic flights requires many altitude changes since saving fuel consumption is related to flying at optimal flight levels considering wind conditions and turbulence. Aircraft operating in oceanic airspace may end up flying at non-optimal flight levels due to traffic conflicts either at the desired flight level or at flight levels between the existing flight level and the optimal flight level. Greater operational efficiency is one

of the advantages of using flight level change procedures enabled by ADS-B ITP.

The third challenge is matching and balancing the traffic flow demand with the capacity of airspace resources. The North Atlantic (NAT) region is the busiest U.S. controlled oceanic airspace which is shaped between Canada, the United Kingdom, and the United States. Because of the time zone differences, airport noise restrictions, and passenger demands, the air traffic between Europe and North America creates two concentrated unidirectional flows over the North Atlantic region: westbound traffic departing from Europe to North America in the morning, and eastbound traffic departing from North America to Europe in the evening.

To better serve the two traffic flows, two Organized Track Systems (OTS) are created on a daily basis to accommodate as many flights as possible. Flights may fly on User-Preferred Routes (UPR) which remain clear of the OTS or may fly on any route that joins or leaves an outer track of the OTS. The current OTS assignment procedure used by oceanic air traffic controllers is a greedy algorithm based on the "First Come, First Serve" method. This method is easy to implement since it does not require much effort for air traffic controllers to optimize the OTS assignment. In the low traffic situation, most of the flights can be assigned to their requested tracks and flight levels. However, the current heuristic procedure could not produce highly satisfactory assignments during congestion periods. According to historical data, Shanwick (United Kingdom) and Gander (Canada) regions were not able to assign approximately 35% and 20% of flights to their requested tracks and flight levels in high traffic conditions. This study proposes a new procedure to improve the OTS assignment based on collaborative decision making philosophy. The main contribution of the proposed methodology is changing the current greedy algorithm (i.e., individual assignment) to a group assignment procedure using optimization algorithms.

1.2 Objectives

The Federal Aviation Administration (FAA) and the International Civil Aviation Organization (ICAO) need to evaluate the benefits and costs of advanced technologies and procedures to justify the NextGen implementation. These decision-makers have employed computer simulation tools to

support decisions for infrastructure investments and encourage airlines to invest in more advanced avionics. This research effort aims to estimate the operational benefits of advanced procedures for improving oceanic flight operations in the following three chapters:

1. Remote Oceanic Meteorology Information Operational (ROMIO) Benefit Analysis:
   The FAA Weather Technology in the Cockpit (WTIC) program has sponsored the ROMIO demonstration to evaluate the feasibility of uplinking convective weather products into the flight deck of oceanic flights. This study aims to estimate the operational benefits of providing satellite-based meteorological information to oceanic flights in two phases: 1) statistical flight analysis, and 2) simulation-based analysis. In the first phase, the goal is identifying the pilots' strategies in avoiding convective weather events through analyzing deviation maneuvers in historical flights. In the second phase, the objective is implementing the extracted rules in a flight simulation tool and quantifying the operational benefits of more strategic decision-making beyond airborne radar.

2. Collaborative Decision Making in Oceanic Air Traffic Flow Management:
   The goal is measuring the potential benefits of an optimization technique for assigning flights to the organized track system in the North Atlantic oceanic airspace. The proposed methodology is based on the Collaborative Decision Making (CDM) concept giving more decision-making responsibilities to airspace users.

3. In-Trail Procedure for Improved Oceanic Air Traffic Operations:
   The aim is evaluating operational improvements of In-Trail Procedure (ITP) as one of the advanced surveillance operations in the Pacific and Atlantic oceans using computer simulation tools. The Global Oceanic (GO) model is employed to quantify the benefits of the proposed concept of operations in terms of efficiency, capacity, and safety. The GO Model is a microscopic flight simulation tool developed jointly by the Air Transportation Systems Laboratory at Virginia Tech and the FAA offering quick, inexpensive, and realistic evaluations on the new policies, procedures, and technologies for improving flight operations over global oceanic airspace.

1.3 Organization of the Dissertation

This dissertation will outline the research effort and improvements to the GO Model using the following structure:

- Chapter 2 outlines the research done for the benefit analysis of the Remote Oceanic Meteorology Information Operational (ROMIO) demonstration. This chapter is divided into two parts: 1) statistical flight analysis, and 2) simulation-based analysis.
- Chapter 3 presents the research effort for improving flight assignment procedure to the Organised Track System (OTS) in the North Atlantic oceanic airspace using an optimization technique.
- Chapter 4 provides the research for evaluating the operational benefits of In-Trail Procedure (ITP) as one of the advanced surveillance operations in oceanic airspace.
- Chapter 5 outlines the summary and recommendations for future study.

Chapter 2

Remote Oceanic Meteorology Information Operational (ROMIO) Benefit Analysis

2.1 Introduction

One of the challenges for air traffic flow management is airspace capacity shortfalls caused by convective weather conditions. According to the Operational Network (OPSNET) standard "Delay by Cause" reports, adverse weather was the main cause in 69% of system delays (more than 15 minutes) from 2008 to 2013. Pilots have access to various weather information (e.g., Significant Weather (SIGWX) charts, Pilot Reports (PIREPS), and visual observations) that assist them in gaining a holistic understanding of the weather which affects flight safety. As the primary source of weather information, pilots rely on airborne weather radar for tactical flight planning [21]. Utilizing airborne radar has two main shortcomings. First, the range of aircraft's airborne radar is limited. Although the maximum range of onboard weather radar is about 320 nautical miles (nm), most weather radars only have a useful range of about 80 nm to 150 nm. Second, "attenuation" is a phenomenon that prevents the airborne weather radar from detecting additional cells that might lie behind the front edge of a convective event. This effect occurs when a cell absorbs or reflects all of the radio signals sent by the radar system [57].

The Federal Aviation Administration (FAA) Weather Technology in the Cockpit (WTIC) program has sponsored an operational demonstration to provide satellite-based meteorological information

to commercial flights in remote and oceanic regions. This effort is called the Remote Oceanic Meteorology Information Operational (ROMIO) demonstration. National Center of Atmospheric Research (NCAR) supports the overall project as the principal investigator. NCAR has developed two weather products: 1) Cloud Top Height (CTH), and 2) Convection Diagnosis Oceanic (CDO). The CTH product displays cloud top contours at flight altitudes of FL320, FL340, FL360, FL380, and FL400. The CDO product displays hazards associated with the storm updraft, lightning, and overshooting tops in four intensity levels (Medium, High, Severe, and Extreme). NCAR distributes the CTH and CDO products in XML format utilizing the FAA NextGen System Wide Information Management (SWIM) technology, and Embry-Riddle Aeronautical University NextGen Testbed is used to demonstrate the capabilities [17].

Basic Commerce and Industries, Inc. (BCI) supports software applications and communications. The BCI has provided a web-based application for displaying weather information from CDO and CTH products. This application is available on iOS, Windows 10, and the web. Figure 2.1 shows the functionality and appearance of the ROMIO application viewer [4]. The participating airlines in this study are Delta Air Lines, United Airlines, and American Airlines, and Panasonic and Gogo provide data-link to aircraft for receiving the weather information.

Currently, ROMIO provides services in the area of 160E to 10W degrees longitude and 50S to 65N degrees latitude. Scanning areas of the Geostationary Operational Environmental Satellite (GOES)-East and GOES-West satellites are the domain of the ROMIO demonstration, and the current rate of updates for CDO and CTH contours is 10 minutes. The two primary aims of the ROMIO application are 1) providing real-time weather information in oceanic airspace for strategic planning beyond the airborne radar, and 2) facilitating common information sharing among different user groups of pilots, dispatchers, and air traffic controllers on electronic flight bags (EFBs) [17].

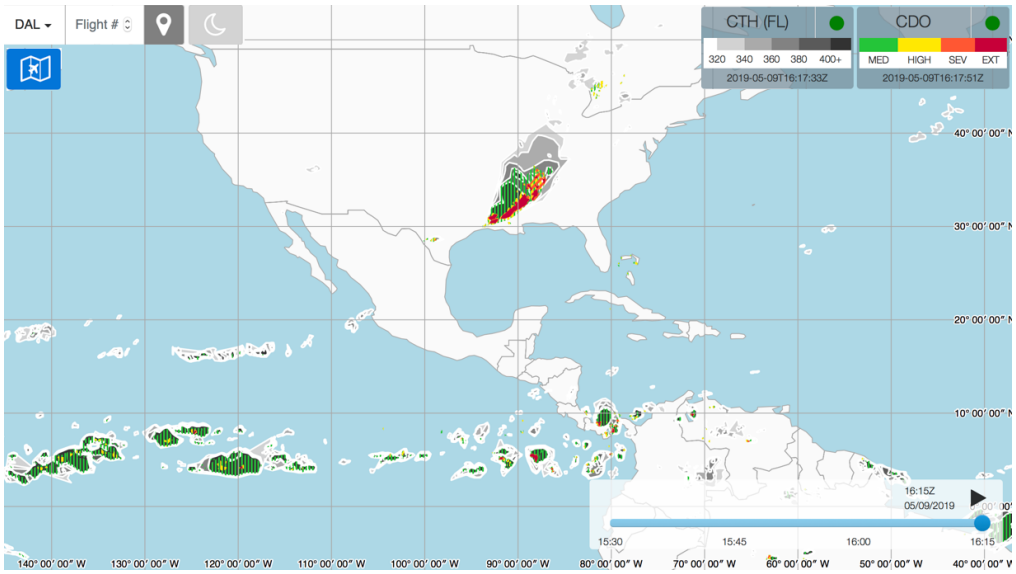

Figure 2.1: Functionality and appearance of the ROMIO application viewer.

The benefit analysis of the ROMIO demonstration consists of three phases including 1) survey analysis, 2) statistical flight analysis, and 3) simulation-based analysis. Virginia Tech created a pilot survey to have a qualitative measure of the benefits of using the ROMIO application and to assess pilots' acceptance of the new airborne information technology. The questions in the survey are mainly categorized into five groups: decision making, workload, situational awareness, efficiency, and quality of information. The pilots from participating airlines in this study are invited to fill out the survey upon completion of their ROMIO-enabled flights. The Virginia Tech Institutional Review Board (IRB) approved this survey, and Qualtrics distributed the electronic version of pilots' responses. This report studies the potential benefits of using the ROMIO application by analyzing the historical flight trajectories. The goal of this analysis is to quantify the operational benefits of enhanced situational awareness and strategic decision making for convective weather deviation maneuvers.

2.2 Literature Review

Access to accurate weather information in the cockpit enables pilots to make safer decisions in avoiding hazardous weather conditions. The use of satellite-based cockpit technology can enhance pilots'

situational awareness and assist in strategic weather-related decision making. Better weather information helps in optimizing flight tracks and reducing flight crew workload and avoid human errors. Previous research efforts have shown promising techniques to adapt simulation and optimization-based approaches for rerouting flights encountering severe weather conditions [36], [48], [41]. There are numerous studies of the operational benefits of weather information technologies in the cockpit.

Wu, et al. (2010) evaluated the use of electronic flight bags to provide enhanced traffic and weather displays on the flight deck. The study showed that displaying the weather and traffic information separately increase the required time to modify routes around weather and negatively impacted the quality of deviations maneuvers [61]. Grasse, et al. (2008) executed a study concerning the depiction of strategic real-time weather data on electronic displays. The first step of this study was analyzing the current weather information and the provided sources to pilots. Next, several human factors and their relative impacts on the development of a weather display were analyzed [19].

Sauer, et al. (2019) assessed the potential benefits of using weather uplinks (e.g., electronic flight bag) compared to the limited information available through the onboard radar. They examined different flight routing approaches regarding multiple weather hazards and various time horizons for decision makings [45]. The studies on cockpit weather information technologies show that more updated meteorological systems create a trade-off between flight safety and pilot workload. Some of the benefits of advanced weather information technologies are as follows: reduction of fuel consumption [46], improved life cycle cost of the aircraft [53], minimized pollutant emission [35], minimized inefficient detours [30], enhanced situational awareness [10], reduced pilot workload [39], improved controller-pilot interactions [16], reduced arrival delays, airborne holding delays, reduced flight cancellation [30], improved Safety [49], and minimized noise production [46].

Feltz, et al. (2008) described an oceanic convection diagnosis and nowcasting system whose domain of interest is the region between the southern continental United States and the northern extent of South America. In this system, geostationary satellite imagery is used to define the locations of deep convective clouds through the weighted combination of three independent algorithms [28]. Frazier, et al. (2018) developed the Remote Oceanic Meteorology Information Operational (ROMIO) demonstration which was a collaborative project between the FAA, the weather research

community, the airlines, and airline in-flight entertainment communications (IFEC) providers. The ROMIO demonstration project shows the operational strategies for the use of rapidly updated CTH and CDO products on the flight deck in the Oceanic Air Route Traffic Control Centers (ARTCC) and flight dispatch operations of Airline Operations Centers (AOC) [17].

2.3 Statistical Flight Analysis

In this study, the Application Programming Interface (API) service from (`www.flightaware.com`) is used to collect historical flight data. The historical 4-dimensional flight trajectories include aircraft position (latitude, longitude), altitude, and time information for reported waypoints. We performed an interpolation analysis on the collected flight tracks to estimate the aircraft position every one nautical mile along the flown route. This step is necessary because many oceanic flights have gaps in the reported flight trajectory in areas where there is no ground-based radar or multilateration coverage. We selected 45 bi-directional flights (90 flights) over the Pacific Ocean, North Atlantic Ocean, and flights crossing the Inter-Tropical Convergence Zone (ITCZ), mainly between North America and South America. Figure 2.2 illustrates the ITCZ region near the equator where the winds of the northern and southern hemispheres meet [3]. The ITCZ area is characterized by convective weather activities involving thunderstorms over large areas.

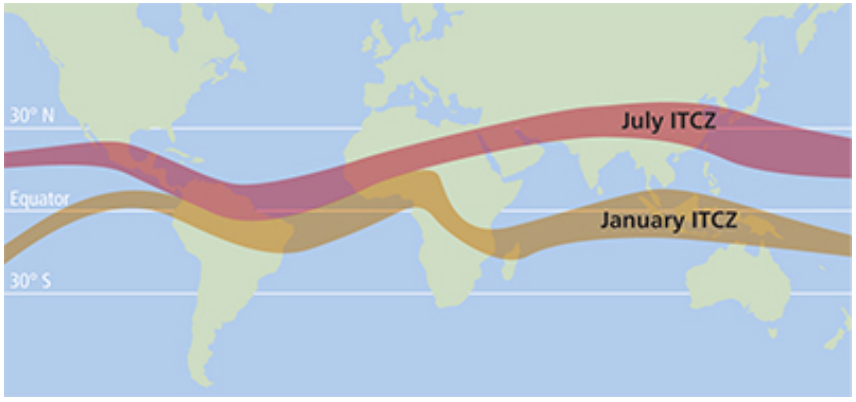

Figure 2.2: Inter-Tropical Convergence Zone (ITCZ).

The scope of this analysis encompasses flights crossing ITCZ since they are likely to encounter potentially hazardous convective weather. We analyzed 18,326 flights flown between March 2018

to August 2019. This interval is divided into two periods, including Pre-ROMIO and Post-ROMIO periods. The Pre-ROMIO period spans from March to July 2018. The Post-ROMIO period spans from August 2018 to August 2019. The rate of updates for convective weather information is 15 minutes for ROMIO data (i.e., CDO and CTH contours) from March 2018 to May 2019, and 10 minutes between June 2019 to August 2019. Figure 2.3 shows the origins and destinations of the selected flights. The blue flights show 30 bi-directional flights (60 flights) among 18 airports including Hartsfield-Jackson Atlanta International Airport (KATL), Dallas/Fort Worth International Airport (KDFW), Detroit Metropolitan Wayne County Airport (KDTW), Newark Liberty International Airport (KEWR), George Bush Intercontinental Airport (KIAH), John F. Kennedy International Airport (KJFK), Los Angeles International Airport (KLAX), Orlando International Airport (KMCO), Miami International Airport (KMIA), O'Hare International Airport (KORD), San Francisco International Airport (KSFO), Ezeiza International Airport (SAEZ), Rio De Janeiro Galeao Airport (SBGL), Sao Paulo International Airport (SBGR), Santiago International Airport (SCEL), Jorge Chavez International Airport (SPJC), Sydney Airport (YSSY), and O.R. Tambo International Airport (FAOR).

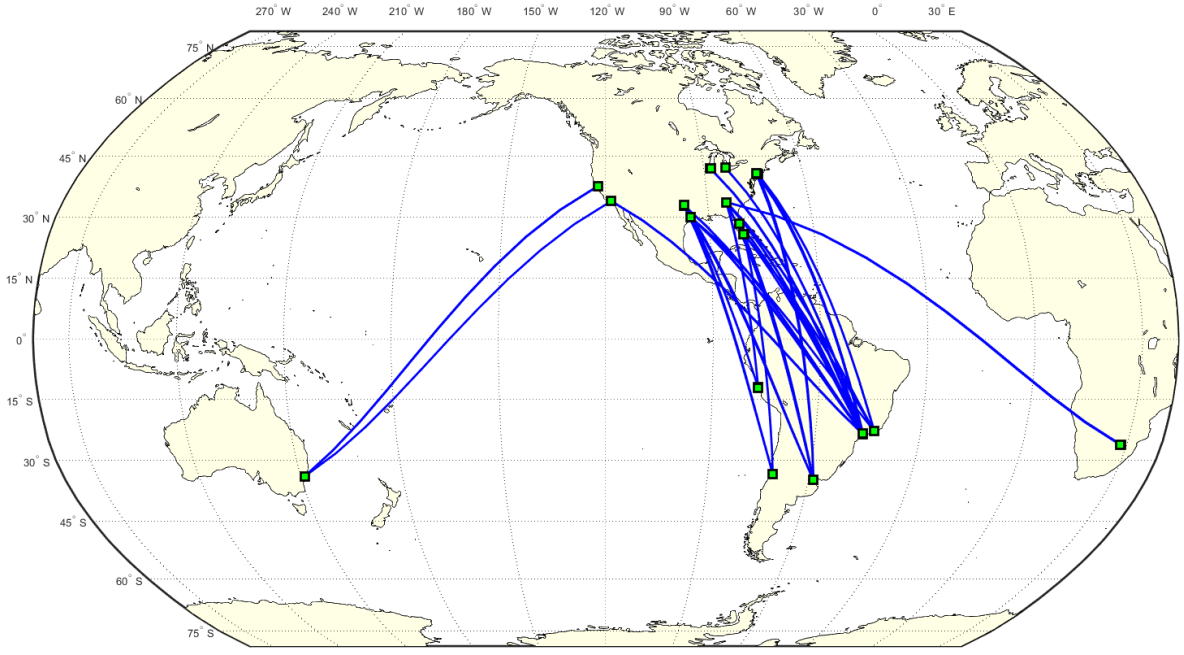

Figure 2.3: Selected origin-destination pairs.

Figure 2.4a shows the proportions of the historical flights from three main airlines, including Delta

Air Lines (DAL), American Airlines (AAL), and United Airlines (UAL). Figure 2.4b shows the fleet mix of historical flights.

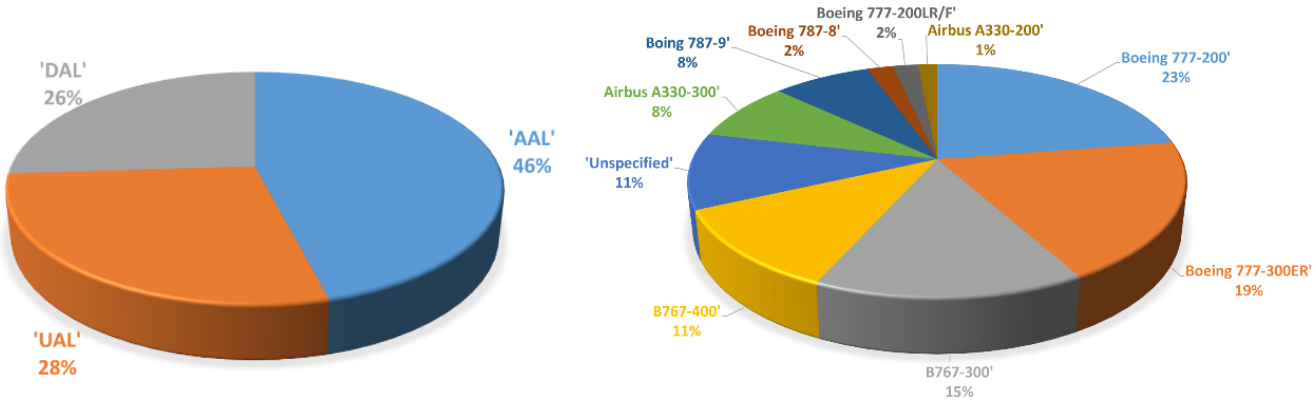

(a) Airlines composition. (b) Fleet composition.

Figure 2.4: Airline and fleet proportions.

2.3.1 Event-Based Flight Analysis

We analyzed the historical 4-dimensional flight trajectories considering the corresponding CDO and CTH contours. In this approach, if the waypoints are outside the CDO and CTH contours, the Closest Point of Approach (CPA) to each weather polygon is measured. If the waypoints are inside the contours, travel distances and travel times in each polygon are determined. Weather events are identified as parts of flight trajectories between entering and exiting a set of CDO and CTH contours. Figure 2.5 illustrates four weather event types based on different layers of CDO contours, and Figure 2.6 shows the proportions of weather events.

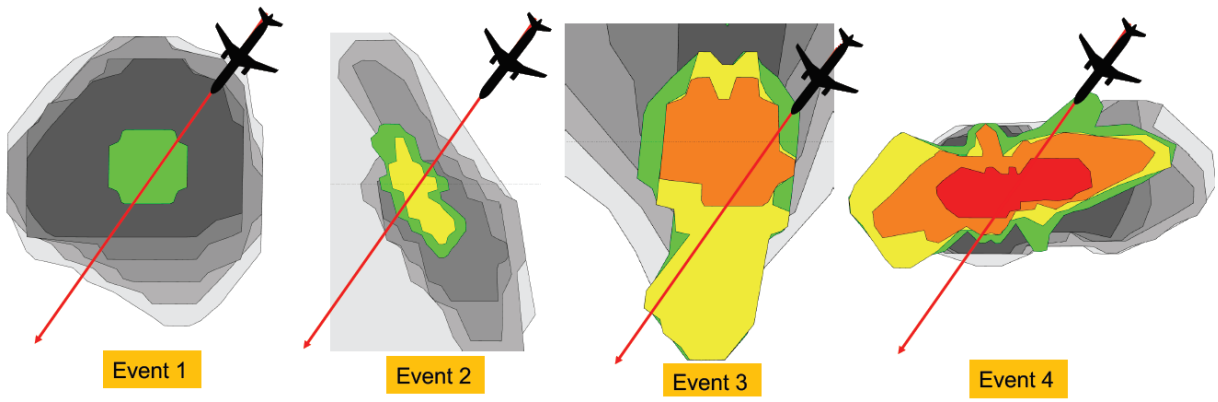

Figure 2.5: Weather event types.

- Event 1: flights enter the Medium CDO contours.
- Event 2: flights enter the Medium and High CDO contours.
- Event 3: flights enter the Medium, High, and Severe CDO contours.
- Event 4: flights enter the Medium, High, Severe, and Extreme CDO contours.

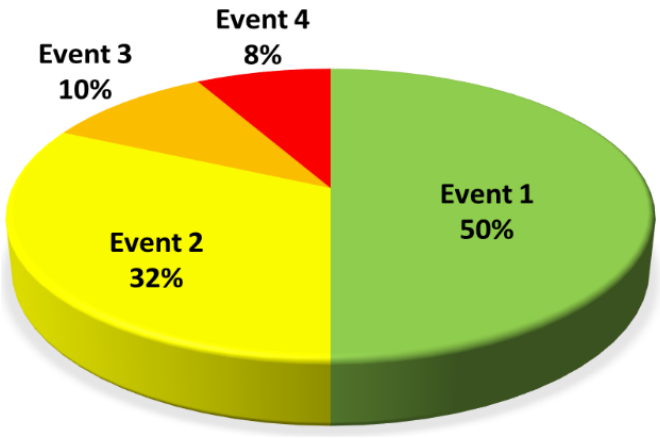

Figure 2.6: Proportion of weather event types.

Figure 2.7 shows the Cumulative Distribution Function (CDF) of travel distances inside each layer of CDO contours. The results show fewer travel distances inside CDO contours with increasing the severity of CDO contours. The distribution of travel distance inside medium CDO contours in Event 4 has a significant shift compared to other CDO categories. Event type 4 mainly involves flight operations near terminal areas.

For having a better understanding of the movements of CDO and CTH polygons, we developed a script in MATLAB to create animations showing the flight trajectory and weather dynamics simultaneously. This study uses the travel time, travel distance, and CPA statistics to find the deviation rules and strategies used by pilots to avoid hazardous weather events. Figure 2.8 shows the travel time in each CDO polygons (Medium, High, Severe, and Extreme). The statistics are related to the flight (AAL905) from Miami to Rio de Janeiro (Brazil) on September 25, 2018.

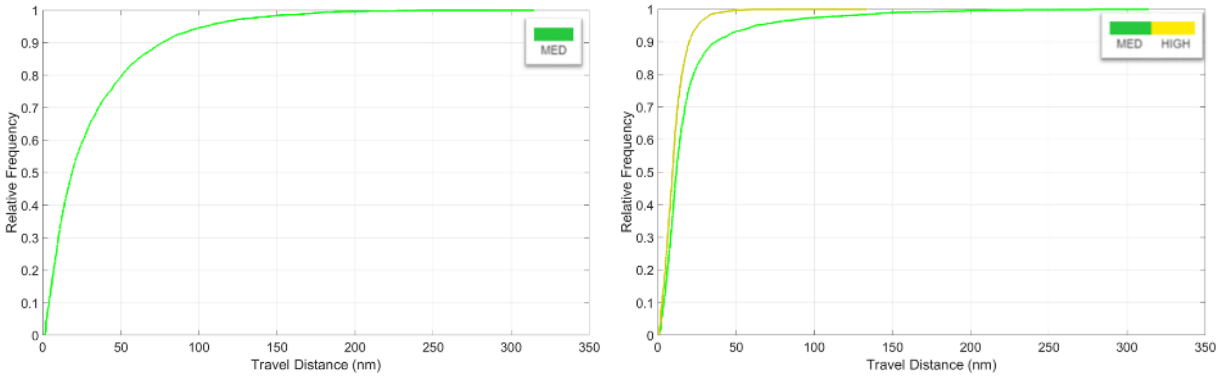

(a) Distribution of travel distances for Event 1. (b) Distribution of travel distances for Event 2.

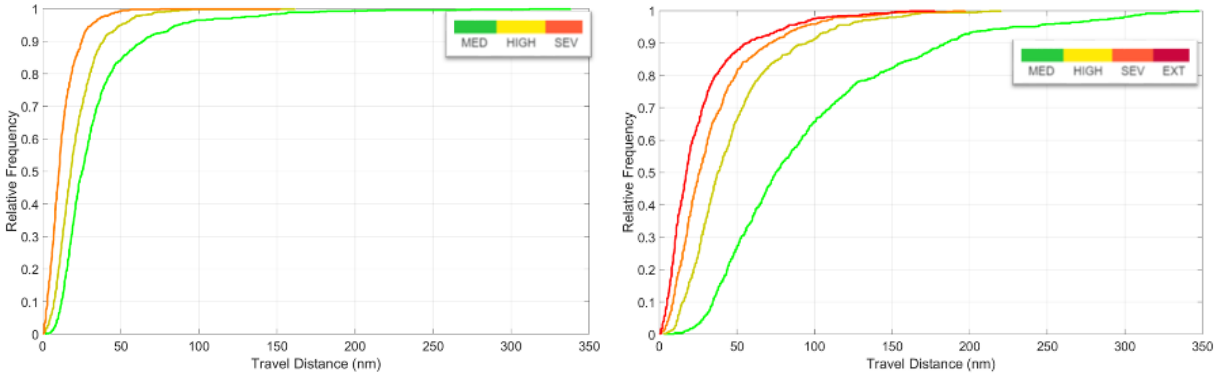

(c) Distribution of travel distances for Event 3. (d) Distribution of travel distances for Event 4.

Figure 2.7: Distribution of travel distances for event types.

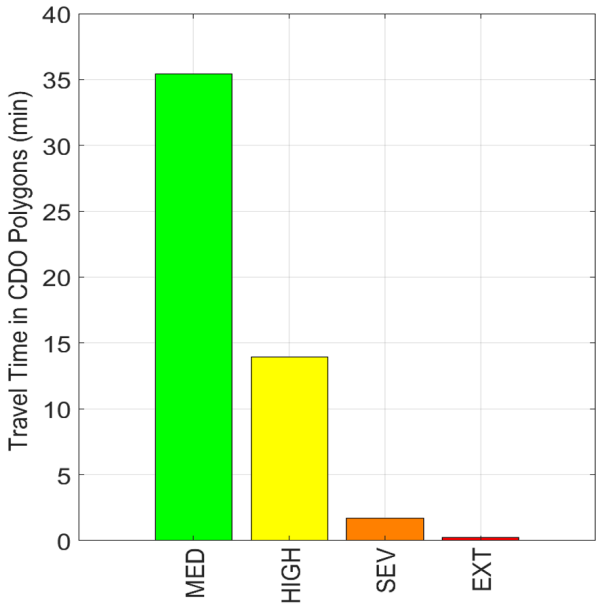

Figure 2.8: Travel time inside CDO contours.

Figure 2.9 depicts the travel time in each layer of CTH polygons (32,000 ft, 34,000 ft, 36,000 ft, 38,000 ft and 40,000 ft).

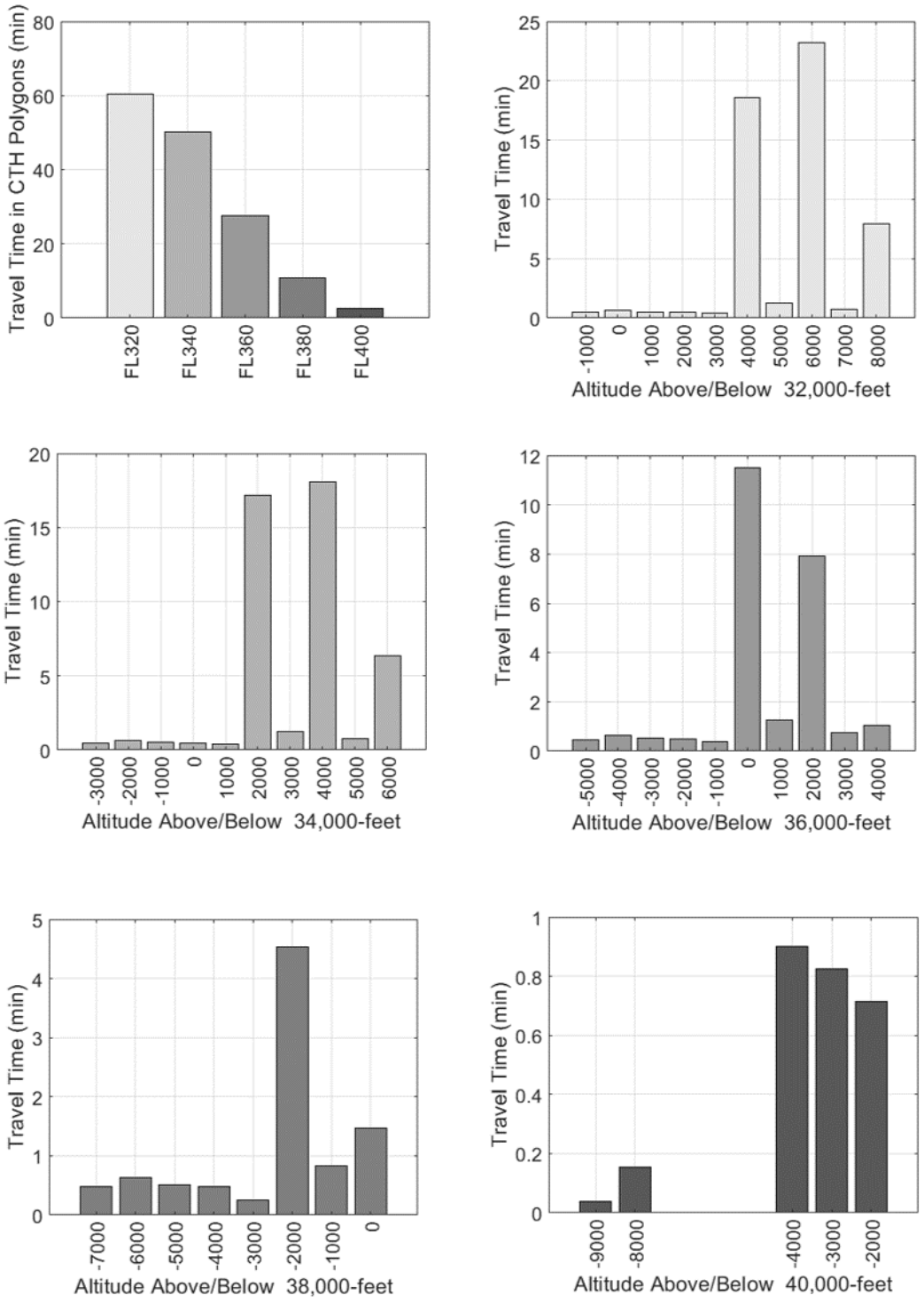

Figure 2.9: Travel time through CTH contours.

Also, the exposure and proximity of flight tracks which are outside convective weather activities are investigated. Figure 2.10 and Figure 2.11 show the closest point of approach to CDO and CTH polygons, respectively.

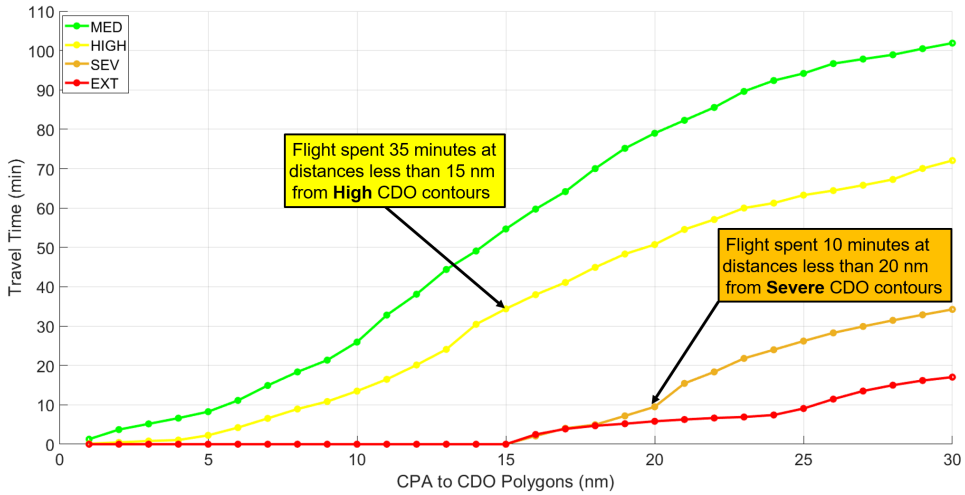

Figure 2.10: Closest point of approach to CDO contours.

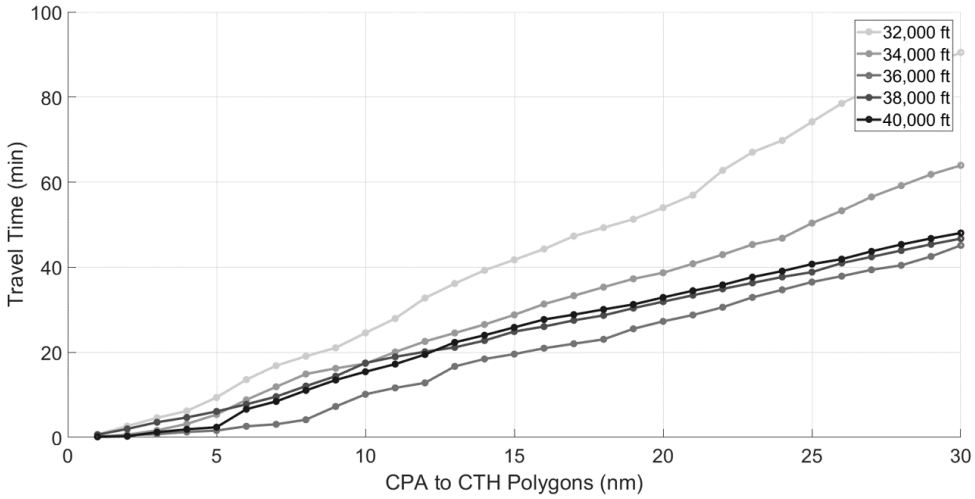

Figure 2.11: Closest point of approach to CTH contours.

In this study, flight azimuth (heading) profiles are analyzed to distinguish two types of weather deviation maneuvers: deviation segments and deviation sections. A deviation section is defined as successive waypoints with azimuth changes more than seven degrees, where the maximum allowed time gap between waypoints with heading change is one minute. In other words, deviation sections

show microscopic deviation maneuvers considering these assumptions. For each recognized weather deviation section, we measured deviation angles, deviation times, and Closest Point of Approach (CPA) to CDO and CTH contours. A deviation segment is a part of flight trajectory when a flight starts deviating (changing azimuth more than seven degrees) until it returns to its planned flight route. Deviation segments show more macroscopic deviation maneuvers, and they can include multiple deviation sections. For each recognized deviation segment, the maximum lateral deviation from the flight plan is measured. Note that the deviation maneuvers in the terminal areas (160 nautical miles radius from origin and destination airports) are not considered. Figure 2.12 shows an example of deviation sections and segments in red trajectories.

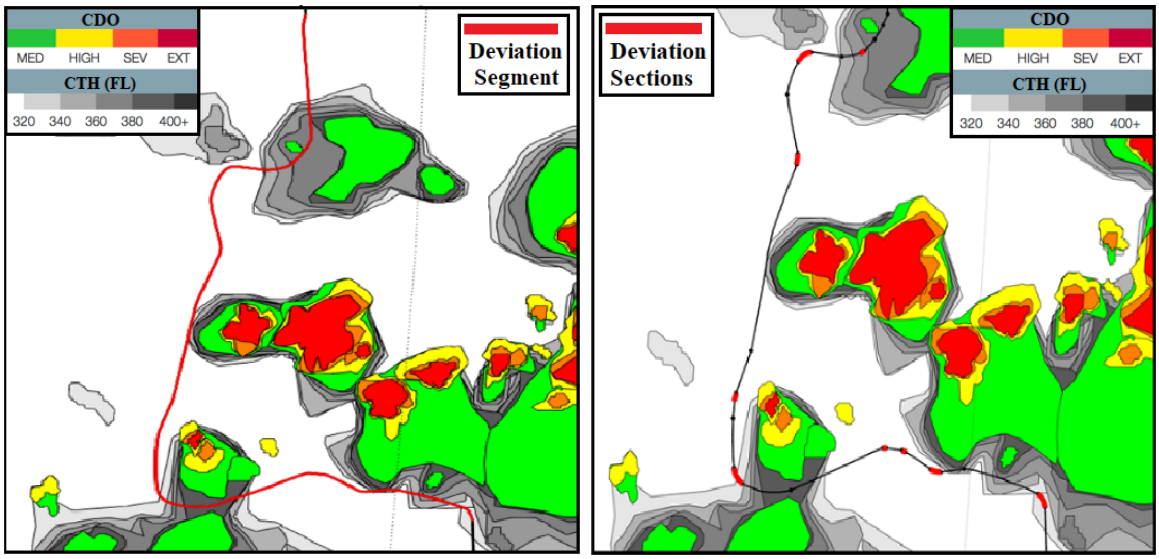

(a) Example of a Deviation Segment. (b) Example of Deviation Sections.

Figure 2.12: Deviation maneuvers types.

2.3.2 Weather Deviation Segment Analysis

Analysis of heading changes within 18,326 flights allows us to find parts of flight trajectories from the first point of deviation until the flight returns to its planned flight route. Figure 2.13 illustrates an example of a deviation segment analysis for a flight between Miami to Sao Paulo, Brazil, on September 30, 2018. The highlighted trajectory shows a weather deviation segment to avoid a large section of convective weather south of the Hispañiola Island. The actual travel distance and time for this deviation segment are 518 nm and 65 minutes, respectively. The black trajectory shows

the great circle route (418 nm) between the first and last point of the weather deviation segment. The maximum lateral deviation is defined as the maximum distance between the actual deviation segment and the great circle route. In this example, the maximum lateral deviation is 145 nm.

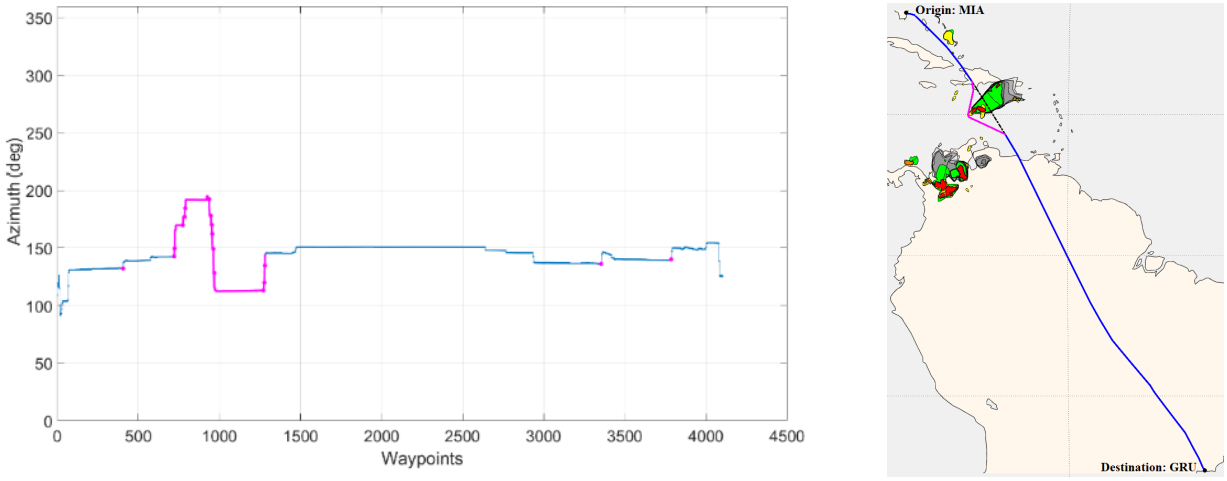

(a) Azimuth profile. (b) Flight trajectory.

Figure 2.13: Deviation segment analysis.

We analyzed the deviation segments of the 18,326 flights to measure the operational benefits of improved situational awareness and strategic decision-making for avoiding convective weather. One of the pilots who used the ROMIO application commented in the pilots' survey that "The threat of adverse weather was first identified with ROMIO, and then within approximately 10 minutes was validated by onboard radar and visual sighting". More strategic deviation alternatives are considered with 10 minutes (80 nm), 15 minutes (120 nm), and 20 minutes (160 nm) earlier deviations.

Figure 2.14 shows an example of a deviation segment with a 240 nm lateral deviation from the flight plan. We do not have information about the aircraft mass in historical flights. Therefore, the EUROCONTROL Base of Aircraft Data (BADA) 3.13 model and the nominal mass for each aircraft type is used to find the fuel flow in the cruise phase [37]. This example is related to a twin-engine wide-body aircraft, and the fuel flow for the nominal mass at 33000 feet is 319 lb/minute. Table 2.1 shows the operational savings of three strategic deviations alternatives (10-minute, 15-minute, and 20-minute earlier deviations) regarding travel distance, travel time, fuel consumption, and greenhouse gas emissions.

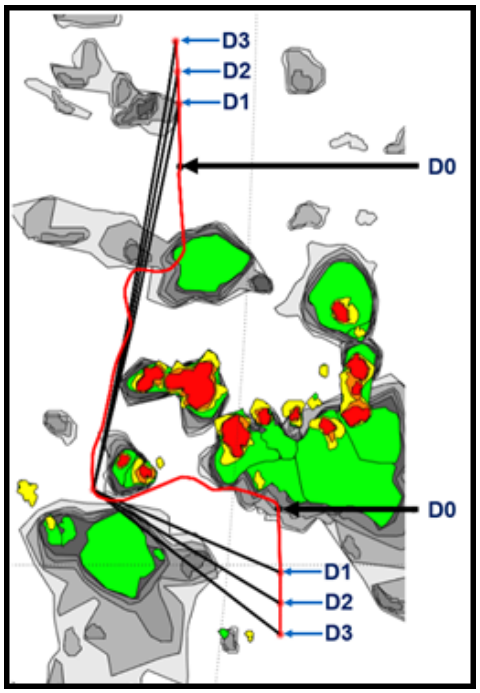

Figure 2.14: Strategic deviation alternatives.

Table 2.1: Operational benefits of deviation maneuvers.

Deviation Alternative	Earlier Strategic Deviation	Travel Distance Savings (nm)	Travel Time Savings (min)	Fuel Consumption Savings (lb)	Greenhouse Gas Emission Savings (lb)
D1	10 min (80 nm)	133	16.1	5,136	16,050
D2	15 min (120 nm)	154	18.6	5,934	18,543
D3	20 min (160 nm)	171	20.6	9,571	20,534

Figure 2.15 shows the distribution of travel time savings with 10-minute earlier deviations regarding lateral deviations larger than 10 nm. According to the Controller-Pilot Data Link Communication (CPDLC) messages analysis, pilots request permission from air traffic controllers for lateral deviations exceeding 10 nm to avoid convective weather [24]. The average travel time saving is 1.6 minutes and the average of lateral deviations is 33 nautical miles (shown in the red dot). Based on the cumulative distribution function, 97% of the lateral deviation are less than 100 nm. The observed lateral deviations with high travel time savings and large lateral deviations are associated with situations in which pilots did not deviate strategically for avoiding convective weather and

were forced to have large deviation maneuvers close to convective activities (an example is shown in Figure 2.14).

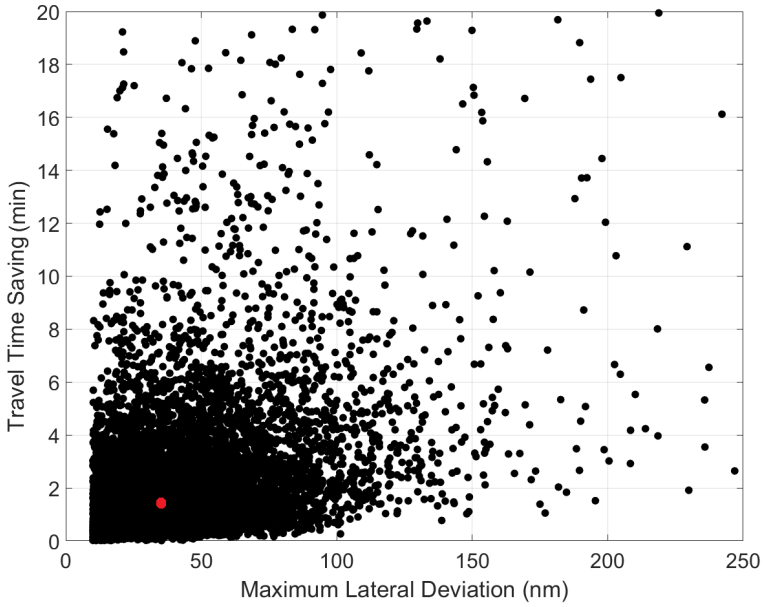

Figure 2.15: Distribution of travel time savings derived from the 18,326 flights.

Table 2.2 shows the operational benefit of 10-minute earlier deviation maneuvers for all aircraft types in terms of average travel distance, travel time, fuel consumption, and greenhouse gas emission savings. Figure 2.16 shows the distribution of travel time savings for three strategic deviations

Table 2.2: Operational benefits for 10-minute earlier weather deviation maneuvers derived from the 18,326 flights.

No.	Aircraft Type	Average Travel Distance Savings (nm)	Average Travel Time Savings (min)	Average Fuel Consumption Savings (lb)	Average Greenhouse Gas Emission Savings (lb)
1	Airbus A330-300	12.9	1.60	318	992
2	Boeing 767-400	10.1	1.25	230	717
3	Boeing 777-200	12.3	1.50	355	1111
4	Boeing 777-300	13.8	1.80	534	1669
5	Boeing 787-9	14.8	1.85	339	1062
	Average	**12.8**	**1.6**	**355**	**1110**

maneuvers. The cumulative distribution functions show higher travel time savings that are the consequences of more strategic weather deviations. According to this analysis for the selected

flights, an annual fuel consumption saving of 6.8 million pounds or 1.8 million dollars is attainable assuming 320 operational days per year and $1.82 per gallon as the average jet fuel price (2019).

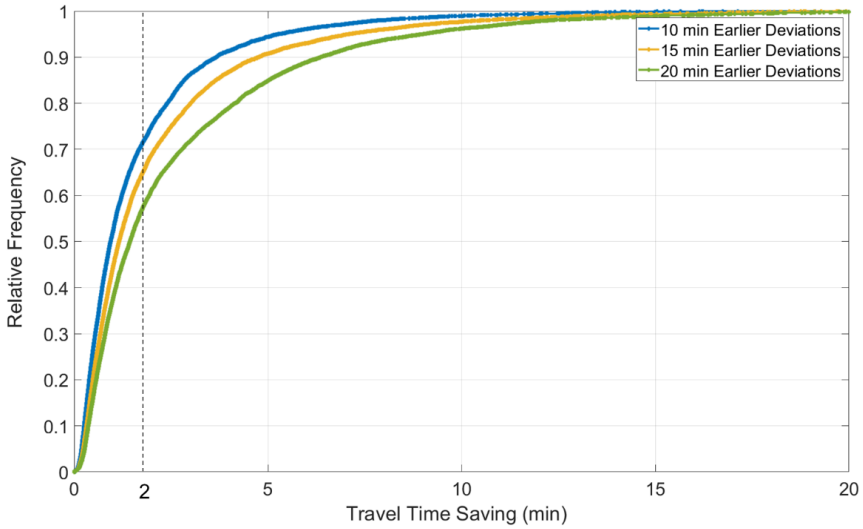

Figure 2.16: Distribution of travel time savings for strategic deviation alternatives for the 18,326 flights.

We conducted statistical tests to check significant differences among aircraft types and airlines. The confidence level for the statistical tests is 95%. Since the p-values of the tests are less than 0.05, we can accept that the distribution of travel time savings for aircraft types and airlines are different. The results show that deviation maneuvers with Airbus A330-300 and Boeing 777-200 have similar distributions in travel time savings with 10-minute earlier deviations. Figure 2.17 and Figure 2.18 show the cumulative distribution functions and the results of statistical t-tests for the travel time savings for each aircraft type and airline.

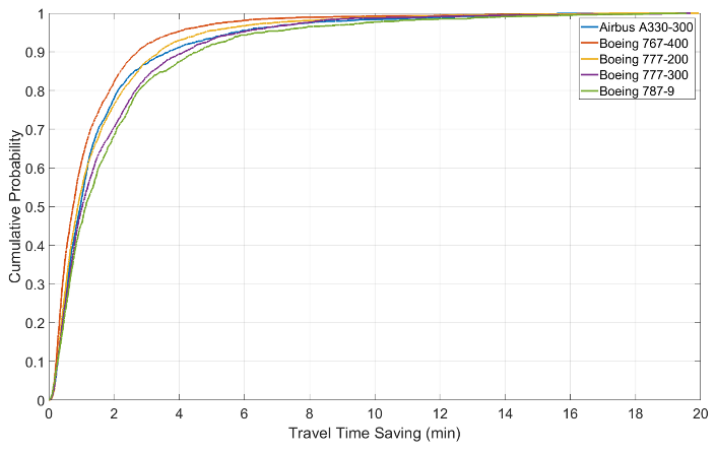

Analysis of Variance

Source	DF	Sum of Squares	Mean Square	F Ratio	Prob > F
Aircraft	4	958.649	239.662	57.7294	<.0001*
Error	16154	67062.951	4.151		
C. Total	16158	68021.600			

Connecting Letters Report

Level		Mean
B789	A	1.9909373
B773	B	1.7993898
A333	C	1.6293448
B772	C	1.5448623
B764	D	1.2647057

Levels not connected by same letter are significantly different.

Figure 2.17: Statistical test for comparing travel time savings for several aircraft types.

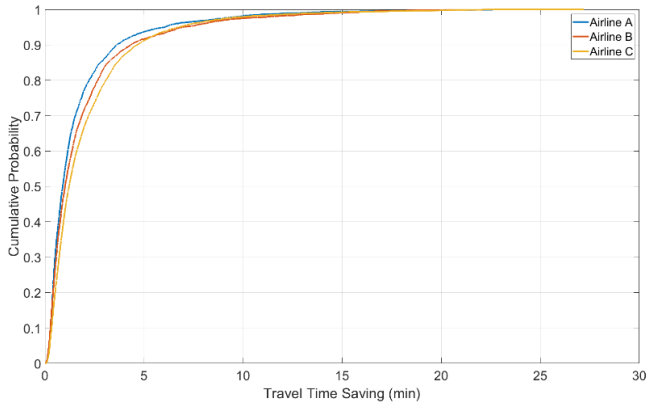

Analysis of Variance

Source	DF	Sum of Squares	Mean Square	F Ratio	Prob > F
Airline	2	371.140	185.570	44.3170	<.0001*
Error	16156	67650.460	4.187		
C. Total	16158	68021.600			

Connecting Letters Report

Level			Mean
Airline A	A		1.7066883
Airline B		B	1.4877184
Airline C		C	1.3125760

Levels not connected by same letter are significantly different.

Figure 2.18: Statistical test for comparing travel time savings for airlines.

2.3.3 Weather Deviation Section Analysis

We analyzed the historical flight trajectories and defined deviation sections in the cruise phase. For each deviation section, the deviation angle and CPA to each CDO contour are measured. This approach aims to find deviation sections with high deviation angles where the CPA is low to CDO contours. The FAA Advisory Circular, AC 00-24C (thunderstorms) stated, "do avoid by at least 20 miles any thunderstorm identified as severe or giving an intense radar echo. This is especially true under the anvil of a large cumulonimbus"[2]. Thus, we evaluated the deviation sections where the CPA to severe and extreme CDO contours are less than 20 nm. Then, the distributions of deviation angles in the Pre-ROMIO and Post-ROMIO periods are compared. Figure 2.19 displays the profile of the azimuth difference and parts of the flight trajectory related to deviation sections highlighted in red. Identified deviation sections have successive waypoints with heading changes more than seven degrees, where the maximum allowed time gap between waypoints is one minute. For example, deviation section 1 is identified with 60 degrees heading change in 75 seconds (10 nm). Figure 2.20 shows the distribution of deviation sections concerning deviation angles and deviation times. This figure shows three clusters of deviation sections. 1) small deviations where the deviation angles are less than 15 degrees, 2) normal deviations with a positive correlation between deviation times and deviation angles, and 3) deviation sections showing holding patterns with around 180 deviation angle degrees. In this figure, 7% of deviation sections are shown in red points indicating

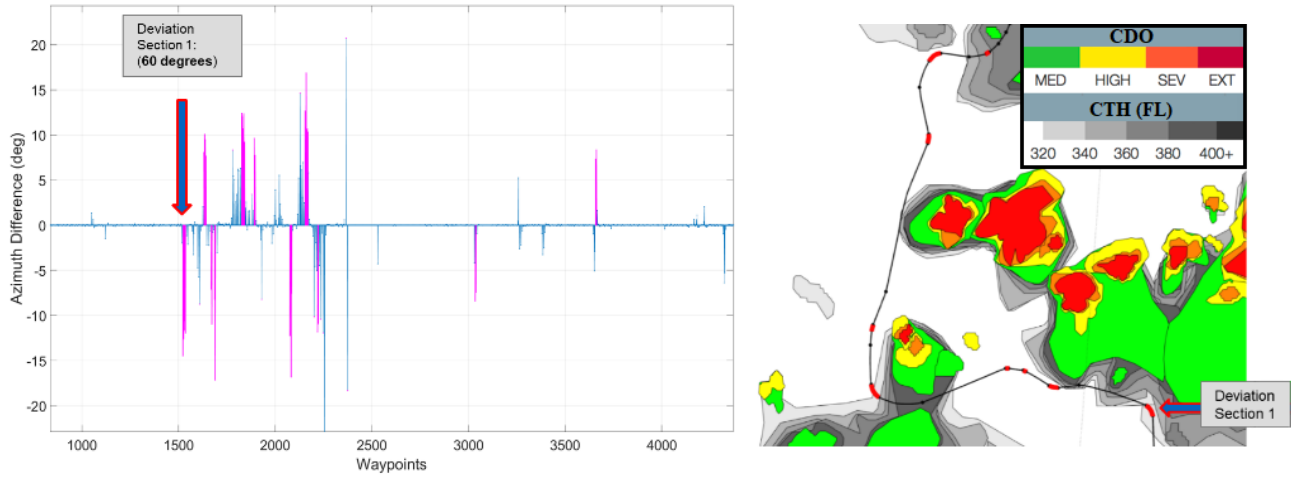

(a) Azimuth difference profile. (b) Corresponding deviation sections.

Figure 2.19: Deviation section analysis.

deviation sections with CPA less than 20 nm to severe and extreme CDO contours. Note that based on the design of the ROMIO application, CDO contours represent the convective activities more generously compared to airborne radars.

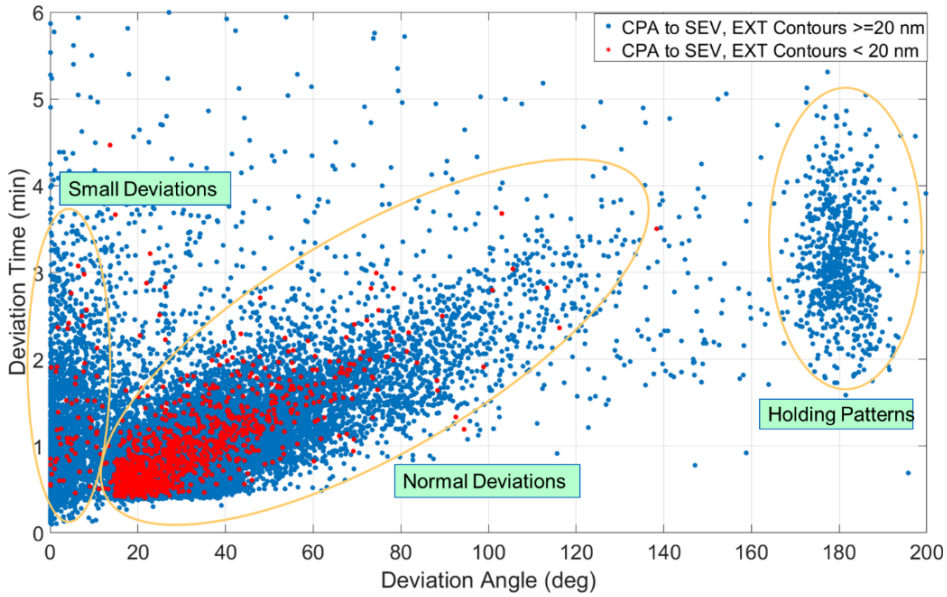

Figure 2.20: Distribution of deviation sections regarding the CPA to CDO contours for 18,326 flights.

The ROMIO application with displaying satellite-based meteorological information provides enhanced situational awareness of rapidly changing convective weather compared to onboard radars. The hypothesis is that flights using ROMIO display will benefit from ROMIO-aided strategic de-

cision making with executing smoother deviation maneuvers (i.e., lower deviation angles) for convective weather avoidance. For testing the hypothesis, we used the pilots' survey to select the flights employed the ROMIO application and compared their distributions of deviation angles in the Pre-ROMIO and Post-ROMIO periods.

To strengthen the statistical comparison tests, the Principal Component Analysis (PCA) is employed to identify deviation maneuvers with similar convective weather exposure (i.e., CDO and CTH contour levels) in the Pre-ROMIO and Post-ROMIO periods. PCA is a dimensionality-reduction method that is used to extract important variables (components). PCA rotates the original data space such that the axes of the new coordinate system point into the directions of the highest variance of data. To extract the relevant features for deviation sections close to convective weather events, we considered areas with a 50 nm radius around the flight trajectory segments and measured the area of the CDO and CTH contours in these zones. The weather events behind the flights are ignored in the buffer zones. Figure 2.21 displays an example of a buffer zone with a deviation section close to CDO contours. Table 2.3 shows the area occupancy features for this example as the percentages of the CDO and CTH contours area to the area of the buffer zone.

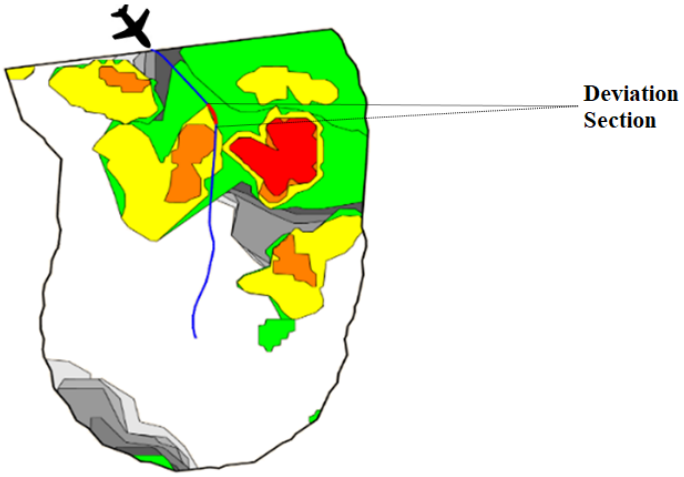

Figure 2.21: Example of a deviation section inside the buffer zone.

One of the flights in the pilot's survey which used ROMIO frequently for weather deviations is Delta 110 between Ezeiza, Argentina, and Atlanta, GA. We selected all DAL110 flights in the Pre-ROMIO

Table 2.3: Area occupancy features for deviation sections.

CTH Contours	Percent of CTH Contours' Area Inside the Buffer Zone
32000 ft	41 %
34000 ft	38 %
36000 ft	35 %
38000 ft	29 %
40000 ft	27 %

CDO Contours	Percent of CDO Contours' Area Inside the Buffer Zone
Medium	43 %
High	24 %
Severe	7 %
Extreme	3 %

(145 flights) and Post-ROMIO (261 flights) periods. For this analysis, the Post-ROMIO period is considered between August 2018 to May 2019 (10 months) to have a consistent rate of ROMIO update (15 minutes) with the Pre-ROMIO period. Using PCA analysis enables us to identify 347 deviation sections with similar convective weather exposure. Figure 2.22 shows the distribution of deviation angles in the Post-ROMIO and Pre-ROMIO periods with probability density function and cumulative distribution function. Based on the results, the distribution of deviation angle in the Post-ROMIO period has a shift to the lower deviation angles.

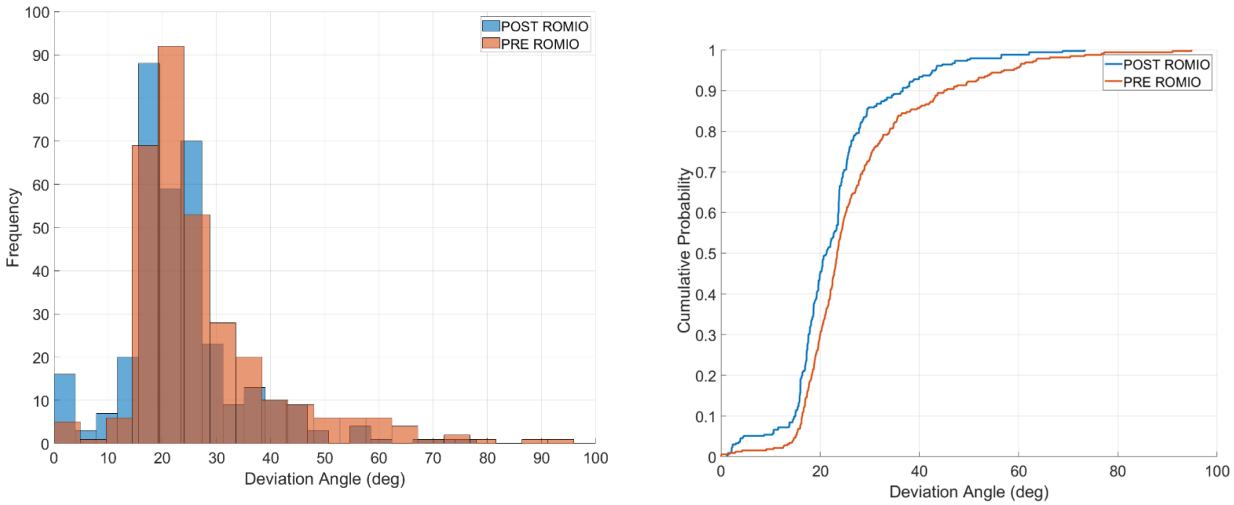

(a) Probability density function. (b) Cumulative distribution function.

Figure 2.22: Distribution of deviation angles (DAL110).

Figure 2.23 and Figure 2.24 show the cumulative distribution and box plots of deviation angles where the CPAs of deviation sections to CDO layers are less than 20 nm. The results show that the deviation angles associated with the CDO layers in the Post-ROMIO period are distributed toward

lower deviation angles compared to the Pre-ROMIO period.

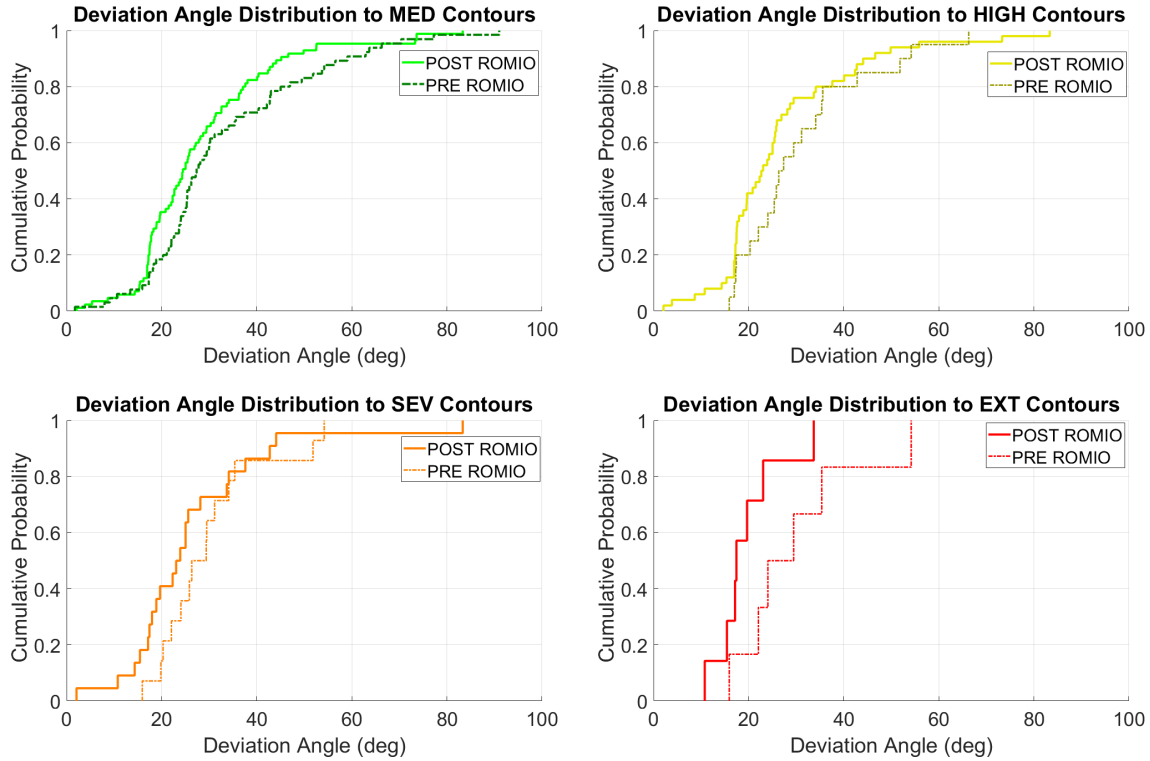

Figure 2.23: Cumulative distribution of deviation angles with CPA less than 20 nm.

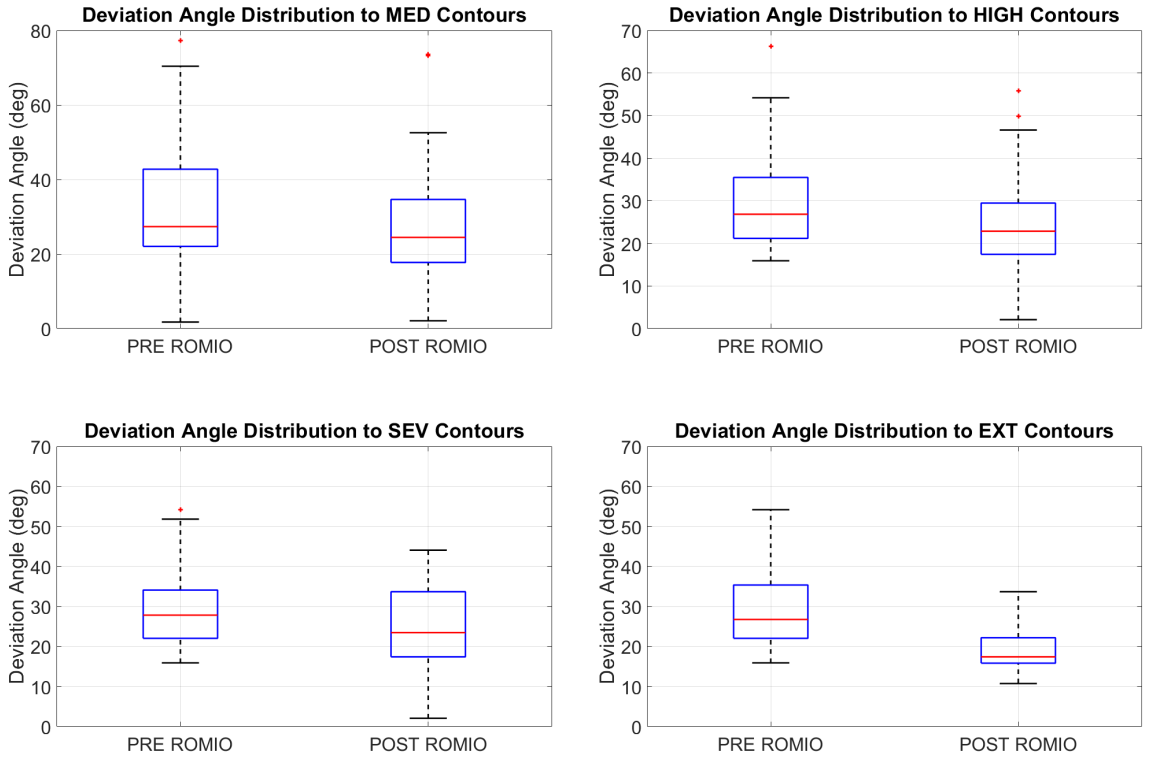

Figure 2.24: Box plot of deviation angles with CPA less than 20 nm.

We specified all the flights in the survey, which crossed the ITCZ and used the ROMIO application to avoid the convective weather. The list of six flights from Delta Air Lines that were selected for comparison in the Post-ROMIO and Pre-ROMIO periods is as following: 1) DAL110: SAEZ-KATL, 2) DAL101: KATL-SAEZ, 3) DAL151: KATL-SPJC, 4) DAL61: KATL-SBGL, 5) DAL472: SBGR-KJFK, and 6) DAL147: KATL-SCEL. It is assumed that all the selected historical flights in the Post-ROMIO period used the ROMIO application for weather-related decision making. The daily log files (between August 2019 to December 2019) verifies that the selected flights used ROMIO frequently in this period.

We integrated the selected flights in the Pre-ROMIO and Post-ROMIO periods and identified all deviation maneuvers segments and sections. The total number of flights in the Pre-ROMIO period (5 months) is 760, and in the Post-ROMIO (10 months) period in 1479 flights. We applied the PCA analysis to check the similarity among deviation maneuvers and defined 1479 similar deviation sections in the Pre-ROMIO and Post-ROMIO periods. The result of the statistical test with a 95% confidence level shows that the p-value of the t-test is less than 0.05 (see Figure 2.25). It means we can accept the hypothesis that the average deviation angles in the Post-ROMIO period are lower than the Pre-ROMIO period. In other words, the lower deviation angle in the Post-ROMIO period shows that the selected flights take advantage of the improved situational awareness and more strategic decision making for avoiding the inclement weather.

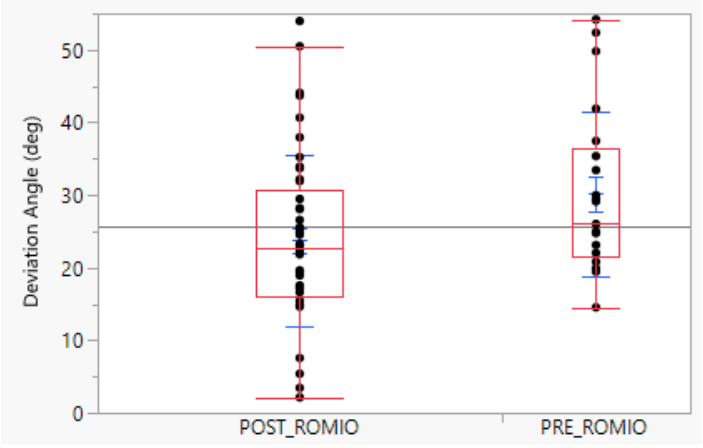

(a) Deviation angles comparison (boxplot).

t Test

PRE_ROMIO-POST_ROMIO

Difference	6.4383	t Ratio	2.125691
Std Err Dif	3.0288	DF	40.61236
Upper CL Dif	12.5568	Prob > |t|	0.0397*
Lower CL Dif	0.3197	Prob > t	0.0198*
Confidence	0.95	Prob < t	0.9802

(b) Statistical t-test results.

Figure 2.25: Deviation angle comparison between the Pre-ROMIO and Post-ROMIO periods.

Figure 2.26 compares the distribution of maximum lateral weather deviation for flights in Pre-ROMIO and Post-ROMIO periods. The result of the statistical test with a 95% confidence level shows a significant difference in the distribution of lateral weather deviation in the Post-ROMO and Pre-ROMIO periods. The lower average lateral deviation in the Pre-ROMIO period substantiates the benefits of ROMIO-aided more strategic deviations. The results show that the average lateral weather deviations for deviation segments more than ten nautical miles are 34 nm and 30 nm in the Pre-ROMIO and Post-ROMIO periods, respectively.

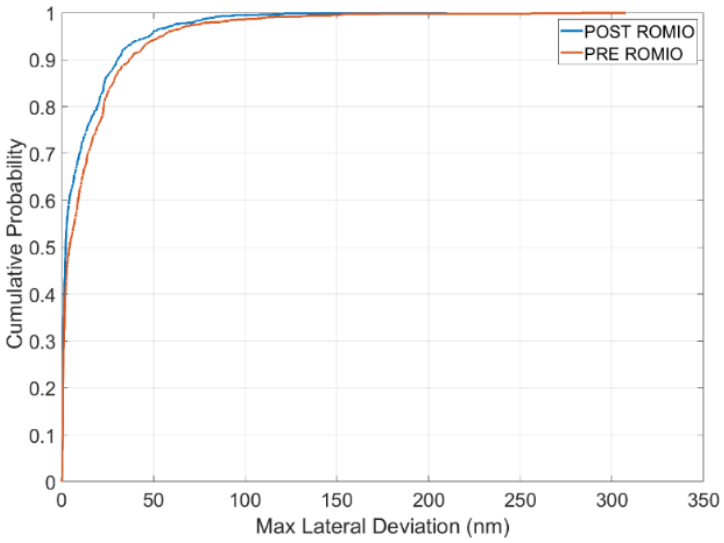

(a) Lateral deviations comparison.

t Test

PRE-ROMIO-POST-ROMIO

Difference	2.4912	t Ratio	1.77922
Std Err Dif	1.4001	DF	1417.798
Upper CL Dif	5.2377	Prob > |t|	0.0754
Lower CL Dif	-0.2554	Prob > t	0.0377*
Confidence	0.95	Prob < t	0.9623

(b) T-statistical test results.

Figure 2.26: Lateral deviation comparison between the Pre-ROMIO and Post-ROMIO periods.

2.4 Simulation-Based Analysis

This section presents a simulation-based approach to estimate the operational benefits of providing satellite-based meteorological information using the ROMIO demonstration. Fast-time, computer simulation tools to evaluate the operational benefits of novel technologies, procedures, and policies for supporting future infrastructure and avionics investment decisions. In this study, we used the Global Oceanic (GO) model which is developed jointly by Virginia Tech Air Transportation Systems Laboratory and the Federal Aviation Administration (FAA).

2.4.1 Global Oceanic (GO) Model Overview

The GO Model is a microscopic flight simulation model developed to evaluate the operational benefits of advanced concepts of operations for flights over global oceanic airspace. The model employs a discrete-time simulation algorithm that can simulate all phases of flight from takeoff to landing [31]. Figure 2.27 describes how the GO Model solves the aircraft equations of motion numerically and updates the position ($x_{t+\delta t} = x_t - (v)\delta t$), altitude ($h_{t+\delta t} = h_t - (\frac{dh}{dt})\delta t$), and aircraft mass ($m_{t+\delta t} = m_t - (\frac{dm}{dt})\delta t$) based on the user-defined simulation time step (δt).

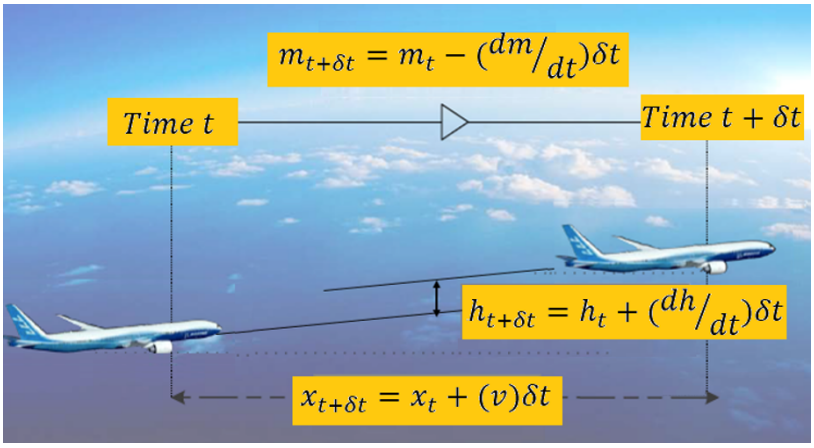

Figure 2.27: Simulation model paradigm.

To simulate the real-world traffic and model the interactions between flights over oceanic airspace, the GO Model uses five modules including wind, aircraft performance, flight planning, track assignment, and conflict detection and resolution modules. The wind module in the model uses the National Center for Atmospheric Research (NCAR) Reanalysis wind data. The aircraft performance module includes the EUROCONTROL Base of Aircraft Data (BADA) 3.13 and 4.0 models. The GO Model has conflict detection and resolution algorithms to detect and resolve strategic and tactical potential conflicts. The strategic conflict detection and resolution modules check the projection of flight trajectories before entering the oceanic boundary. These modules assign flights with conflict-free flight level and Mach number at the entry to oceanic airspace. Tactical conflict detection and resolution modules monitor the projection of flight trajectories to have a user-defined conflict-free horizon. Figure 2.28 demonstrates conflict resolution rules implemented in the GO Model which are changing cruise flight levels, changing cruise Mach numbers, and lateral deviations.

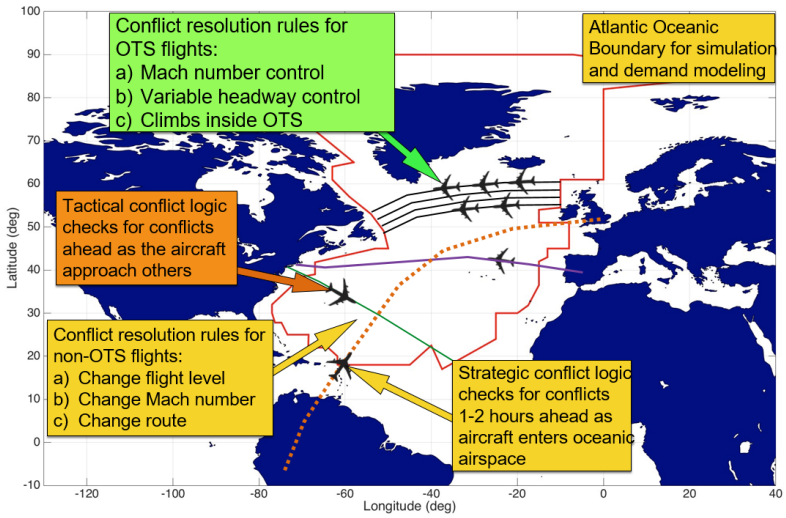

Figure 2.28: Conflict detection and resolution logic.

To model the interactions between pilots and Air Traffic Controllers (ATC), we implemented three routines in the model including a pilot routine, an ATC routine, and a system update routine. The pilot routine controls each aircraft by simulating the behaviors of pilots. The ATC routine controls all the aircraft within Flight Information Regions (FIRs) by simulating the behaviors of air traffic controllers. The system update routine updates the status of all aircraft in the simulation according to the pilot routine and ATC routine.

The FAA uses the Advanced Technologies and Oceanic Procedures (ATOP) system to control the oceanic airspace system. We had interviews with air traffic controllers in the New York (ZNY) and Oakland oceanic centers in 2016 and 2018. These interviews provide insight into the priorities of the conflict resolution strategies used by the ATC to resolve the conflicts. Figure 2.29 depicts the flowchart of the GO Model.

To address the task of simulating traffic in diverse FIRs with distinct separation standards, the GO Model was enhanced to include multi-region simulation capabilities with multiple separation standards and various aircraft equipage levels. Another feature of the GO Model applied in this analysis is the use of a flight plan optimization tool for generating wind-optimal flight trajectories using the National Center for Atmospheric Research (NCAR) Reanalysis wind and air temperature model. This module is employed to create User-Preferred Routes (UPR) for flight plans contained in the TFMS demand sets.

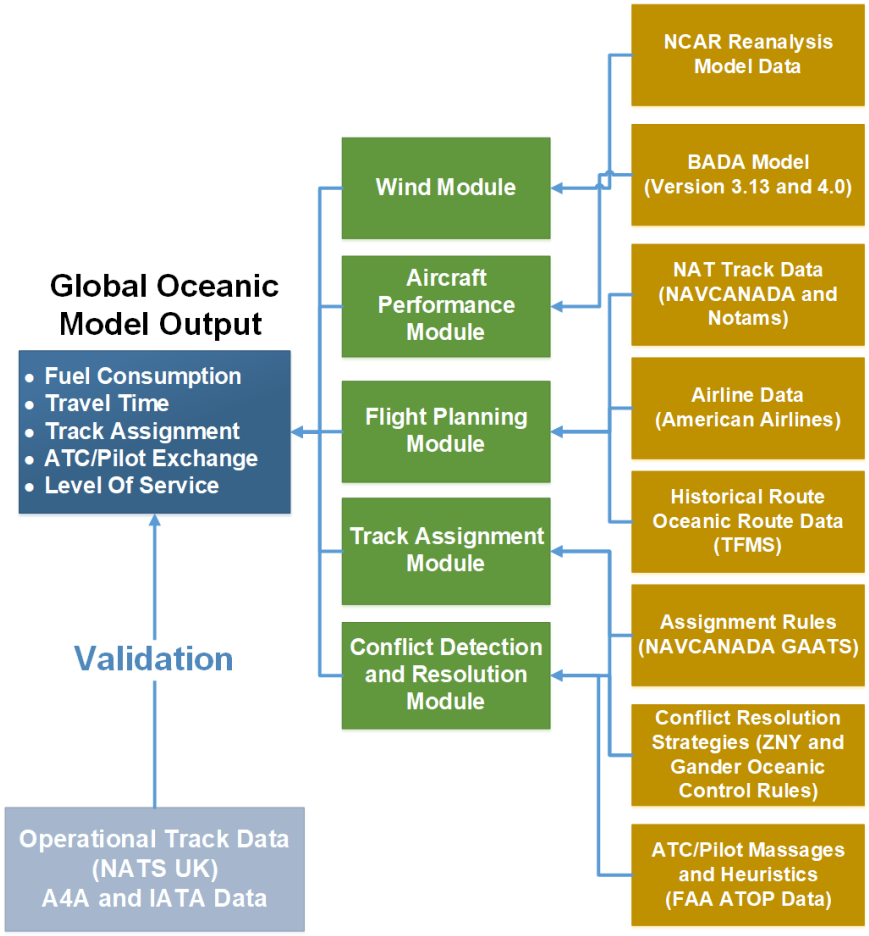

Figure 2.29: Global Oceanic model flowchart.

2.4.2 Weather Conflict Detection and Resolution Logic

To study the benefits of providing ROMIO-aided weather information, the conflict detection and resolution module is enhanced with independent algorithms for detecting and resolving conflicts due to traffic and weather. This enhancement enables the GO Model to measure the operational benefits of different weather-related scenarios with fixed traffic-related settings.

Traffic conflict detection and resolution logic monitors the projection of flight trajectories inside the oceanic airspace. This module assures that flights have their conflict-free horizon (i.e., user-defined parameter) by applying three resolution maneuvers (i.e., changing flight level, changing Mach Number, and lateral detours). The weather conflict detection algorithm checks the projection of flight trajectories against convective weather (i.e., CDO contours) and detects any potential exposure of flights with convective areas. Then, the weather conflict resolution algorithm generates

different deviation alternatives and evaluates them to find a conflict-free maneuver.

We used two sources to define the rules and strategies for convective weather avoidance: 1) historical flight analysis, and 2) the FAA advisory circular for thunderstorms (AC-0024C). According to the analysis of over 18,326 oceanic flights, we measured the travel distance flown inside convective weather events when flights pierce CDO contours. Four types of convective weather events based on the number of involved CDO contours are shown in Figure 2.5.

To visualize multivariate data, "parallel coordinates diagrams" are a commonly used tool for showing a set of points in a multi-dimensional space. A point in N-dimensional space is represented as a polyline with vertices on N parallel vertical axes. Figure 2.30 shows the parallel coordination diagrams showing 4-dimensional values of travel distance in four types of piercing events. The black lines in this figure illustrate the threshold of maximum allowable travel distance for each event type. These thresholds are defined based on 95 percentile of observations with travel distance inside each CDO contours. The green areas below the threshold are safe, and the red area above the threshold should be avoided.

Figure 2.30a shows that flights would tolerable 100 nm travel distance inside Medium convective weather contours in event type 1. Figure 2.30b shows that flights would tolerable 85 nm and 30 nm travel distance inside Medium and High convective weather contours in event type 2. Figure 2.30c shows that flights would tolerable 40 nm, 30 nm, and 15nm travel distance inside Medium, High, and Severe convective weather contours in event type 3. Figure 2.30d shows that flights would tolerable 65 nm, 30 nm, 20 nm, and 12 nm travel distance inside Medium, High, Severe, and Extreme convective weather contours in event type 4.

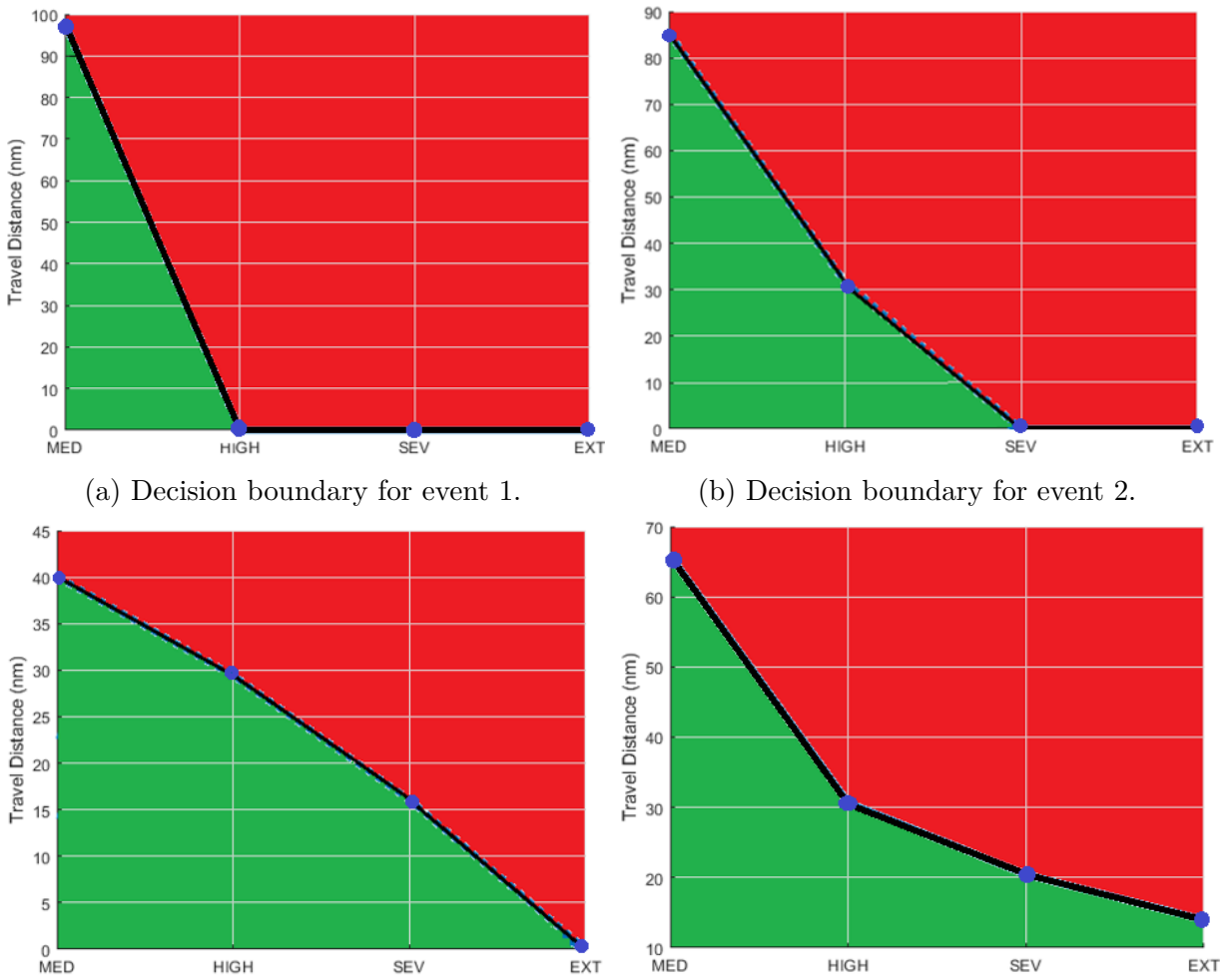

(a) Decision boundary for event 1.

(b) Decision boundary for event 2.

(c) Decision boundary for event 3.

(d) Decision boundary for event 4.

Figure 2.30: Decision boundaries for allowable travel distance in CDO Contours.

The FAA advisory circular for thunderstorms (AC-0024C) is the second reference to define the convective weather avoidance rules. In the AC-0024C, it is suggested that to avoid by at least 20 miles from 1) any thunderstorm identified as severe or giving an intense radar echo, 2) the anvil of a large cumulonimbus [2]. The ROMIO application demonstrates the convective weather events with four severity levels (i.e., Medium, High, Severe, Extreme). In this study, convective weather contours with severity level 4 (Severe: orange color) and severity level 5 (Extreme: red color) are considered as severe thunderstorms. Thus, we implemented this rule for checking the deviation alternatives to maintain a minimum distance to severe and extreme CDO contours. Note that based on the design of the ROMIO demonstration, CDO contours represent the convective weather polygons more generously compared to airborne radars. For consistency with the real-world observations,

the GO Model is programmed to maintain the flight tracks 10 nautical miles away from the Closest Point of Approach (CPA) to Severe and Extreme CDO contours. Based on the FAA standard and historical flight analysis, the weather conflict detection and resolution module in the GO Model considers the following rules for evaluating the deviation maneuvers:

- A flight can fly less than 100 nm in Medium CDO weather contours in a piercing event.
- A flight can fly less than 85 nm in Medium and 30 nm in High CDO weather contours in a piercing event.
- A flight cannot fly in Severe and Extreme CDO contours.
- A flight should fly with at least 10 nm as the minimum distance (i.e., CPA) to Severe and/or Extreme CDO contours.

The weather conflict detection and resolution module in the GO Model have the following parameters:

1. **Weather detection look-ahead horizon:**

   This parameter defines the look-ahead horizon in monitoring flight trajectory projections and detecting convective weather contours. In scenarios with flights equipped with onboard radar technology, this parameter is set to 20 minutes ($\sim$ 160 nm) representing the usable onboard radar range. In scenarios with ROMIO-enabled technology, this parameter is increased to 25 minutes, 30 minutes, 40 minutes, and 60 minutes.

2. **Weather conflict detection and resolution cycle:**

   This parameter defines the frequency of running the weather conflict detection and resolution module. This parameter is set to 2 minutes. Note that the traffic conflict detection and resolution cycle (10 minutes) determines the frequency of running the traffic conflict detection and resolution module.

3. **Maximum lateral deviation:**

   This parameter defines the maximum lateral deviation from the flight plan for avoiding the convective weather. A study on the Controller-Pilot Data link Communication (CPDLC)

messages determined that the minimum lateral deviation maneuver requested by pilots is 10 nm [24]. Figure 2.31a shows the cumulative distribution function of lateral deviations derived from historical flight analysis. This figure shows that 97% of the deviation maneuvers (more than 10 nm) deviated less than 100 nm laterally.

4. **Maximum deviation angle:**

   Figure 2.31b shows the cumulative distribution function of deviation angles associated with historical long-range flights. The figure shows the maximum deviation angles of 60 degrees or less for most of the weather avoidance maneuvers. This parameter varies among scenarios in the study.

5. **Buffer time for creating deviation alternatives:**

   Buffer time for creating deviations alternatives is the time required for air traffic controllers and pilots to communicate and verify deviation alternatives. This parameter is set to 120 seconds (2 minutes).

6. **The minimum distance of deviation alternatives to Severe and Extreme CDO contours:** this is a user-defined parameter set as 10 nautical miles in this study.

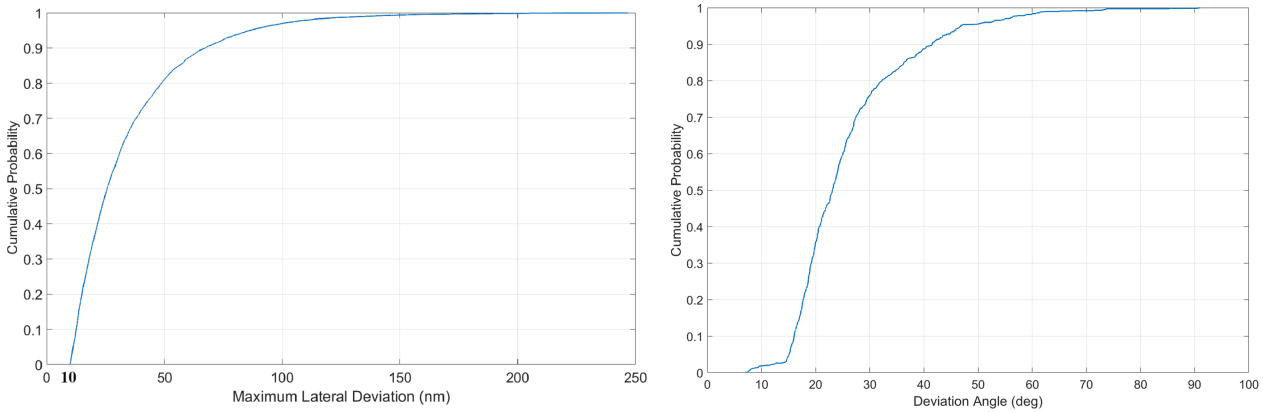

(a) Lateral deviations distribution. (b) Deviation angles distribution.

Figure 2.31: Cumulative distribution functions of lateral deviations and deviation angles.

Figure 2.32 displays a flight example inside the simulation when the weather conflict detection algorithm finds a potential conflict in the flight plan (shown in D1 trajectory) with convective

weather events 20 minutes ahead. This is an example of event type 3. If this flight continues the projected flight trajectory based on its flight plan, it will traverse 28 nm in Medium, 26 nm in High, and 4 nm in Severe CDO contours. Based on the mentioned evaluation rules, this is not allowable. The weather conflict resolution module receives the details of this potential conflict such as the beginning and end of exposure to CDO polygons, and generates deviation alternatives based on the maximum lateral deviation parameter (i.e., 100 nm). This module creates deviation alternatives at 10 nm increments to the right and left sides of the flight trajectory segments.

Figure 2.32 shows that all the deviation maneuvers to the right are not acceptable since they would fly in Severe and Extreme CDO contours. Table 2.4 shows the details of two deviation alternatives (i.e., D2, D3) to the left without any piercing to Severe and Extreme contours. Both deviation alternatives satisfy the travel distance in Medium and High contours. D2 has 22 nm in Medium and 22 nm in High while its CPA to Severe and Extreme contours is 4 nm. This alternative satisfies the travel distance requirement but it does not comply with the FAA CPA standard. D3 does not pierce any contours and the CPA is 24 nm which satisfies both rules. Thus, in this example, D3 is selected as the deviation resolution to avoid the convective weather area.

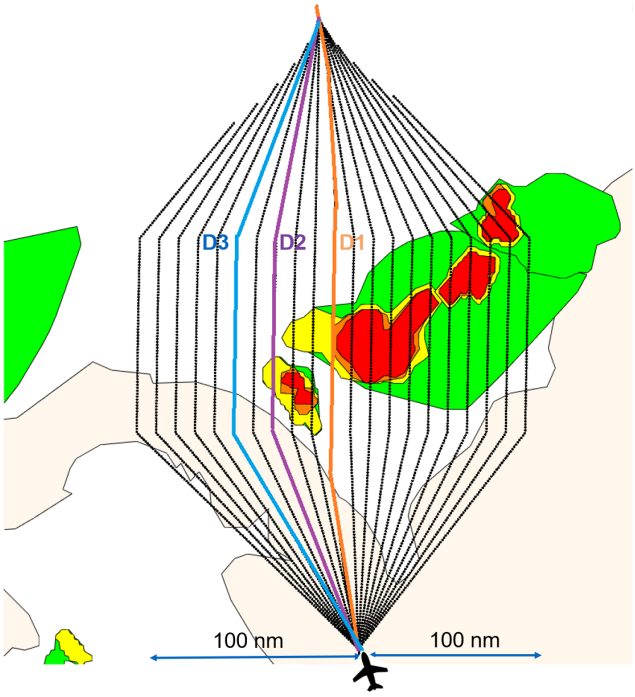

Figure 2.32: Evaluated deviation alternatives.

Table 2.4: Example of deviation alternatives evaluations.

Deviation Alternative	Lateral Deviation	Travel Distance in CDO Contours	Min Distance to Severe and Extreme CDO Contours
D1	0 (Flight Plan)	Medium: 28 nm High: 26 nm Severe: 4 nm	0 nm
D2	30 nm to the Left	Medium: 22 nm High: 22 nm	4 nm
D3	50 nm to the Left		24 nm

2.4.3 Simulation Scenarios

The simulation model is driven by a set of input files including a daily flight demand, FIR boundaries for each air traffic control region, weather data (i.e., CDO and CTH contours), and wind data sets. In this study, the Geographic Information System (GIS) database of the International Civil Aviation Organization (ICAO) is used for defining the boundaries of FIRs in the North Atlantic, Caribbean, and South America airspace. Figure 2.33 shows the domain of the traffic simulation which is consistent with coverage of the ROMIO application. The list of regions and FIRs included in each region are as follows:

- SA: South America region consists of twenty-seven FIRs in lower and upper Latin America.
- NA1: North Atlantic 1 region consists of New York East, New York West, and Santa Maria FIRs.
- NA2: North Atlantic 2 consists of 5 FIRs including Gander, Shanwick, Reykjavik, Sondrestrom, and Bodo.
- CA1: Caribbean Airspace 1 consists of 3 FIRs including Mexico, Houston, and Miami.
- CA2: Caribbean Airspace 2 consists of eleven Caribbean FIRs including San Juan, Habana, Kingston, Santo Domingo, Maiquetia, Panama, Port au Prince, Barranquilla, Curacao, Piarco, and Central America.

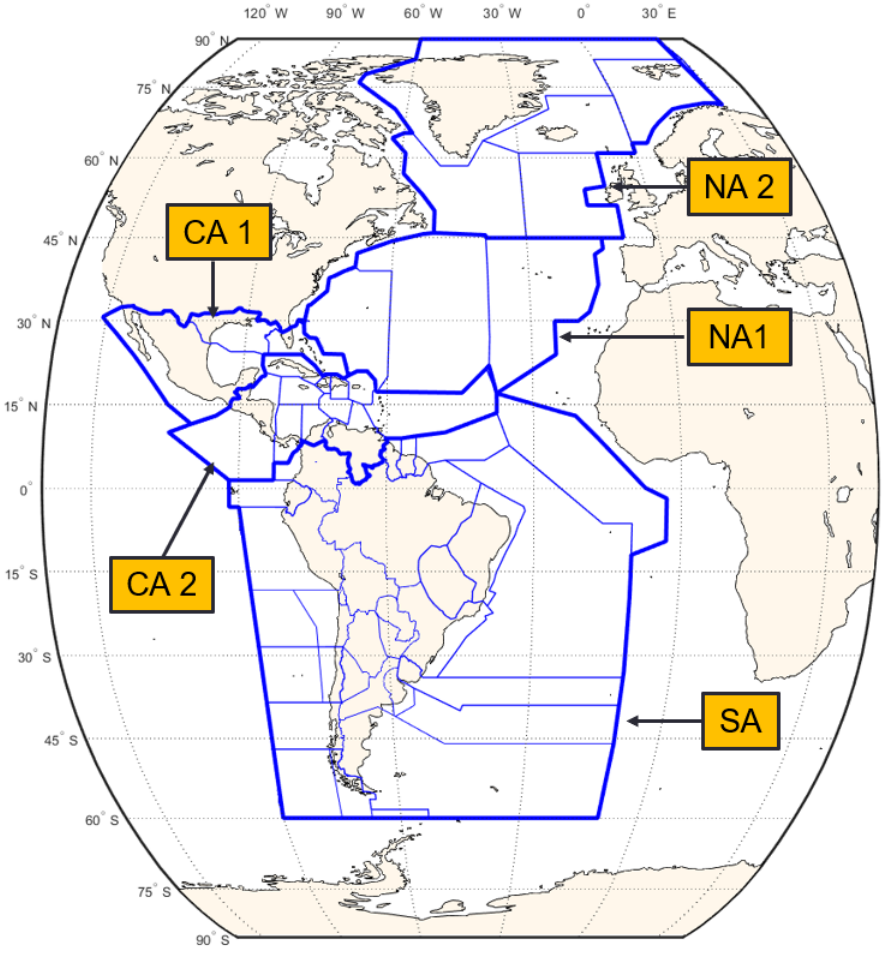

Figure 2.33: Simulation airspace: regions and FIRs.

Table 2.5 shows the minimum vertical, lateral, and longitudinal separations in each FIR. Note that the North Atlantic regions (i.e., NA1 and NA2) are the airspace where the step climbs are 1000 feet, and flights in other regions execute 2000 feet step climbs complying with hemispherical rules. According to the hemispherical rules, eastbound flights shall cruise in odd flight levels and westbound flights shall cruise in even flight levels.

Table 2.5: Separation minima.

Flight Information Regions (FIRs)	Vertical Separation Minimum (feet)	Lateral Separation (nm)	Longitudinal Separation (nm)
SA	2000	30	80
NA1	1000	30	30
NA2	1000	23	40
CA1	2000	15	15
CA2	2000	30	80

In this study, we used the real-scale traffic derived from the Traffic Flow Management System (TFMS) to simulate flight operations in the specified airspace boundary. TFMS is a data exchange system including flight data such as aircraft types, flight plans, origin, and destination information in one record per flight. The traffic data set used in this analysis is related to June 24,25,26, 2019. A traffic forecast function provided by the FAA is used for growing the traffic to the year 2019. We specified two traffic data set as medium traffic (2050 flights) and high traffic (4437 flights) in the simulation airspace (see Figure 2.34). We also determined two weather data set as follows: 1) moderately-dynamic weather derived from June 24,25,26, (2019), 2) highly-dynamic weather derived from November 9,10,11 (2019). The dates with highly-dynamic weather are selected to have convective areas in the North Atlantic regions (see Figure 2.35). The GO Model uses the wind data derived from the NCAR Reanalysis II wind model developed by the National Oceanic and Atmospheric Administration (NOAA). Table 2.6 demonstrates four scenario cases based on different traffic and weather data sets. Table 2.7 shows the simulated scenarios in each scenario set.

Table 2.6: Scenario cases.

Scenario cases		**Traffic**	
		Medium	High
Weather	Moderately-Dynamic	Medium Traffic, Moderately-Dynamic Weather	High Traffic, Moderately-Dynamic Weather
	Highly-Dynamic	Medium Traffic, Highly-Dynamic Weather	High Traffic, Highly-Dynamic Weather

Table 2.7: Simulated scenarios.

No.	Scenarios	Weather Conflict Detection Look-Ahead Horizon	Maximum Deviation Angle
1	Onboard Radar	20 minutes (∼160 nm)	75
2	ROMIO-Enabled	25 minutes (∼200 nm)	65
3	ROMIO-Enabled	30 minutes (∼240 nm)	65
4	ROMIO-Enabled	40 minutes (∼320 nm)	65
5	ROMIO-Enabled	60 minutes (∼480 nm)	55

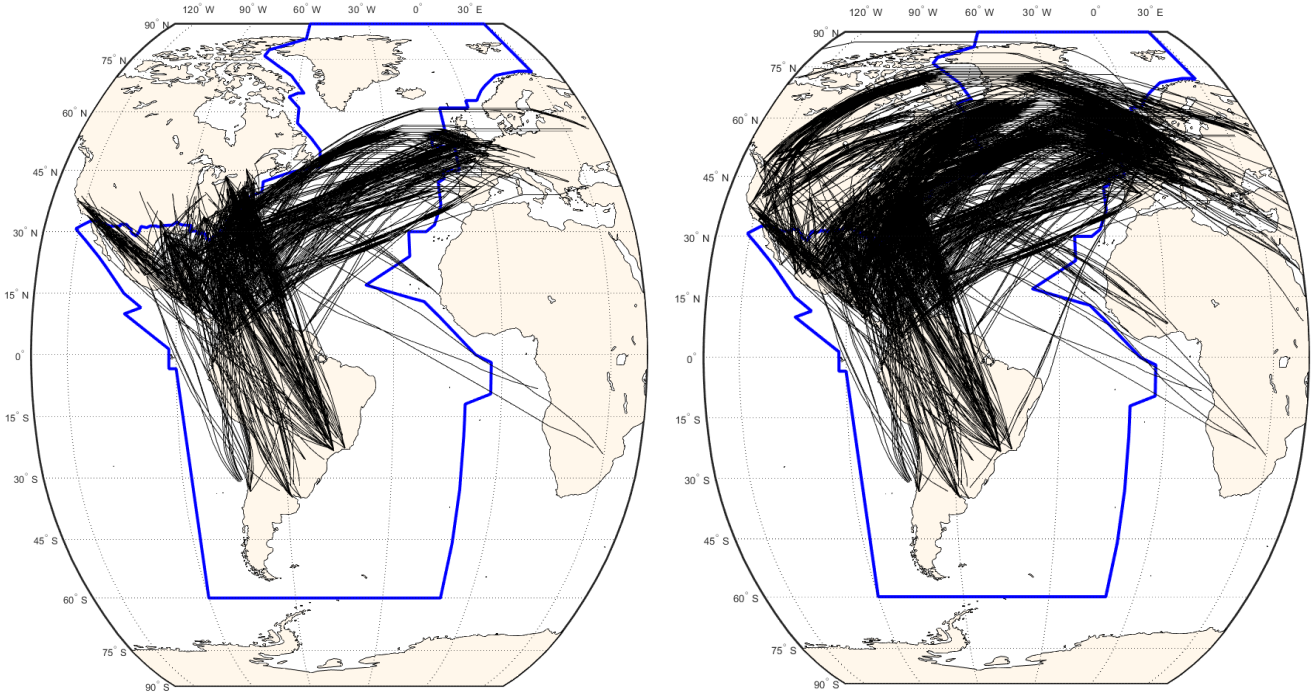

(a) Medium traffic. (b) High traffic.

Figure 2.34: Simulated flight traffic.

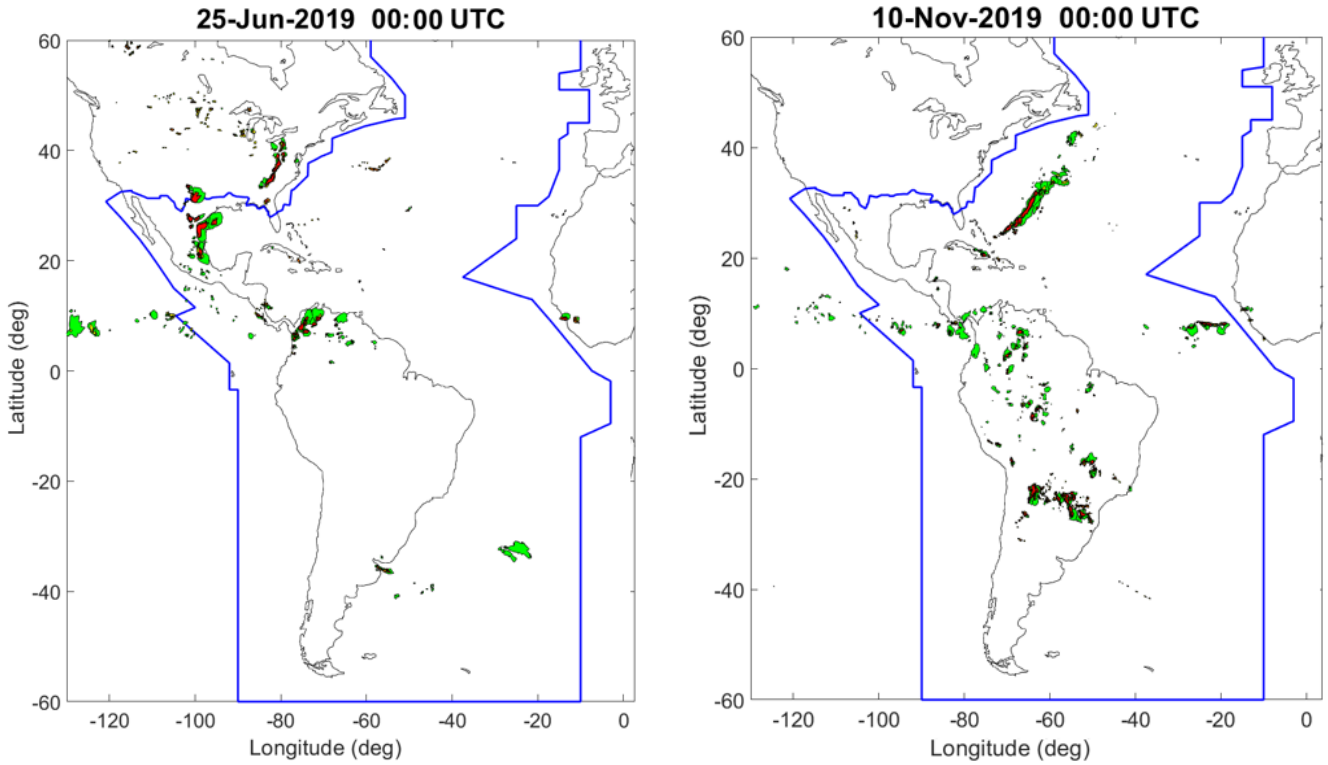

(a) Moderately-Dynamic weather. (b) Highly-Dynamic weather.

Figure 2.35: Simulated weather conditions.

2.4.4 Simulation Results

We simulated five scenarios per scenario case and compared the average fuel consumption, travel distance, and travel time of flights in the middle day of the simulations. Figure 2.36 shows the normalized fuel consumption, travel distance, and travel time for all the simulated scenarios. Equation (2.1) is used to normalize the data, where $x = (x_1, x_2, x_3, ..., x_n)$ and z_i is the i^{th} normalized data.

$$z_i = \frac{x_i - min(x))}{max(x) - min(x)))} \tag{2.1}$$

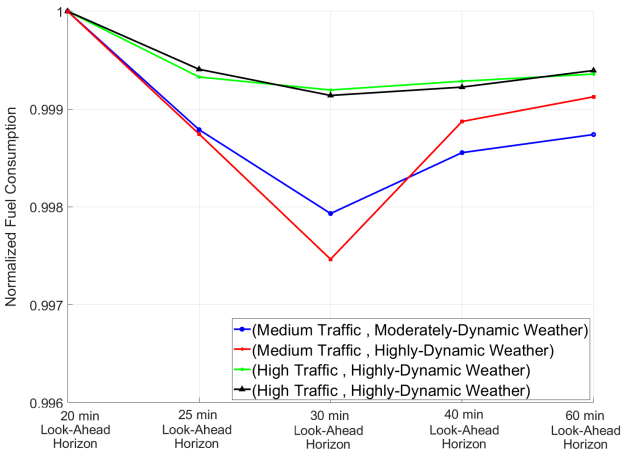

(a) Normalized fuel consumption.

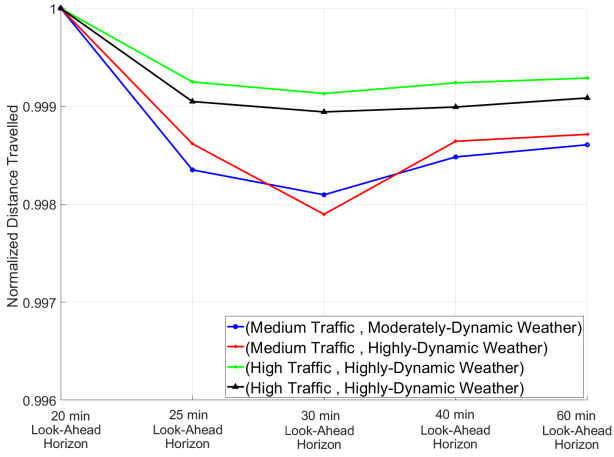

(b) Normalized travel distance.

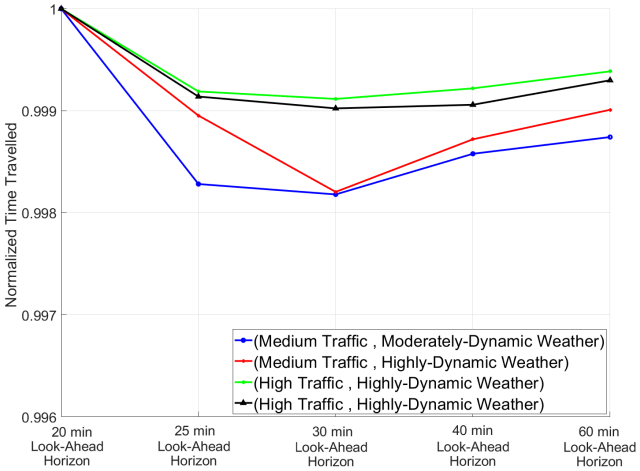

(c) Normalized travel time.

Figure 2.36: Normalized fuel consumption, travel distance, and travel time.

The simulation results show that the ROMIO-enabled scenarios have lower fuel consumption, travel

distance, and travel time compared to the onboard radar scenario. Also, the ROMIO-enabled scenario with 30-minute look-ahead horizon has the minimum average fuel consumption, travel distance, and travel time compared to other ROMIO-enabled scenarios.

Note that the ROMIO demonstration nowcasts the meteorological information. In ROMIO-enabled scenarios with 40 minutes and 60 minutes of look-ahead horizons, the model uses the present weather information to make decisions for avoiding convective weather events in the next 40 minutes and 60 minutes. This uncertainty of weather information is the reason for operational inefficiency (i.e, higher fuel consumption, travel distance, and travel time) in ROMIO-enabled scenarios with 40 minutes and 60 minutes of look-ahead horizons.

Figure 2.37 shows the changes in fuel consumption for the scenarios investigated. The scenario case with high traffic, highly-dynamic weather conditions is subject to further analysis since it has the highest number of flights with fuel consumption benefits comparing the onboard radar and the ROMIO-enabled (30-minute look-ahead horizon) scenario. Figure 2.38 demonstrates the distribution of fuel consumption savings and travel distance savings for the flights in the high traffic, highly-dynamic weather conditions scenario case.

The blue dots show the flights with different travel distances in the onboard radar and the ROMIO-enabled scenarios. The red dots show the flights which gain or lose fuel consumption due to different vertical profiles. These flights are called affected flights since they do not have differences in travel distance among the onboard radar and the ROMIO-enabled scenarios. Figure 2.39 illustrates the average fuel consumption, travel distance, and travel time savings and losses for deviated flights in scenario cases.

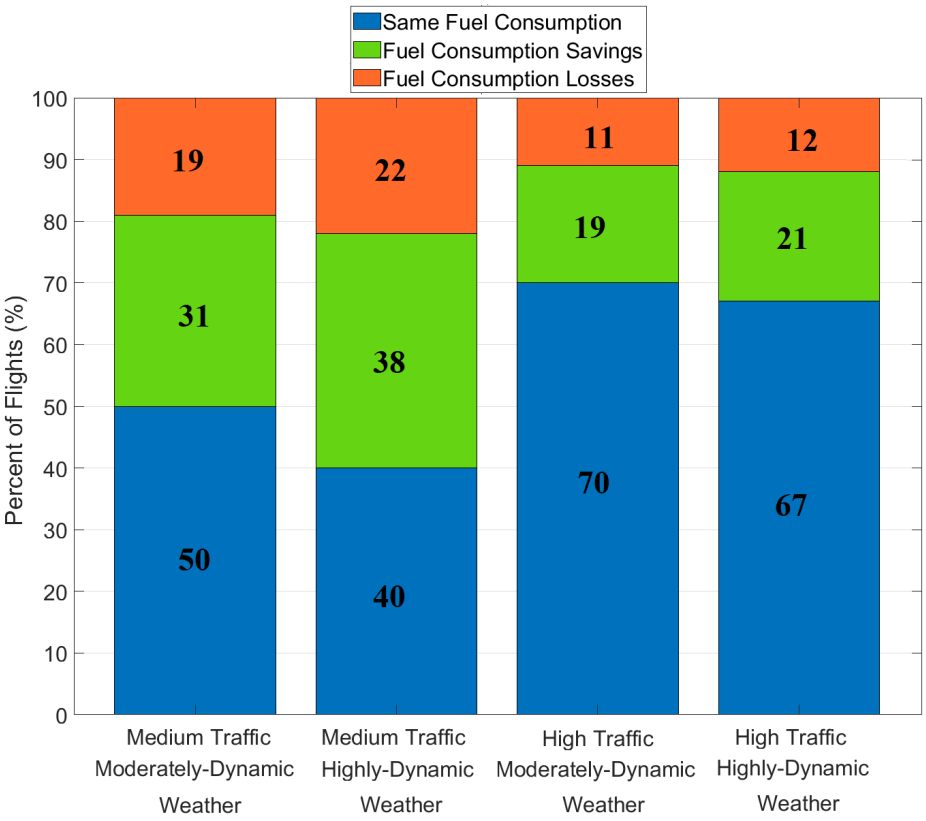

Figure 2.37: Distribution of fuel consumption benefits.

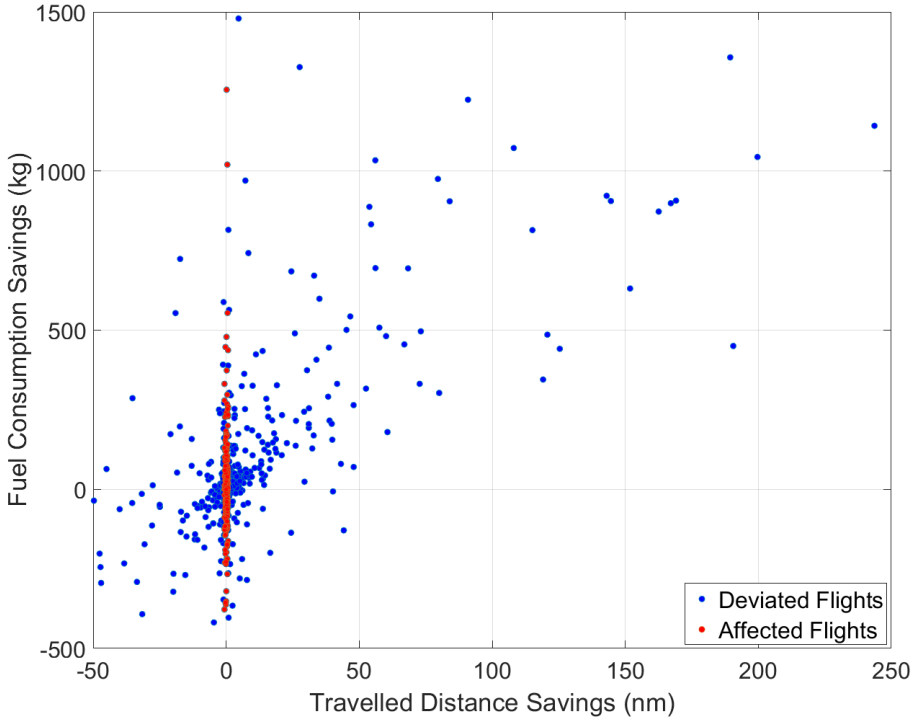

Figure 2.38: Distribution of fuel consumption savings and travel distance savings.

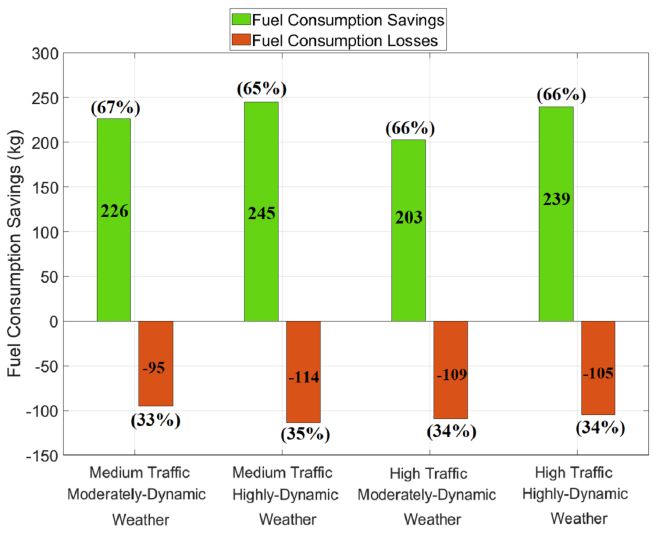

(a) Fuel consumption benefits.

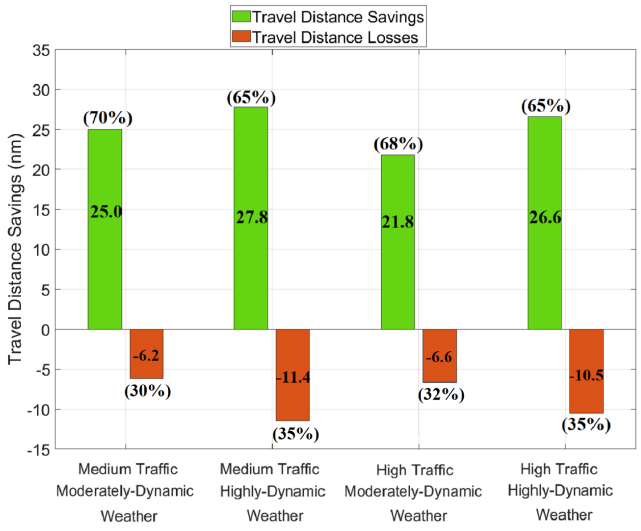

(b) Travel distance benefits.

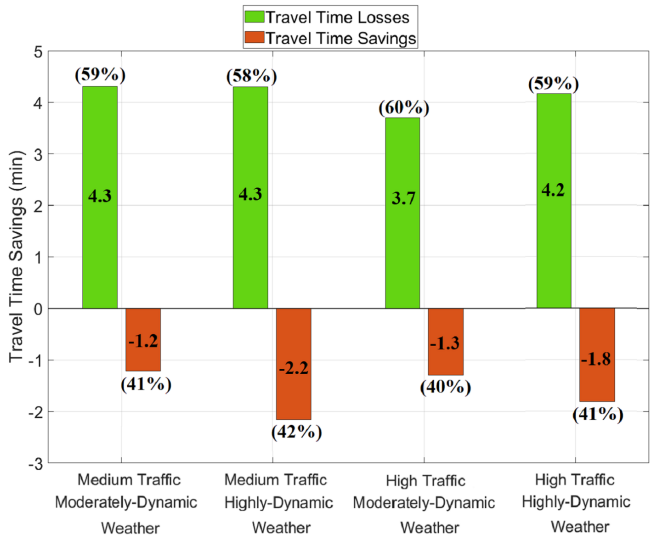

(c) Travel time benefits.

Figure 2.39: Average fuel consumption, travel distance, and travel time savings.

Table 2.8 summarizes the operational benefits for deviated flights and affected flights, and Table 2.9 summarizes the operational benefits of deviated flights. Table 2.10 indicates the deviation maneuver statistics in all the scenarios. Figure 2.40 shows the number of flights with at least one deviation and the number of total deviation maneuvers due to traffic and weather. The results show that the ROMIO-enabled scenario with 30-minute look-ahead horizon has the minimum deviation maneuvers per flight. Figure 2.41 illustrates the spatial distribution of deviation maneuvers in the onboard radar and the ROMIO-enabled (30-minute look-ahead horizon) scenarios.

Table 2.8: Summary of operational benefits for deviated and affected flights.

Scenario Set	Average Fuel Consumption Saving (kg)	Average Travel Distance Saving (nm)	Average Travel Time Savings (min)	Average Greenhouse Gas Emission Saving (kg)
Medium Traffic, Moderately-Dynamic Weather	86	9.1	1.5	271
Medium Traffic, Highly-Dynamic Weather	84	7.6	1.0	264
High Traffic, Moderately-Dynamic Weather	88	8.3	1.4	277
High Traffic, Highly-Dynamic Weather	91	6.9	1.0	289
Average	**87**	**8.0**	**1.2**	**275**

Table 2.9: Summary of operational benefits for deviated flights.

Scenario Set	Average Fuel Consumption Saving (kg)	Average Travel Distance Saving (nm)	Average Travel Time Savings (min)	Average Greenhouse Gas Emission Saving (kg)
Medium Traffic, Moderately-Dynamic Weather	120	13.6	1.7	379
Medium Traffic, Highly-Dynamic Weather	119	12.7	1.7	377
High Traffic, Moderately-Dynamic Weather	97	14.1	1.6	306
High Traffic, Highly-Dynamic Weather	122	15.7	2.0	386
Average	**115**	**14.0**	**1.8**	**363**

Economists estimate the "Social Cost of Carbon" (SCC) to study the impact of greenhouse gas emissions in cost-benefit analyses. The SSC is a measure of the economic impact of emitting one ton of carbon dioxide into the atmosphere. Howard, et al, (2015) estimated that the median value of the social cost of carbon is over $50 per ton [22]. The fuel consumption and carbon dioxide savings are annualized and monetized using the Official Airline Guide (OAG) data. The OAG data (2016) analysis shows that three participating airlines (i.e. DAL, UAL, AAL) have 588,582 operations annually in the simulation region. The annual fuel consumption savings for the participating airlines could reach 15.3 million kilograms of fuel consumption and 8.97 million dollars, considering $1.82 per gallon as the average jet fuel price in 2019. The annual saving of carbon dioxide is 48.3 million kilograms, and the social cost of carbon could reach 2.4 million dollars.

Figures 2.41a–2.41b shows the spatial distribution of deviations maneuvers in the onboard radar Scenario and ROMIO-enabled Scenario. Table 2.11 provides the percent of deviation maneuvers to the flights flown in each FIR.

Table 2.10: Deviation maneuver statistics.

No.	Scenarios	Number of Flights with Deviations	Number of Total Deviation Maneuvers	Average Deviation Maneuvers Per Flight
1	20 min Look-Ahead Horizon	356	683	1.92
2	25 min Look-Ahead Horizon	349	575	1.65
3	30 min Look-Ahead Horizon	335	554	1.65
4	40 min Look-Ahead Horizon	351	587	1.67
5	60 min Look-Ahead Horizon	360	685	1.90

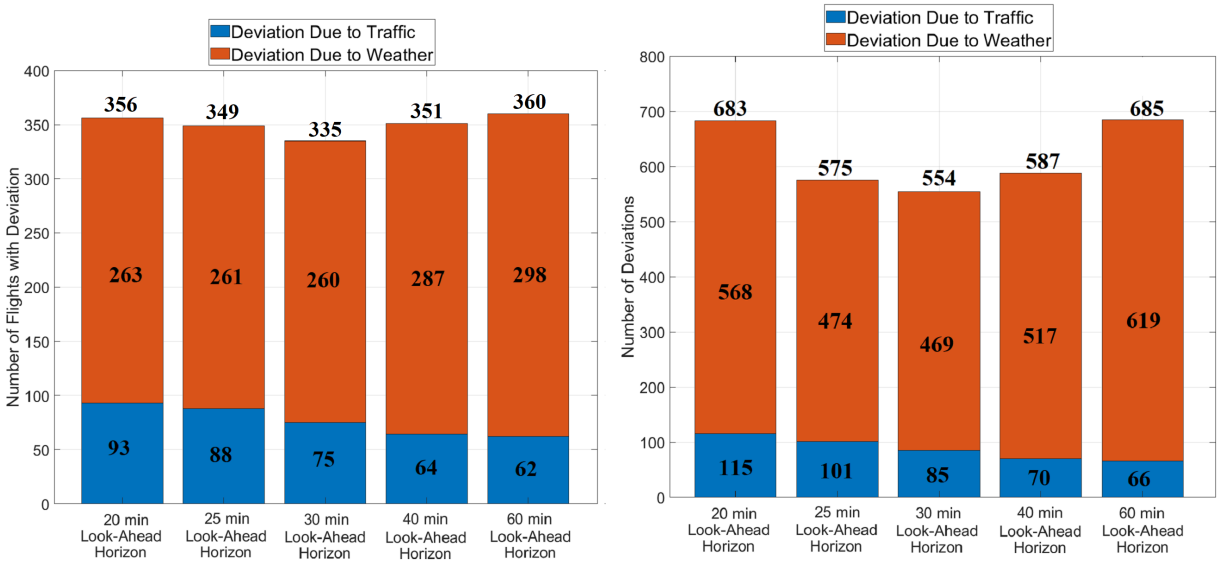

(a) Frequency of flights with deviations.

(b) Frequency of deviation maneuvers.

Figure 2.40: Deviation maneuvers due to traffic and weather.

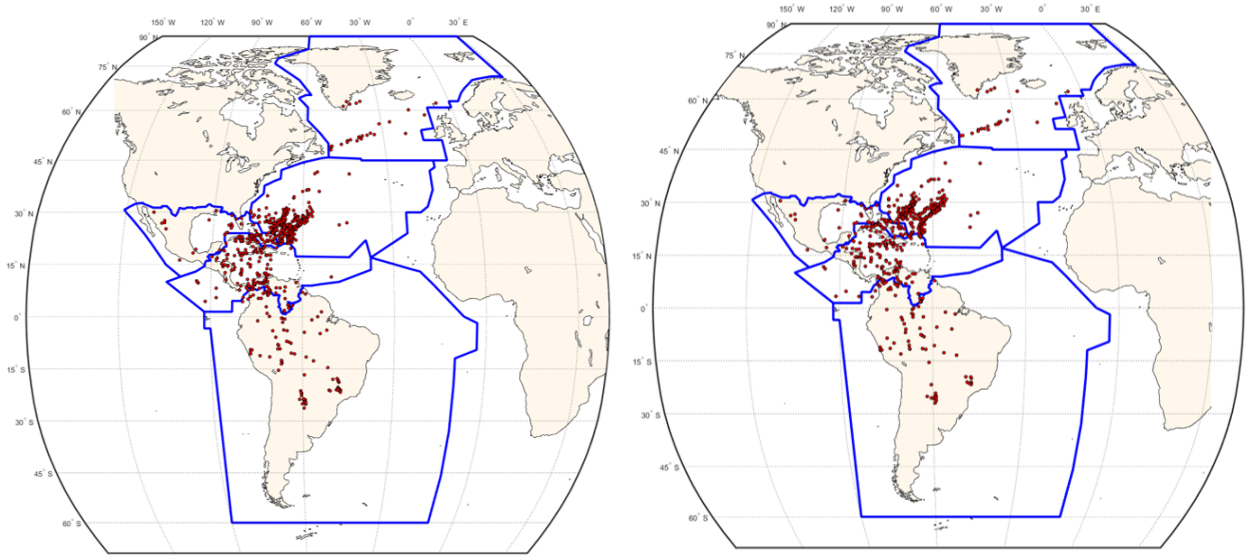

(a) 683 deviations in onboard radar scenario (20 min look-ahead horizon).

(b) 554 deviations in ROMIO-enabled scenario (30 min look-ahead horizon).

Figure 2.41: Spatial distribution of deviation maneuvers.

Table 2.11: Deviation maneuvers to the flights flown in FIRs.

FIRs	Number of Flights Flown	Deviation Maneuvers in 20 min Look-Ahead Horizon	Deviation Maneuvers in 30 min Look-Ahead Horizon	Percent of Deviation Maneuvers to Flights Flown in 20 min Look-Ahead Horizon	Percent of Deviation Maneuvers to Flights Flown in 30 min Look-Ahead Horizon	Reduction in Percent of Deviation Maneuvers to Flights Flown Comparing 20 min and 30 min Look-Ahead Horizon
SA	213	94	88	44.1%	41.3%	2.8%
NA1	793	334	252	42.1%	31.8%	10.3%
NA2	1062	28	26	2.6%	2.4%	0.2%
CA1	1208	52	46	4.3%	3.8%	0.5%
CA2	951	175	142	18.4%	14.9%	3.5%
Simulation Domain	**2258**	**683**	**554**	**30.2%**	**24.5%**	**5.7%**

Figure 2.42 shows the reduction in deviation maneuvers to flights flown in each FIR. The results show that the North Atlantic (NA1) region (i.e., New York East, New York West, and Santa Maria FIRs) has the highest reduction in deviation maneuvers to flights flown.

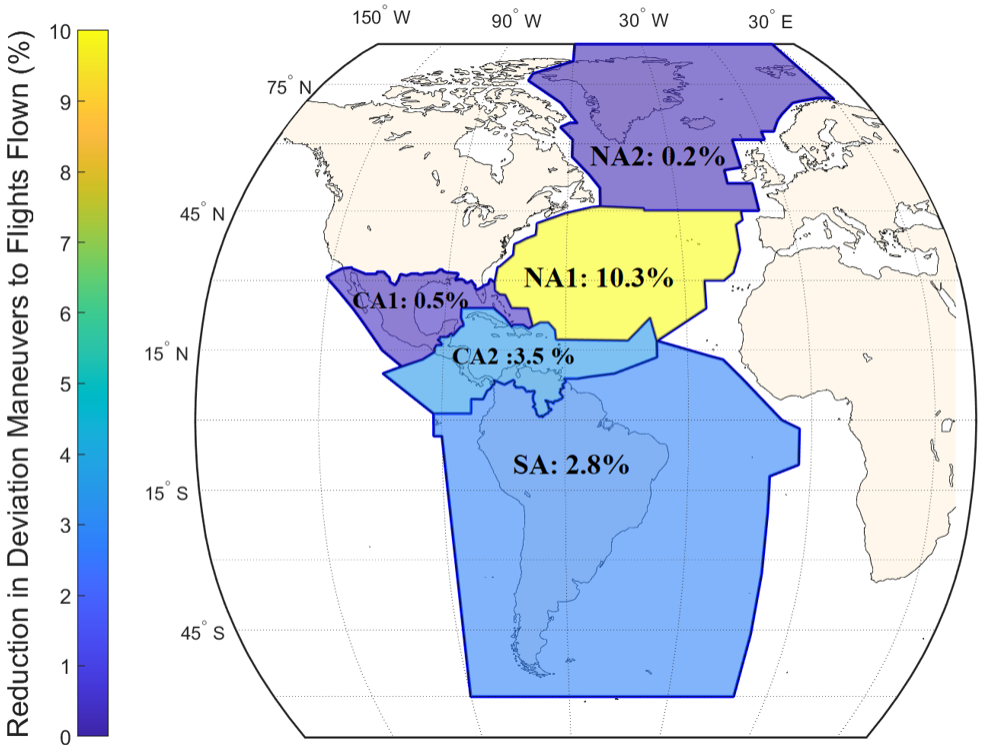

Figure 2.42: Reduction in deviation maneuvers to flights flown.

Simulating the flights with the GO Model allows us to consider the interactions between pilots and ATC using three routines in the model including a pilot routine, an ATC routine, and a system update routine. The pilot routine simulates the behaviors of pilots, and the ATC routine simulates the behaviors of air traffic controllers. We proposed two measures for evaluating the potential air

traffic controllers' workload using the simulation results derived from interactions between the ATC routine and pilot routine.

First, the number of tactical resolution maneuvers directly impacts the potential ATC workload, since the pilots and ATC need to communicate through the Controller-Pilot Data Link Communications (CPDLC) system for verifying resolution maneuvers. In other words, air traffic controllers need to send and receive several text-based messages before granting flight level changes, Mach Number changes, or detour maneuvers.

Second, oceanic air traffic controllers start evaluating different alternatives to resolve potential conflicts when the Advanced Technologies and Oceanic Procedures (ATOP) system detects potential separations violations in the projection of flight trajectories. It is assumed that oceanic air traffic controllers start monitoring flights when two aircraft are located within a percent above the separation minima. This monitoring threshold can vary regarding different FIRs and air traffic controllers' confidence. This assumption is consistent with the interviews done with real air traffic controllers [25].

To study the benefits of using the ROMIO demonstration on the number of events creating potential workload for ATC, we considered larger rectangular separation envelopes with a 50% increase above the minimum longitudinal and lateral separations (see Figure 2.43). Then, the number of events required close ATC monitoring in the onboard radar Scenario and the ROMIO-enabled Scenario are identified to investigate the impact of providing satellite-based meteorological information to flights in oceanic airspace. We analyzed each pair of simulated flight trajectories and check the CPA among them. If two aircraft are located in the larger rectangular separation envelope, it is considered as an event making potential workload for the air traffic controllers. Figure 2.44 demonstrates the number of monitoring events in each FIR for the onboard radar Scenario (20-minute look-ahead horizon) and the ROMIO-enabled Scenario (30-minute look-ahead horizon). Comparing the onboard radar and ROMIO-enabled scenarios show a 6% reduction in the number of events requiring close ATC monitoring.

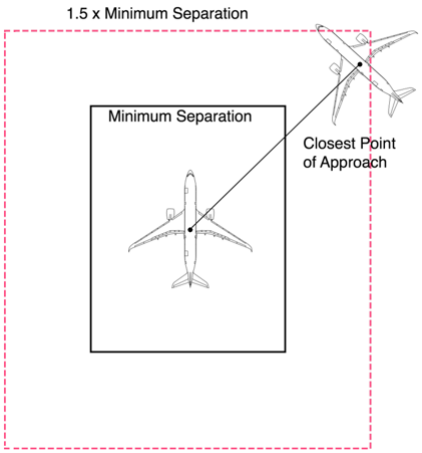

Figure 2.43: Separation envelope for detecting events requiring close ATC monitoring.

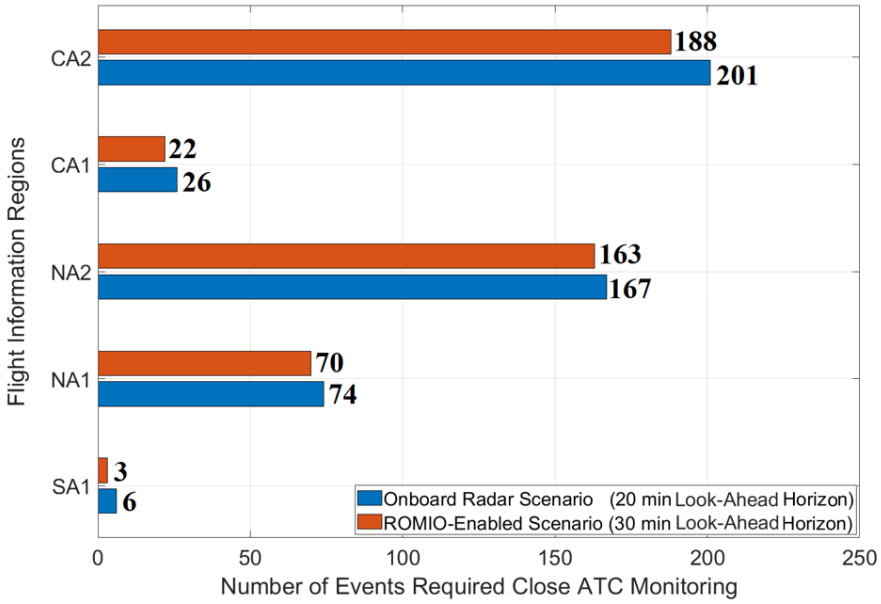

Figure 2.44: ATC monitoring events statistics.

Figure 2.45 shows the number of conflicts resolution maneuvers for the simulated flights in the middle day of simulation. Figure 2.46 shows the distribution of lateral deviation for the onboard radar Scenario (20-minute look-ahead horizon) and ROMIO-enabled Scenario (30-minute look-ahead horizon). The distributions of lateral deviations indicate two following points: 1) the flights in the ROMIO-enabled Scenario requested fewer deviation maneuvers for avoiding convective weather events, 2) the flights in the ROMIO-enabled Scenario requested more deviations related to maneuvers with large lateral deviations (i.e., 70 nm, 90 nm, 110 nm). The result depicts that these large

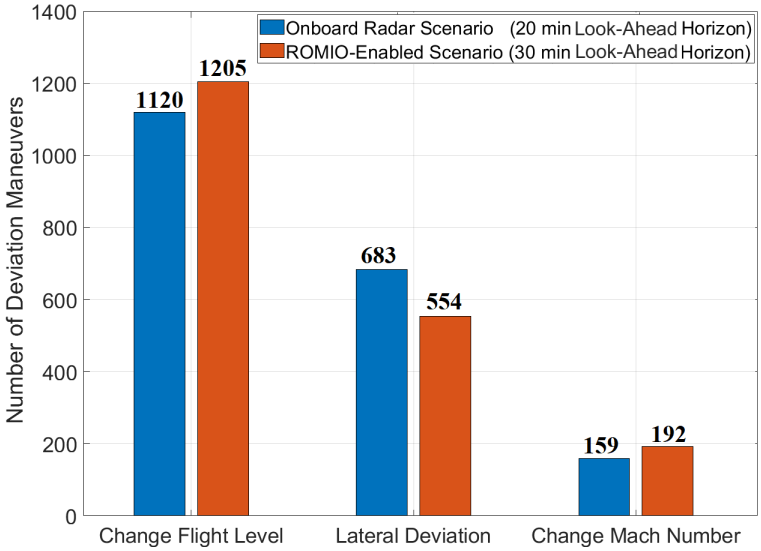

Figure 2.45: Resolution maneuvers statistics.

deviations are requested by flights exposing to the large convective areas and enhanced situational awareness derived from the ROMIO application enabled them to initiate more strategic deviations for convective weather avoidance.

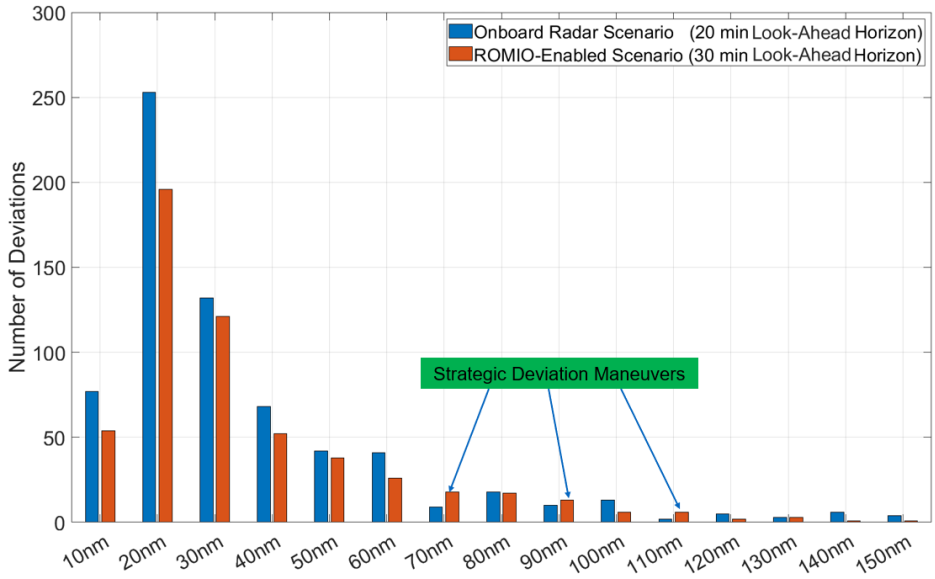

Figure 2.46: Distribution of lateral deviations.

Figure 2.47 shows the cumulative distribution functions of deviation angles for all the scenarios. Figure 2.48 shows the distribution of deviation angles in the form of boxplot graphs. The Analysis of Variance (ANOVA) test proves that the average deviation angle executed in the ROMIO-enabled scenarios is statistically lower compared to the onboard radar scenario (20 min look-ahead horizon).

This is attributed to the additional weather situational awareness provided by the ROMIO display.

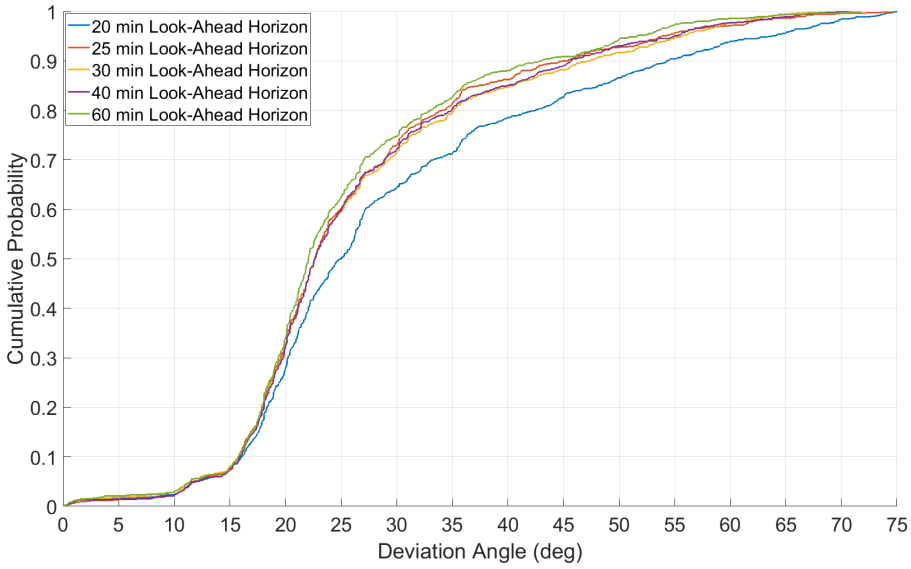

Figure 2.47: Cumulative distribution function of deviation angles.

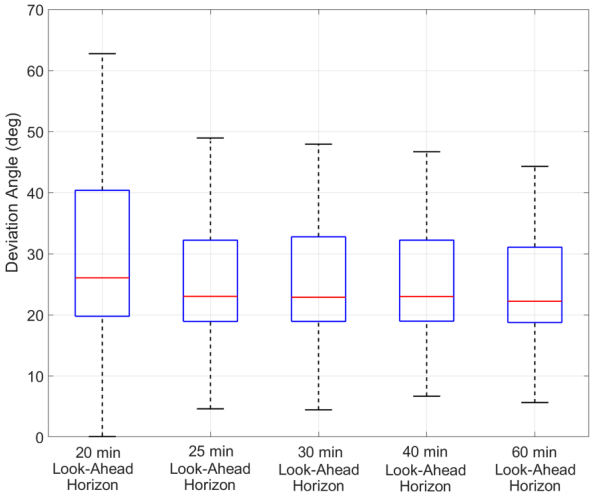

(a) Boxplot of deviation angles.

LSMeans Differences Tukey HSD

Connecting Letters Report

Level		Mean
'20 minutes Look_Ahead Horizon'	A	36.090715
'60 minutes Look_Ahead Horizon'	B	31.988215
'30 minutes Look_Ahead Horizon'	B	31.953911
'40 minutes Look_Ahead Horizon'	B	31.518964
'25 minutes Look_Ahead Horizon'	B	31.313753

Levels not connected by same letter are significantly different.

(b) Analysis of Variance (ANOVA) results.

Figure 2.48: Distribution of deviation angles (boxplot).

Figure 2.49 indicates the average travel distance in CDO contours for all the scenarios. The result shows that the ROMIO-enabled Scenario (30 min look-ahead horizon) had the minimum travel distance in CDO contours. Figure 2.50 shows the 95 percentile and 50 percentile (median) of travel distance inside CDO contours. The result shows that the distribution of travel distance inside CDO contours for simulated flights is consistent with the distribution of exposure to CDO contours for

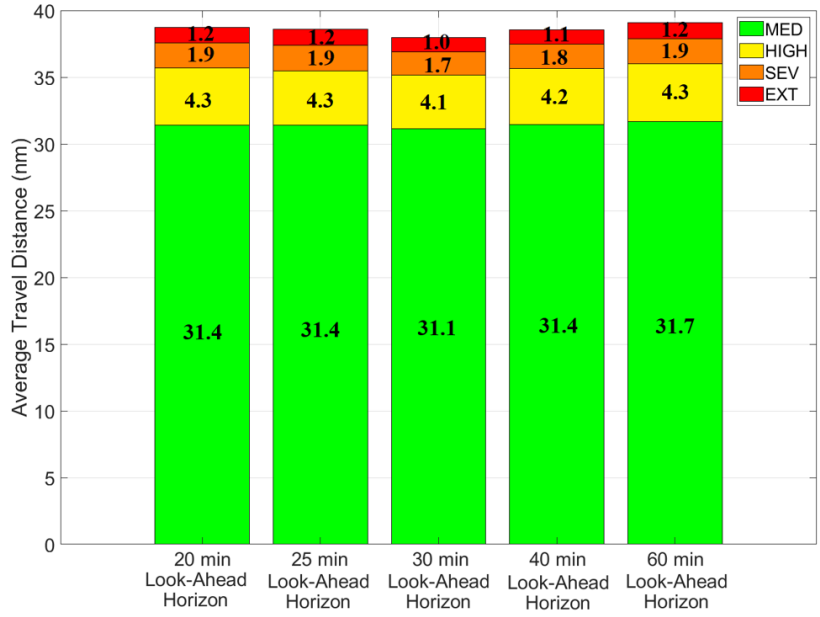

Figure 2.49: Average exposure to CDO contours.

the analyzed historical flights. It means that the GO Model replicates the distribution of allowable travel distance inside CDO contours derived from 18,326 historical flights which were programmed in the weather conflict detection mad resolution module.

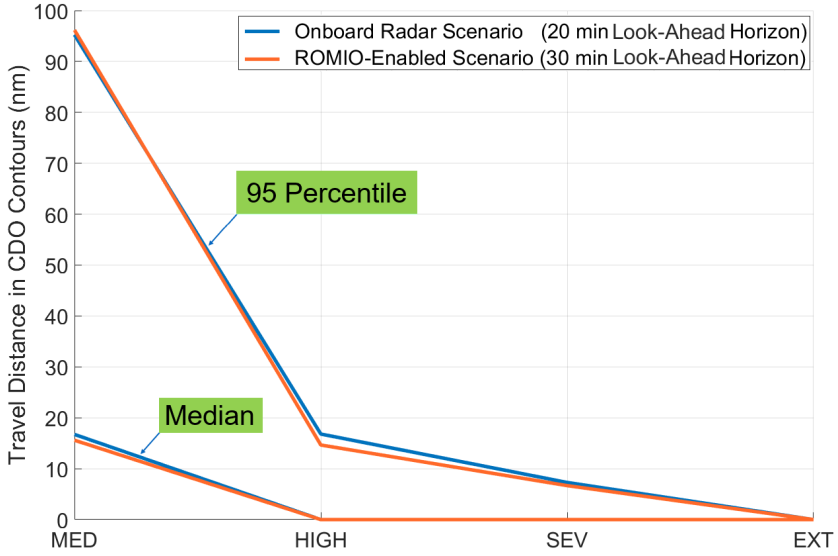

Figure 2.50: Distribution of travel distance inside CDO contours.

Figure 2.51 shows a simulated flight in scenarios with different look-ahead horizon ranges. This example indicates how the ROMIO demonstration contributes to decision making for convective weather avoidance by providing satellite-based meteorological information. Figure 2.51a shows

the CDO contours available to the pilot routine for convective weather avoidance in the onboard radar scenario (20-minute look-ahead horizon). Based on the weather information, the pilot routine considers the detours to the right side since the onboard radar detects the front edge of the extreme convective area on the left side. Figures 2.51b–2.51c–2.51d show the meteorological information in ROMIO-aided scenarios with enhanced look-ahead horizons enabled the flights to make better decisions (i.e., deviation to the left side) for avoiding the convection area.

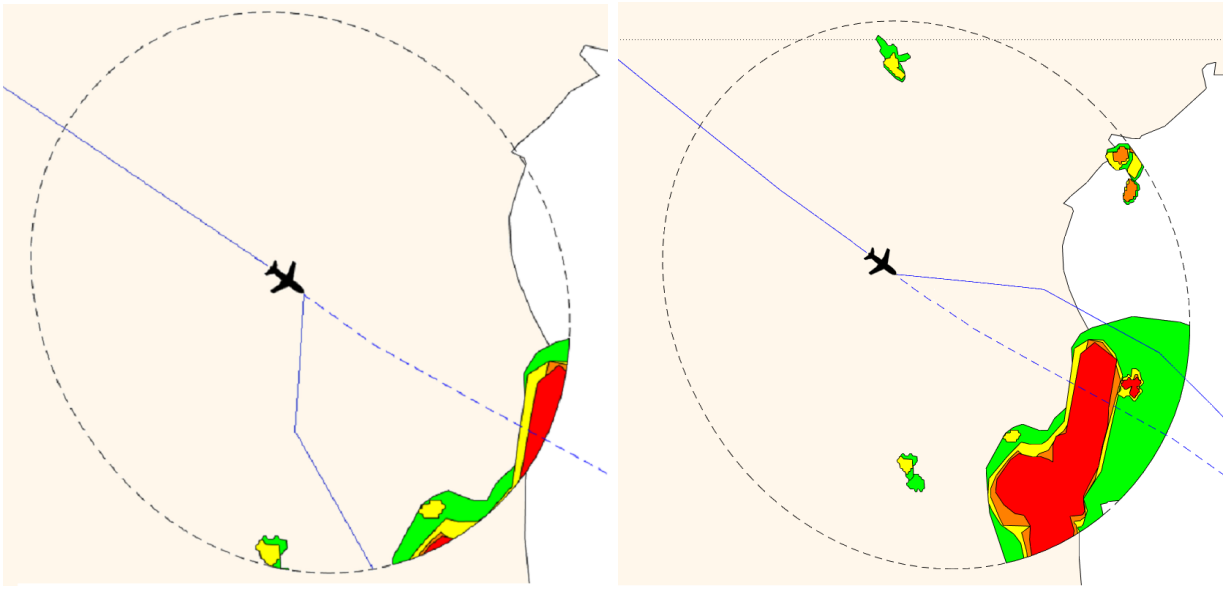

(a) Onboard radar scenario (20-minute look-ahead horizon).

(b) ROMIO-enabled scenario (30-minute look-ahead horizon).

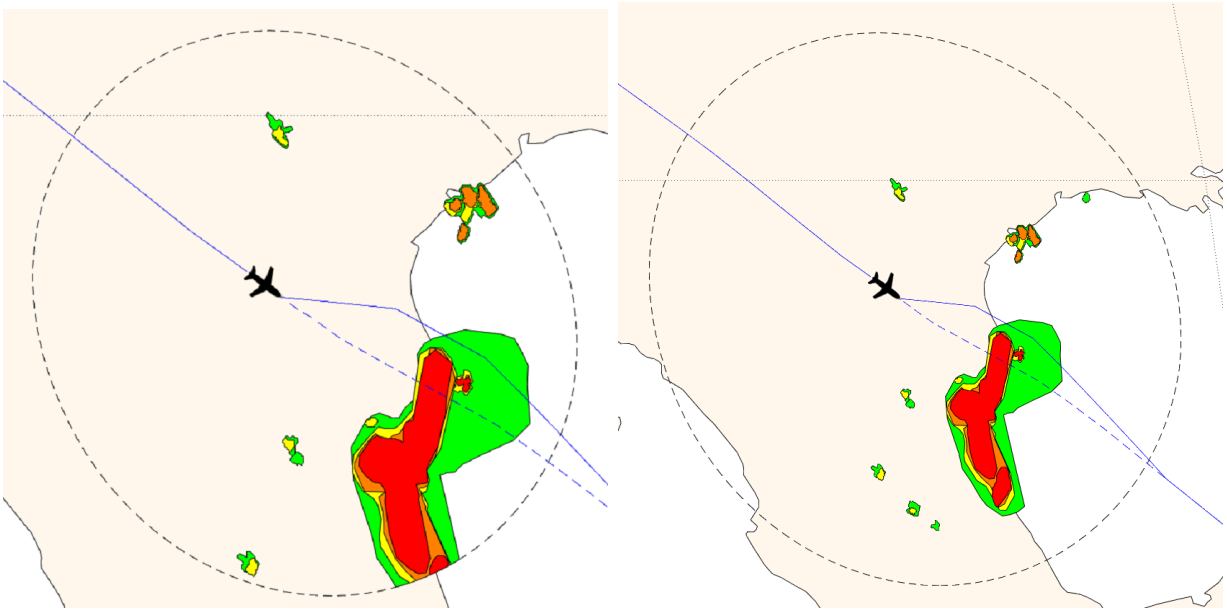

(c) ROMIO-enabled scenario (40-minute look-ahead horizon).

(d) ROMIO-enabled scenario (60-minute look-ahead horizon).

Figure 2.51: A sample flight with different weather information in the simulated scenarios.

2.5 Conclusions

Convective weather is a significant hazard to air transportation operations due to convective-induced turbulence that causes injuries to passengers and crew. Weather is uncertain and dynamic, requiring technologies to be updated quickly. Remote Oceanic Meteorology Information Operational (ROMIO) is a web-based application that provides near real-time weather information for rapidly changing weather to flight crews, dispatchers, and air traffic controllers. ROMIO aims to enhance user situational awareness of hazardous weather over oceanic regions where the coverage of ground-based and airborne weather radars are limited or lacking. ROMIO provides the information of two weather products: Cloud Top Height (CTH) and Convection Diagnosis Oceanic (CDO). CTH visualizes the cloud top structure by altitude and the CDO displays the location of convective weather events. This study quantified the operational benefits of the ROMIO demonstrations using two approaches: 1) statistical flight analysis, and 2) simulation-based analysis.

In the first approach, 18,326 historical flights crossing Inter-Tropical Convergence (ITCZ) among 30 bi-directional flights (60 flights) are studied. This study analyzed flight azimuth profiles to identify two types of weather deviation maneuvers for avoiding convective weather events: 1) deviation segments showing the macroscopic deviation maneuvers from the flight plan, and 2) deviation sections showing microscopic heading changes in flight trajectories.

The statistical analysis shows the benefits of ROMIO-aided strategic decision-making and having earlier deviation maneuvers for convective weather avoidance as follows: 161 kilograms of fuel consumption savings, 12.8 nautical miles of travel distance savings, 1.6 minutes of travel time savings, and 508 kilograms of greenhouse gas emission savings. This study targets the flights in the pilot survey which had employed the ROMIO application for weather deviations and compares the distributions of lateral deviations and deviation angles where the CPA is less than 20 nautical miles to convective weather events. The statistical t-tests with a 95% confidence level prove that 1) the deviation maneuvers in the Post-ROMIO period have lower deviation angles in comparison to the Pre-ROMIO period, 2) the average lateral deviation in the Post-ROMIO period is less than the Pre-ROMIO period.

In the second approach, Global Oceanic (GO) Model which is a fast-time simulation tool is employed to simulate real-scale traffic exposing convective weather in the oceanic airspace consistent with the ROMIO application coverage. The scenario cases consist of two traffic data sets (i.e, medium, high) and two convective weather data sets (i.e, moderately-dynamic, and highly-dynamic). The scenario representing the onboard radar with usable coverage is using 20-minute look-ahead horizon ($\sim$ 160 nautical miles) in detecting the convective weather contours. The ROMIO-enabled scenarios have additional ranges with 25, 30, 40, and 60 minutes look-ahead horizons.

The simulation results demonstrate that the ROMIO-enabled Scenario with 30-minute look-ahead horizon has the best operational benefits among ROMIO-enabled scenarios. Comparing the ROMIO-enabled Scenario with 30-minute look-ahead horizon and the onboard radar with 20-minute look-ahead horizon shows the following average benefits for deviated flights: 115 kilograms fuel consumption savings, 14.0 nautical miles travel distance savings, 1.8 minutes average travel time savings, and 363 kilograms greenhouse gas emissions savings. The fuel consumption savings are annualized and then monetized using the Official Airline Guide (OAG) data. The annual fuel consumption savings for three participating airlines (i.e., DAL, UAL, AAL) could reach 15.3 million kilograms of fuel consumption and 8.97 million dollars, considering \$1.82 per gallon as the average jet fuel price in 2019. The annual saving of carbon dioxide is 48.3 million kilograms, and the social cost of carbon could reach 2.4 million dollars.

This study shows that executing more strategic deviation maneuvers beyond onboard radar derived from ROMIO-enabled technology is the main reason for the potential benefits. First, the ROMIO-enabled scenario with 30-minute look-ahead horizon had the minimum number of deviated flights and the minimum number of total deviations due to weather. Besides, traffic-related deviations reduce with fewer weather-related deviations in the ROMIO-enabled scenarios. The distribution of lateral deviations and deviation angles shows that ROMIO-enabled scenarios had fewer deviation maneuvers with lower deviation angles. The analysis of variance (ANOVA) test proved that the average deviation angle executed in the ROMIO-enabled scenarios is statistically lower compared to the onboard radar scenario.

The GO Model results provide two measures for evaluating the potential air traffic controllers'

workload. First, the number of deviation maneuvers to the flights flown in each Flight Information Region (FIR). This measure directly affects the number of text-based communication messages between pilots and oceanic air traffic controllers for verifying deviation maneuvers. Comparing the onboard radar and the ROMIO-enabled scenarios indicate reductions in deviations maneuvers to the flown flights in all the FIRs. Second, the simulation results provide insight into the number of events requiring close ATC monitoring when aircraft pairs are located within 50% above the separation minima. Comparing the onboard radar and ROMIO-enabled scenarios show a 6% reduction in the number of events requiring close ATC monitoring. The distribution of travel distances inside convective weather contours for simulated flights shows the GO Model replicates the similar distribution of exposure to convective areas observed in the historical flight analysis. Note that the ROMIO application is a now-casting weather application demonstrating near real-time weather information, not forecasted weather. The reason for lower efficiencies in ROMIO-enabled scenarios with 40 minutes and 60 minutes of look-ahead horizons stem from making decisions based on uncertain weather information. Our recommendation for improving the ROMIO application is adding the forecast capability enabling the flight to take advantage of more strategic decision-making for convective weather avoidance.

Acknowledgments

Special Thanks to Eldridge Frazier (FAA, ANG-C61), Matthias Steiner (NCAR), and Cathy Kessinger (NCAR) for their technical and financial support of this project. This project was executed as part of a contract between Virginia Tech and the Federal Aviation Administration Administration Weather Technology in the Cockpit program. Also, this work has been supported in parts by the Najeeb E. Halaby Graduate Student Fellowship[1]. The authors would like to thank pilots who provided survey feedback in the project. Any opinions, findings, and conclusions presented herein are those of the authors and do not necessarily reflect the views of the FAA.

[1] https://ral.ucar.edu/opportunity/halaby-fellowship

Chapter 3

Collaborative Decision Making in Oceanic Air Traffic Flow Management

3.1 Introduction

"Air Traffic Management (ATM)" represents all services and procedures supporting safe and efficient flight operations. The two main components of ATM are 1) Air Traffic Control (ATC), and 2) Air Traffic Flow Management (ATFM). ATC refers to processes providing real-time and tactical separation procedures for conflict detection and avoidance. Air traffic controllers perform ATC by monitoring and controlling local aircraft movements over airspace sectors. Their goal is to maintain separations (i.e., vertical, lateral, and longitudinal) between aircraft and conveying traffic to the next sector properly. Each sector can be occupied by a limited number of aircraft, and air traffic controllers' ability and complexity of traffic patterns define this limitation. ATC procedures have more tactical nature and address immediate safety concerns of airborne flights.

On the other hand, ATFM refers to more strategic processes. The objective of ATFM is to match the capacity of air transportation systems with the traffic demand ensuring flights can flow through the airspace safely and efficiently. In the long term, this implies efforts to prevent demand-capacity imbalances by reducing demand or increasing capacity. In the short term, ATFM aims to avoid congestion and delays. When delays must be imposed, the goal is to reduce their impact on airspace users as much as possible. The Federal Aviation Administration (FAA) implemented a systematic form of flow management known as the Ground Delay Program (GDP). With GDP, aircraft departures are restricted until sufficient airspace or airport capacity is available for each aircraft.

The primary challenge for ATFM arises when the system is disrupted. Fluctuating weather conditions, demand surges, and equipment outages cause significant demand-capacity imbalances. Since these disruptions are highly unpredictable, ATFM needs to resolve the resulting structural imbalances dynamically. Establishing appropriate constraints for the impacted airspace can address safety concerns temporarily. For example, ATFM adjusts minimum separation standards and limit the number of operations at an airport to ensure that flights can move safely through the system. ATFM tends to provide equity of access to system resources such as airports. Basic strategies, such as "first come, first served" and "first ready, first served" have long been used in resource assignment. However, the increasing complexity of traffic flow management has shown the limitations of these concepts. These policies can create systematic biases and fail to provide incentives for airspace users [54].

3.2 Collaborative Decision Making

Collaborative Decision Making (CDM) is a process and culture that engages stakeholders to deliver the right information to the right people at the right time to achieve efficient solutions (Metron Aviation, 2018). Under CDM, the management of traffic flows and the resource allocation decisions are conducted in a way that gives significant decision-making responsibilities to airspace users. The overall objectives of CDM can be summarized as follows:

1. Generate better information, by merging flight data from the airspace system.
2. Create better situational awareness, by distributing the same information to traffic flow managers and airspace users.
3. Create better procedures, by allowing traffic flow managers to collaborate with airspace users.

Flow management in the National Airspace System (NAS) is performed by a distributed system in which decision-making responsibilities are shared by various stakeholders. The stakeholders in the NAS are air traffic service providers and airspace users. In the United States, the FAA is the air traffic services provider, and the primary users are airlines; other users are general aviation and

the military. On the FAA's side, operational processes are distributed among three organizational levels. Air Traffic Control System Command Center (ATCSCC) is the first level that supervises traffic flows and monitors the demands and capacity limits. It is the responsibility of ATCSCC to initiate major flow management actions, such as GDPs and rerouting flights around adverse weather.

Air Route Traffic Control Centers (ARTCC), Terminal Radar Approach Control Facilities (TRACONs), and towers form the second organizational level. The entities at this level are responsible for coordinating air traffic in their assigned airspace sectors. Air traffic controllers are the third organizational level. The primary interaction at this level is between controllers at neighboring sectors to send flights properly to the next sectors.

On the airlines' side, daily operations are coordinated at Airline Operational Control centers (AOCs). To monitor and control the flights, there is steady communication among AOCs and pilots. Also, operational planning tasks such as gate assignments are performed in coordination with stations. Figure 3.1 shows the interaction between the FAA and airlines during daily air traffic flow operations which can be categorized into strategic and tactical levels [55].

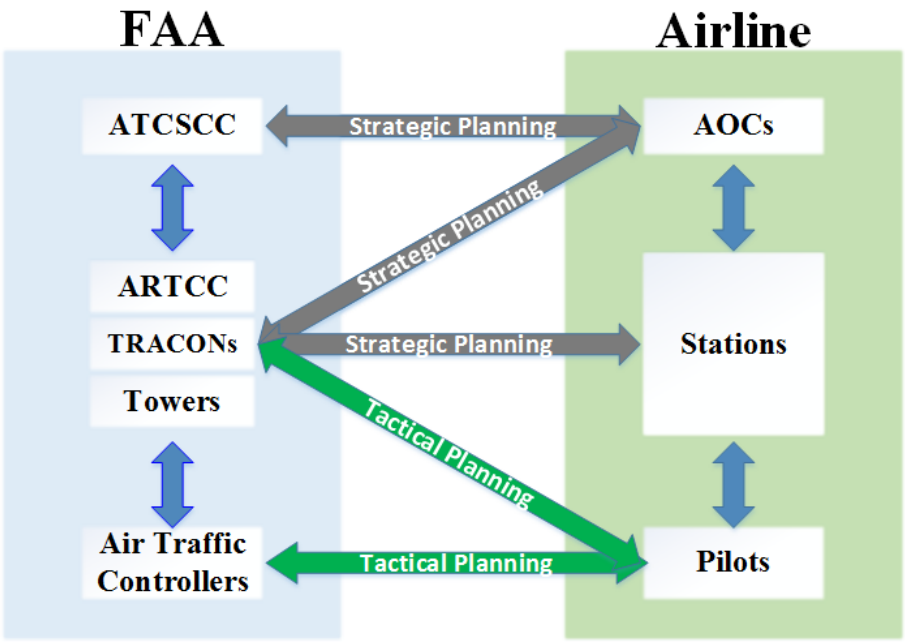

Figure 3.1: Operational interactions between the FAA and airlines.

Air transportation is different from most other modes of transportation in one important aspect: vehicles cannot be stopped en-route. Thus, air transportation systems should hinder developing air traffic jams. As a result, traffic managers implement various Traffic Management Initiatives (TMIs) to restrict demand before congestion occurs. Each TMI can be viewed as a combination of the following control techniques:

- Ground holding controls, which result in delays to flights before their departure. These take the form of GDPs that control flights departing a specific region in a specific period.
- Airborne holding controls, which result in delays to flight after their departure. Airborne delays can be applied using a variety of methods: 1) controlling the separation between successive aircraft traveling in the same direction, 2) speed control aims to ensure safe and efficient flows of aircraft by selectively increasing or decreasing their Mach number, 3) vectoring which corresponds to minor lateral deviations from flight plans.

Currently, CDM procedures for ground delay programs are in operation at all the airports in the United States. CDM is extending to other areas of air traffic management, such as rerouting of aircraft around overloaded airspace sectors. In this research, airborne holding controls and its methods are studied for oceanic flights.

3.3 Literature Review

The problem of adjusting air traffic flows in real-time to balance demand with capacity has been discussed in the literature. Operations Research techniques have been widely used to develop models that can optimize ATFM decisions. Several analytical models have been developed for the air traffic flow management problem at different scales considering various types of resources and control mechanisms.

At the strategic level, ATFM is concerned about managing flights destined for a capacity-constrained airport or planned to fly over capacity-constrained airspace. The Single Airport Ground Holding Problem (SAGHP) introduced a ground holding control mechanism to manage flows to airports with

reduced capacity. The motivation is that delaying aircraft on the ground before departure instead of imposing airborne delays is a better solution regarding costs and safety. The first formulations of the problem were deterministic and static, and capacity was assumed to be known with certainty, and decisions were made once for the entire planning horizon. Richetta and Odoni (1993) and Ball et al. (2003) proposed the stochastic-static models which recognize the uncertainty in airport capacity profiles during the optimization process.

CDM was conceived in the mid-1990s within the FAA airline data exchange project. Originally, this project was created as a short-term experiment to see if updated airline schedules would result in improved flow management decisions [56]. The results of human-in-the-loop experiments led to the initial implementation of CDM. These procedures focused on the development of new decision support tools for implementing and managing ground delay programs, which are used to delay flights experiencing inclement weather conditions. The main idea behind a GDP is to delay these flights before their departure to increase safety and reduce costs.

In GDPs under CDM, airlines send operational schedules to the air traffic control centers continually. The schedule information includes flight delay information, cancellations, and newly created flights. The ATCSCC uses this information to monitor and implement GDPs, using a decision support tool called Flight Schedule Monitor (FSM). Note that this information is shared with all users (e.g., airlines) creating a comprehensive picture of current and projected airport conditions. Other initiatives have aimed to increase airline control over scheduling decisions, within the slot credit substitutions effort [6].

There are numerous studies focused on improving the efficiency of performance in the oceanic airspace including reducing fuel consumption, delays, air traffic controllers' workload, and increasing level of services. The articles studied for this literature review are categorized into two main approaches in their methodology for performance improvement including "discrete-time simulation model" and "mathematical optimization model".

Discrete-Time Simulation Model (North Atlantic Region)

Gunnam, et al. (2014) developed a simulation model called North Atlantic Simulation and Modeling (NATSAM) to analyze the impacts of different Organized Track System (OTS) operational policies in terms of potential fuel savings and level of service improvements. The scenarios tested in this study include reduced lateral and longitudinal separations with the application of the data link mandate. The simulation model creates a cost matrix for each flight by estimating the fuel consumption related to all combinations of OTS tracks and flight levels [20].

Campos, et al. (2013) examined the economic costs for U.S. commercial airlines to equip their aircraft with Future Air Navigation System (FANS 1/A) Data Link Mandate (DLM) in the North Atlantic (NAT) region. The primary motivation behind the DLM was to increase operational safety by increasing the quality of communications, navigation, and surveillance of operators in the NAT. The analysis showed that avionics procurement and installation have high costs for airlines. However, the DLM enables new concepts of operations like reduced separation minima, which are expected to increase the operational efficiency in the NAT oceanic airspace [11].

Chung and Post (2008) developed a North Atlantic Simulation Model (NATSIM), which forecasts future demand and provides long-term operational and financial estimates [15]. NATSIM was a macroscopic model, and it offers relatively fewer details about the microscopic movements of the traffic in the OTS. The scope of the NATSIM includes commercial flights between countries in North America (Canada, United States) and Europe. Besides, NATSIM provides estimations for flight characteristics (e.g., flight distance, block time, and fuel burn) and economic and financial changes.

Chartrand, et al. (2009) tried to assess the benefits of Automatic Dependent Surveillance-Broadcast (ADS-B) and In-Trail Procedure in OTS. This study was performed using the Traffic Manager as the simulation tool and nine days of actual air traffic data collected by the Shanwick Oceanic Center. The results demonstrated improvements in terms of fuel savings and operational parameters like request approval rates when new policies are applied. The main variable used for the assessment of the results was the fuel burned during the entire flight divided by the total travel time [12].

Williams, et al. (2005) focused on the benefits provided by two low complexity Airborne Separation Assurance Systems (ASAS) applications in the North Atlantic Organized Track. First, Climb Advisory Request Assistance Tool (CARAT) provides pilots with increased awareness of the surrounding traffic and facilitates more informed flight level change requests and more frequent step-climbs. Second, ASAS In–Trail Climb (ITC) is a proposed procedure that allows an aircraft to pass another aircraft at an intermediate flight level using an alternate longitudinal separation standard of 10 nautical miles. Benefits from implementing CARAT and ASAS ITC procedures in NAT OTS were examined comparing to a baseline scenario with the longitudinal separations standards of 80 nautical miles [60].

Williams and Greenfeld (2006) developed a discrete event simulation model that estimates the potential benefits from reduced horizontal and lateral separation in the OTS. The authors evaluated three demand sets for 2005, 2010, and 2015 generated using 2004 actual NAT traffic data. For each demand set, they applied five equipage levels, and they assessed the OTS performance regarding fuel and flight time savings, potential cargo revenues, and improvements in system efficiency. The results of this study show potential fuel and time savings per flight that is proportional to the equipage level of all OTS flights [58].

Gerhardt-Falk, et al. (2000) developed a Flight Tracking Model (FTM) to determine the potential fuel savings of proposed changes to NAT airspace separation standards due to future system improvements. The FTM is designed to model the NAT air system and is written in a discrete-time simulation language called SIMSCRIPT II.5. In the FTM, the aircraft is moved from node to node. Before the aircraft moves to the next node on its path, path clearance is checked to determine whether the path from the current node to the next node conflicts with the paths of other aircraft. If the path is clear, the aircraft moves to the next node, and the arrival time is estimated. The processing of the aircraft is suspended until the system reaches its arrival time which moves an aircraft from its current waypoint to the next one, and calculates travel time and fuel consumption [18].

Discrete-Time Simulation Model (South Pacific Region)

Livingston, et al. (1984) developed a computer simulation model for the North Pacific track system to examine the safety impacts of a new separation rule in North Pacific (NOPAC) routes [34]. This is a discrete-time model providing a comparative analysis of the total system fuel consumption, step-climb advantage, and route occupancy due to congestion influences. As a disadvantage, this model is developed only for air traffic over the Pacific airspace.

Williams, et al. (2005) studied the operational benefits of In-trail Climb (ITC) in the South Pacific Oceanic airspace (SOPAC). ITC is a proposed procedure that allows an aircraft to pass a cruising flight at an intermediate flight level with required longitudinal separations. Operational benefits were investigated on one month of actual traffic data by aircraft model and market-pair [59].

Mathematical Optimization Model

Rodionova, et al. (2014) formulated an optimization mathematical model to assess the benefits of reduced separation in the North Atlantic OTS. This study focuses only on the part of the flight that is inside the OTS while it considers only eastbound traffic data collected by the Shanwick oceanic center. The model is even more constrained given that aircraft are allowed to change flight levels only at waypoints, and this change happens instantaneously. Also, a Genetic Algorithm has been implemented to improve aircraft routes and to reduce the congestion at the entry/exit of airspace. The results of this study showed that implementing new technologies will yield a positive effect on the traffic in North Atlantic oceanic airspace [43].

In another study, Rodionova, et al. (2014) introduced a mathematical model approach as "wind networking" for aircraft trajectory prediction in North Atlantic oceanic airspace. Aircraft in the NAT oceanic airspace are subjected to strong winds caused by the jet stream, and the uncertainty in wind forecast often results in large differences between the predicted and the actual cruising times. This approach permits the aircraft to receive the information about the observed winds from preceding aircraft on the same route and increase the precision in flight prediction [42].

3.4 Organized Track System (OTS)

The air traffic between Europe and North America forms two major relatively concentrated unidirectional flows over the North Atlantic. Passenger demand, time zone differences, and airport noise restrictions are the factors in creating traffic peaks for both eastbound and westbound traffic. Westbound traffic departing from Europe to North America in the morning and eastbound traffic departing from North America to Europe in the evening. The peak of the westbound traffic crosses the 30W longitude between 1130 UTC and 1900 UTC, and the peak of the eastbound traffic crosses the 30W longitude between 0100 UTC and 0800 UTC. Figure 3.2 depicts an example of eastbound and westbound OTS tracks configuration related to June 25, 2016 [33].

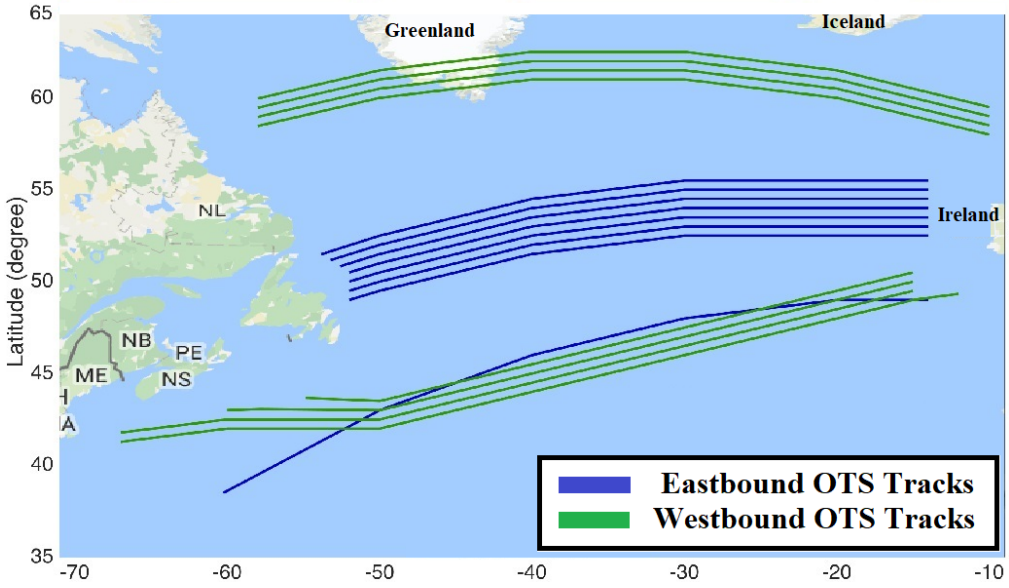

Figure 3.2: OTS tracks configuration (June 25, 2016).

To manage the traffic flows, two organized track systems are created daily to accommodate as many flights as possible. Meteorological conditions such as weather and wind patterns are the significant factors in designing the OTS tracks. The OTS tracks are designed such that eastbound flights could take advantage of the tailwind, and westbound flights could reduce their headwind. The GO Model has a flight plan optimization tool using the NCAR Reanalysis wind data to generate wind-optimal flight trajectories worldwide [50]. This module is used to create User-Preferred Routes (UPR) for flight plans. Note that utilizing the OTS tracks is not mandatory and aircraft can fly on UPR and

remain clear of the OTS tracks.

3.4.1 Modeling North Atlantic OTS Flights

The geographic scope of this analysis is the North Atlantic oceanic airspace shown in Figure 3.3. The NAT airspace includes eight FIRs managed by seven oceanic control centers including New York East and New York West (United States), Gander (Canada), Santa Maria (Portugal), Shanwick (United Kingdom - Ireland), Reykjavik (Iceland), Sondrestrom (Greenland) and Bodo (Norway).

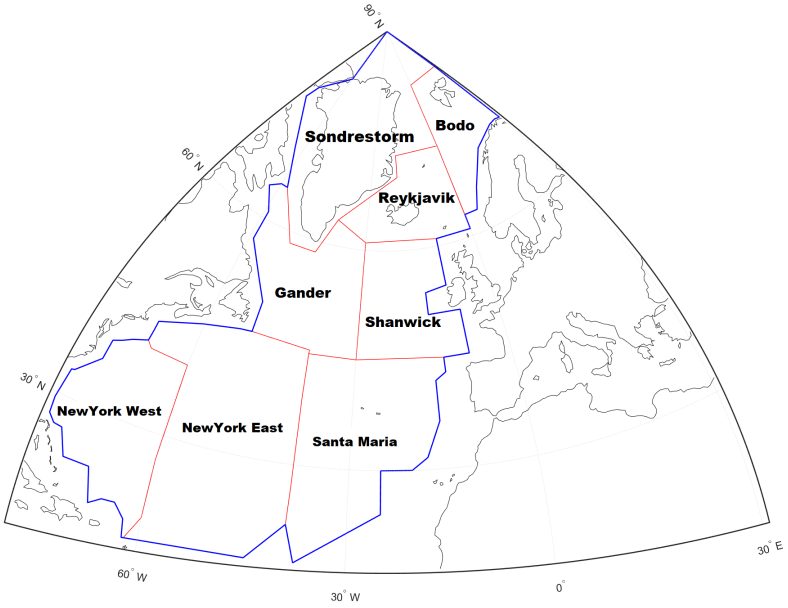

Figure 3.3: Simulation domain in the North Atlantic airspace.

Flights tending to use the OTS tracks should send their request to air traffic controllers at the last domestic point before the entry of oceanic airspace. Then, controllers assign the track and flight level to flights considering the standard longitudinal separations in the OTS and flight path clearance. If the requested assignment (i.e., track and flight level) is not conflict-free, air traffic controllers will consider other flight levels and other tracks until finding a conflict-free assignment. To maintain separations, flights inside the OTS are expected to follow their assigned tracks, flight levels, and Mach numbers. Any changes to the assignment should be reported by pilots and approved by air traffic controllers. The initial assignment of flights to OTS tracks is critical, and the potential violations in the separation standards can be defined based on the initial headway assignment.

Recently, advanced technologies such as FANS 1/A, Automatic dependent surveillance-Broadcast (ADS-B), and Controller-Pilot Data Link Communications (CPDLC) have significantly improved situational awareness and communication between pilots and controllers in remote oceanic areas. Based on the current standard of flight operations in OTS tracks, if both of the leading and following aircraft are equipped with satellite-based avionics, their longitudinal separation can be reduced to 5 minutes. Otherwise, if one or both of the leading and following aircraft are not equipped, their minimum longitudinal separation is 10 minutes [52] (see Figure 3.4).

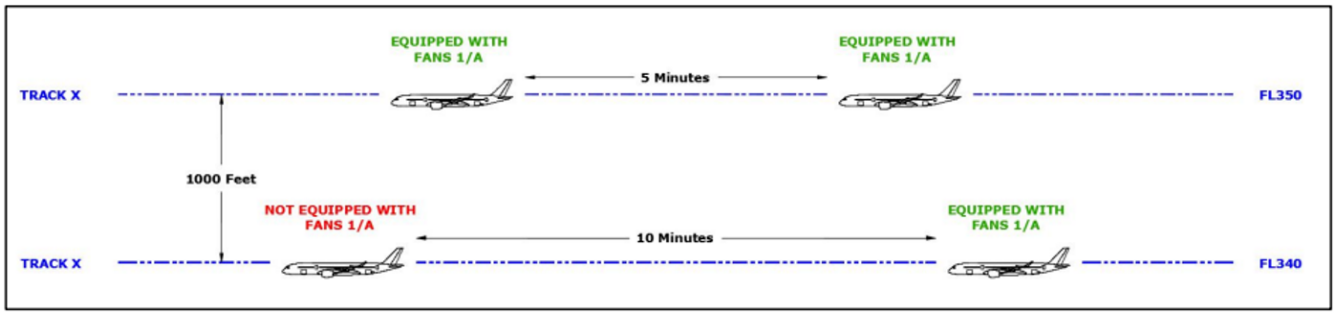

Figure 3.4: Longitudinal and vertical separations in OTS tracks.

Air traffic controllers consider speed differences between leading and following aircraft pairs to calculate the headway at the entry of OTS tracks. If the speeds of both leading and following aircraft are the same, their separation will not be changed along the track. However, there are two other cases that longitudinal separations change along the track due to the relative speed of flight pairs: 1) opening cases and 2) closing cases. In the opening case, the speed of a leading aircraft is higher than the following aircraft. To illustrate the point, consider the example shown in Figure 3.5. A Boeing 747-400 with Mach number 0.84 is faster than a Boeing 777-200 with Mach number 0.82. Flying across the North Atlantic in the same flight level and track, the longitudinal separation increases, and their gap will be greater.

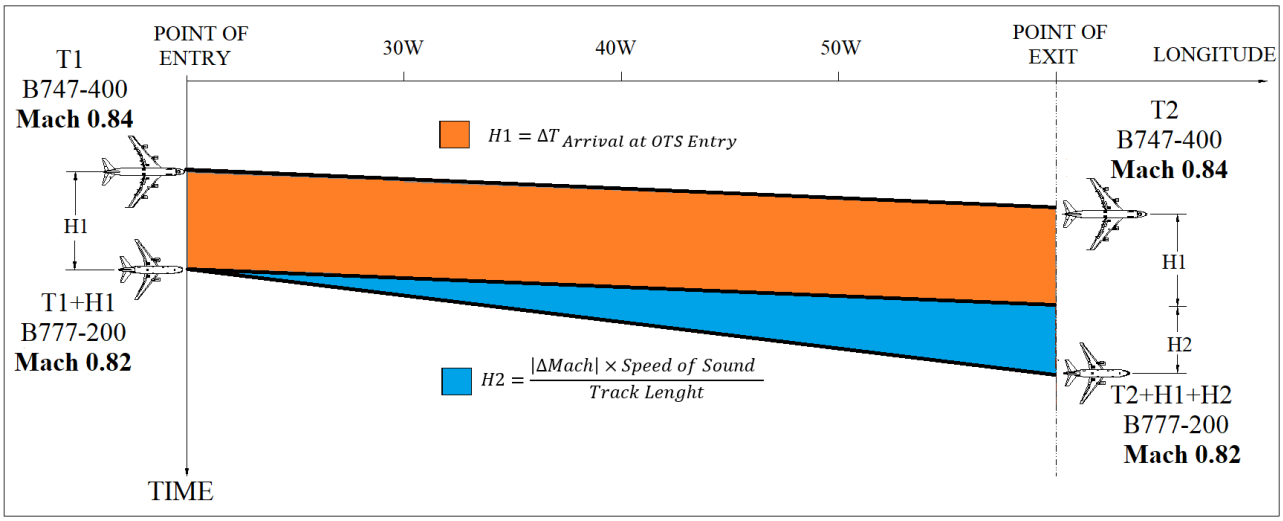

Figure 3.5: Headway rules (opening case).

On the contrary, as it is shown in Figure 3.6, if the following aircraft is faster than the leading flight, their longitudinal separation will be reduced and the gap between them will be shorter as they fly along the track.

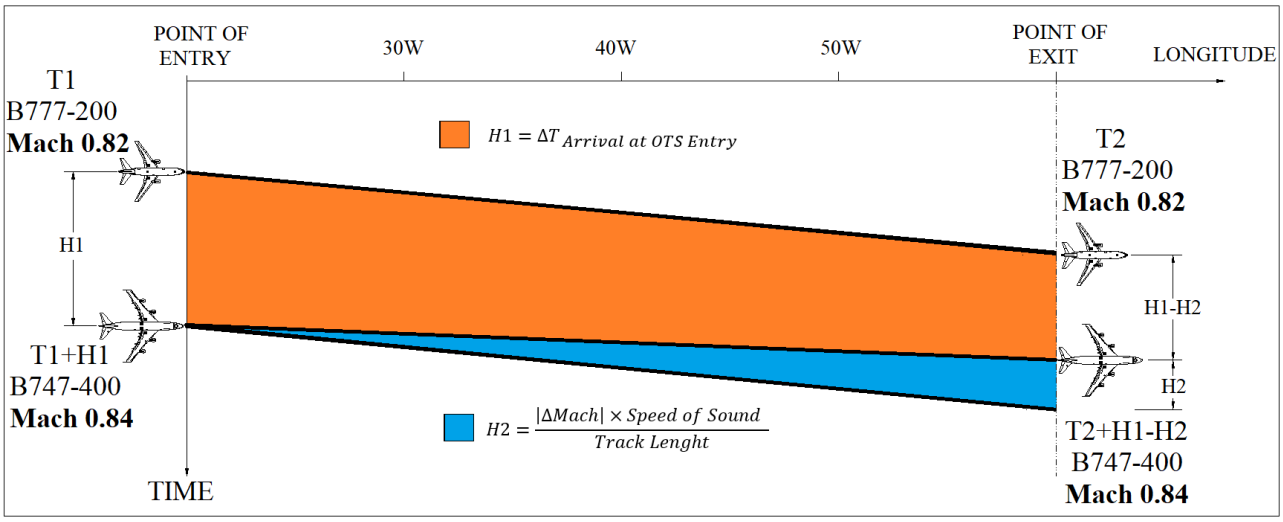

Figure 3.6: Headway rules (closing case).

Flight Cost Module

As it was mentioned, flights can cross the North Atlantic airspace by flying inside the OTS or on free routes. Airlines compare the cost of these two options and choose the one with the least travel cost. If airlines decide to use OTS tracks for some flights, they evaluate the cost of flying in all

alternatives (i.e., tracks and flight levels) and select the alternative with the least fuel consumption cost. Also, they select two additional track and flight level combinations to file in the flight plan as alternate preferences in case the ideal track and flight level is not available. The Global Oceanic model has a flight cost module that creates flight plans by calculating the cost matrix for flights and evaluating the track and fight level combinations.

This module has an OTS cost matrix generator which calculates the fuel consumption, travel distance, and travel time for all the OTS assignments and saves the results in a matrix. Figure 3.7 shows an example of a cost matrix for a flight between John F. Kennedy International Airport (KJFK) to London Heathrow Airport (EGLL) with a Boeing 777-300ER aircraft.

The red cells in the matrix labeled '77,777,777' indicate the flight is not capable of flying in the track and flight level because of track configuration. The yellow cells in the matrix labeled '999,999' are unfeasible track and flight levels due to aircraft performance restrictions at the entry point of the OTS. The greenest cell shows the least fuel consumption alternative. In this example, the ideal track and flight level is track X at 38,000 feet with 46,200 kilograms of expected fuel consumption.

Fuel Cost Matrix (kg)		Eastbound Tracks							
		NAT S	NAT T	NAT U	NAT V	NAT W	NAT X	NAT Y	NAT Z
Flight Level (feet)	40,000	999,999	999,999	999,999	999,999	77,777,777	999,999	999,999	999,999
	39,000	999,999	999,999	999,999	999,999	999,999	999,999	999,999	77,777,777
	38,000	46,836	46,603	46,445	46,331	46,229	46,200	46,232	999,999
	37,000	46,892	46,660	46,505	46,395	46,299	46,278	46,320	77,777,777
	36,000	47,151	46,918	46,766	46,660	46,571	46,560	46,617	77,777,777
	35,000	47,264	47,033	46,885	46,784	46,703	46,701	46,770	77,777,777
	34,000	47,694	47,462	47,316	47,218	77,777,777	47,154	47,238	52,461
	33,000	48,036	47,803	47,654	47,553	77,777,777	47,492	47,578	77,777,777
	32,000	48,748	48,507	48,350	48,241	77,777,777	48,182	48,269	53,794
	31,000	77,777,777	77,777,777	77,777,777	77,777,777	77,777,777	77,777,777	77,777,777	77,777,777

Figure 3.7: An example of a cost matrix.

Track Assignment Module

The GO Model has a track assignment module developed inside the flight simulator. Based on its logic, the decision for the OTS assignment is made 350 nautical miles (∼45 minutes) before the entry point of OTS tracks. The assignment process begins with calculating the maximum operational

altitude attainable by each flight. The ideal flight level may be higher than the maximum operational altitude at the decision point because the GO Model uses the average wind speed in calculating the cost matrix. During simulations, wind data is updated in every time step and this provides a more precise evaluation of the aircraft operational mass at the track entry point.

Note that the traffic in the OTS can be heavy during peak hour conditions. It means that there is no guarantee that all the oceanic flights can achieve their ideal track and flight level. Figure 3.8 illustrates the OTS assignment alternatives. When the requested (ideal) track and flight level is not available, air traffic controllers use three approaches to reassign the flights as following: 1) changing flight levels in the requested track, 2) switching to other OTS tracks, and 3) changing the flight Mach number for adjusting the arrival time and satisfying the required separation at the OTS entry point.

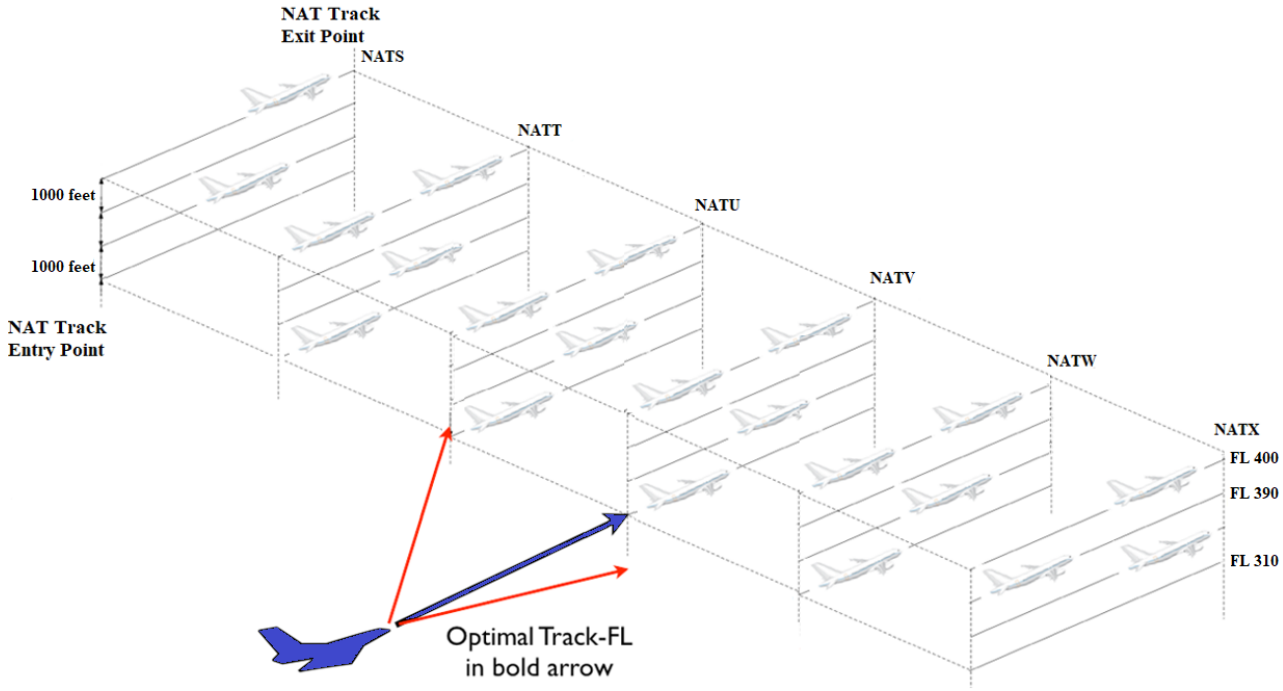

Figure 3.8: OTS assignment alternatives.

According to the current practice, oceanic air traffic controllers have a heuristics logic for reassigning a flight to OTS tracks and flight levels. Based on their logic, the first preference is checking alternatives in the requested OTS tracks and flight levels with climbing 1,000 feet or descending up to 3,000 feet of the requested flight level. If none of the alternatives satisfy the separation

requirements, they check assignment options in other tracks and flight levels until finding a conflict-free assignment. There is another logic for reassigning flight to the OTS track which is based on the flight cost matrix entirely. In this approach, all the OTS alternatives are ranked based on the lower additional fuel cost from the optimal assignment (see Figure 3.9).

Fuel Cost Matrix (kg)		Eastbound Tracks							
		NAT S	NAT T	NAT U	NAT V	NAT W	NAT X	NAT Y	NAT Z
Flight Level (feet)	40,000	999,999	999,999	999,999	999,999	77,777,777	999,999	999,999	999,999
	39,000	999,999	999,999	999,999	999,999	999,999	999,999	999,999	77,777,777
	38,000	636	403	246	131	29	0	32	999,999
	37,000	692	460	306	195	100	78	121	77,777,777
	36,000	951	718	567	460	371	361	418	77,777,777
	35,000	1,064	833	686	584	503	502	571	77,777,777
	34,000	1,494	1,262	1,116	1,018	77,777,777	954	1,038	6,261
	33,000	1,836	1,603	1,454	1,353	77,777,777	1,293	1,378	77,777,777
	32,000	2,549	2,308	2,151	2,042	77,777,777	1,982	2,070	7,594
	31,000	77,777,777	77,777,777	77,777,777	77,777,777	77,777,777	77,777,777	77,777,777	77,777,777

Figure 3.9: Additional fuel cost for non-optimal assignments.

3.5 Group Assignment Procedure

The current OTS assignment procedure used by oceanic air traffic controllers is similar to the greedy algorithm based on the ”First Come, First Serve” (FCFS) method. In the context of this problem, air traffic controllers follow an individual assignment algorithm based on ”first request, first assign”. This method is easy to implement since it does not require much effort for air traffic controllers to optimize the OTS assignment. In situations with low traffic, most of the flights can be assigned to their requested tracks, flight levels, and Mach number. However, the current procedure could not produce highly satisfactory assignments during congestion periods. According to historical data, Shanwick (United Kingdom) and Gander (Canada) flight information regions were not able to assign approximately 35% and 20% of flights to their requested track and flight level, respectively.

This study proposes a new procedure to improve the OTS assignment based on collaborative decision making philosophy. The main contribution of the proposed methodology is changing the current greedy algorithm (i.e., individual assignment) to a Group Assignment Procedure (GAP) using

optimization algorithms. The new procedure improves the OTS assignments by considering a group of flights that have sent their OTS requests within a certain distance before OTS entry.

In the GO Model, the flights send their requests for preferred OTS assignment 350 nautical miles before the OTS entry. Then, the OTS track assignment module receives the requests and performs the decision-making for each OTS flight assignment instantly using the heuristic method. In the group assignment procedure, the OTS track assignment module decides about the OTS flights in an entry zone area for a period of time (e.g, 20 minutes). The entry zone is a predetermined area prior to the OTS track entry where the decision-making occurs in the real-world.

In the group assignment procedure, the flights send OTS requests when they pierce the entry zone areas. The GO Model monitors the number of flights in the entry zone areas based on a user-defined time parameter (e.g., 5 minutes). When there are two or more flights inside the entry zone, the optimization algorithm performs the decision-making for assigning all the flights inside the group to OTS tracks and flight levels simultaneously. This procedure enables the OTS track assignment module to reevaluate the previous OTS assignments as long as the flights are inside the entry zone. At the exit point of the entry area, the module finalizes the OTS assignment decisions for each flight. The mathematical modeling for the group assignment procedure is presented in the next section.

3.6 Mathematical Modeling Formulation

Optimization models have various categories for formulating and solving decision-making problems (Figure 3.10). An optimization problem may be defined by the couple (S, F), where S represents the set of feasible solutions and the objective function to optimize ($F : S \rightarrow R$). The objective function measures the worth of every solution $s \in S$ of the search space with a real number [51].

Linear Programming (LP) is one of the most widely used methods for solving optimization problems. If the feasible region of a problem is a convex set and the objective function is a convex function, the global optimum solution is necessarily a point inside the feasible region. Many real-life applications

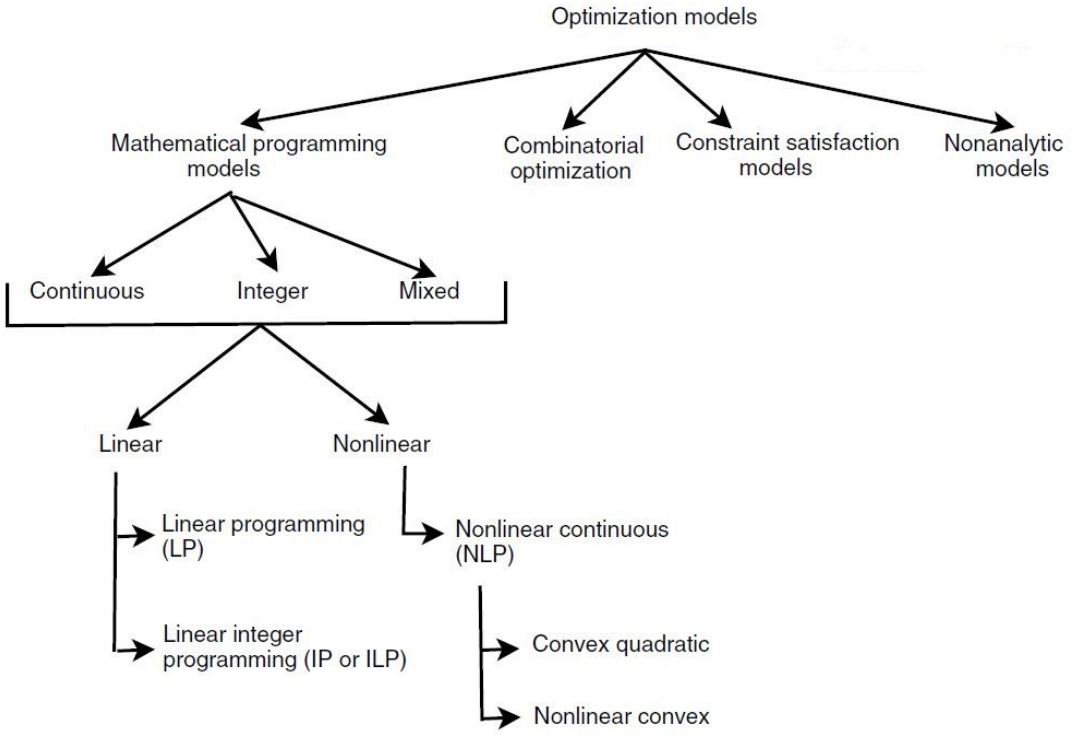

Figure 3.10: Optimization models.

should be modeled with discrete variables since the resources are indivisible such as machines and people. In an Integer Program (IP) optimization model, the decision variables are discrete. When the decision variables are both discrete and continuous, we are dealing with Mixed Integer Programming (MIP) problems. A more general class of IP problems is combinatorial optimization problems. This class of problems is characterized by discrete decision variables and finite search space. The popularity of combinatorial optimization problems stems from the fact that in many real-world problems, the objective function and constraints have different types (e.g., non-linear, non-analytic, black box) whereas the search space is finite.

As an optimization problem, this air traffic flow problem wants to find solutions that minimize the overall cost based on the perspective of the Air Navigation Service Providers (ANSP) and airlines (see Figure 3.11). In this section, the mathematical modeling for assignment of requested flights to the North Atlantic organized track system is formulated.

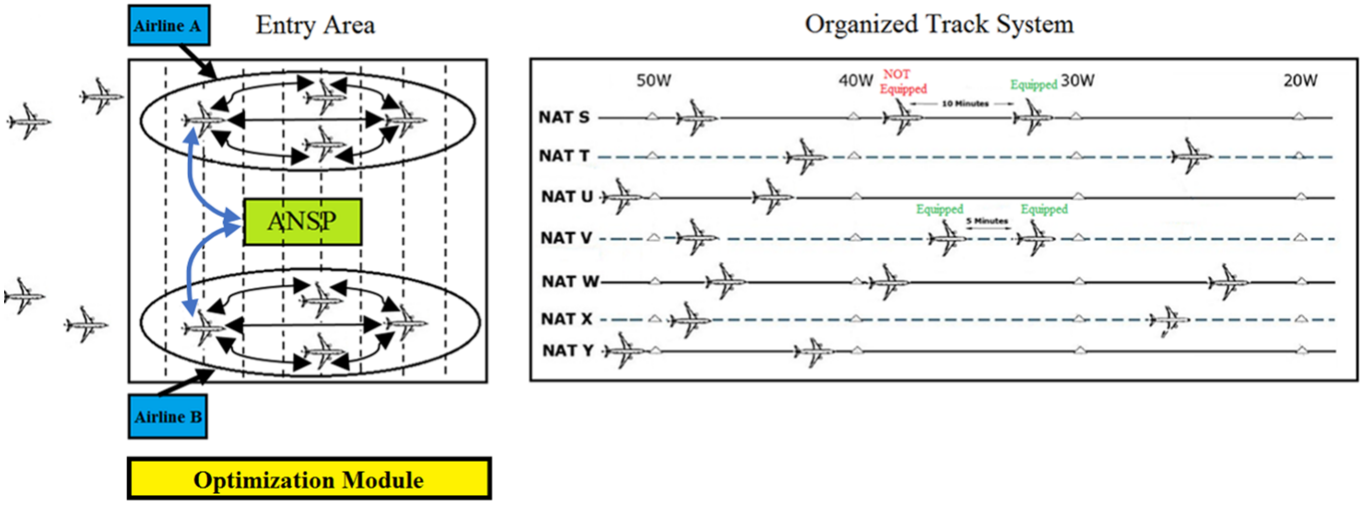

Figure 3.11: Group assignment procedure scheme.

The followings are the list of model index sets, decision variables, parameters, objective function, and constraints.

Index Sets

Set of airlines: $j = 1, 2, ..., J$

Set of flights related to each airline: $i = 1, 2, ..., I$

Set of available OTS tracks for each flight: $k = 1, 2, ..., K$

Set of available flight levels for each flight: $n = 1, 2, ..., N$

Set of available Mach numbers for each flight: $m = 1, 2, ..., M$

Decision Variable

X_{ijknm} : Binary variable, which equals to 1 if flight i from airline j is assigned to track k and flight level n with Mach number m (3.1)

Model Parameters

FC_{ijknm} : Fuel cost related to flight i from airline j which is assigned to track k and flight level n with Mach number m (derived from cost matrices) (3.2)

FEQ_{ijknm} : Equipage level of flight i from airline j which is the following flight requested track k

and flight level n with Mach number m (binary parameter) (3.3)

LEQ_{ijknm} : Equipage level of flight i from airline j which is the leading (most recent) flight assigned to track k and flight level n with Mach number m (binary parameter) (3.4)

FAM_{ijkn} : Mach number of flight i from airline j which is the following flight requested track k and flight level n (3.5)

LAM_{ijkn} : Mach number of flight i from airline j which is the leading (most recent) flight assigned to the track k and flight level n (3.6)

TS_{ijknm} : Time separation among following flight i from airline j requested track k and flight level n with Mach number m to the leading (most recent) flight flying in track k and flight level n with Mach number m (3.7)

TD_k : Distance length of track k (nautical miles) (3.8)

SS : Standard minimum longitudinal separation (e.g., 10 minutes) (3.9)

RS : Reduced minimum longitudinal separation (e.g., 5 minutes) (3.10)

$Z_1 = 0.333$: coefficient for longitudinal separation correction (3.11)

$Z_2 = 0.0018$: coefficient for longitudinal separation correction (eastbound tracks) (3.12)

$Z_3 = 0.0026$: coefficient for longitudinal separation correction (westbound tracks) (3.13)

Objective Function

$$MinZ = \sum_{i=1}^{I} \sum_{j=1}^{J} \sum_{k=1}^{K} \sum_{n=1}^{N} \sum_{m=1}^{M} (FC_{ijknm} \times X_{ijknm}) \quad (3.14)$$

Constraints

$$\sum_{k=1}^{K} X_{ijknm} = 1, \quad \forall i = 1, ..., I, j = 1, ..., J, n = 1, ..., N, m = 1, ..., M \quad (3.15)$$

$$\sum_{n=1}^{N} X_{ijknm} = 1, \quad \forall i = 1, ..., I, j = 1, ..., J, k = 1, ..., K, m = 1, ..., M \quad (3.16)$$

$$\sum_{m=1}^{M} X_{ijknm} = 1, \quad \forall i = 1, ..., I, j = 1, ..., J, k = 1, ..., K, n = 1, ..., N \quad (3.17)$$

Time separation constraints (eastbound tracks) (3.18)

$$TS_{ijknm} \times X_{ijknm} \geq SS - [(SS - RS) \times FEQ_{ijknm} \times LEQ_{knm}] + [(Z_1 + (Z_2 \times TD_k)) \times (\frac{FAM_{ijkn} - LAM_{ijkn}}{0.01})]$$

Time separation constraints (westbound tracks) (3.19)

$$TS_{ijknm} \times X_{ijknm} \geq SS - [(SS - RS) \times FEQ_{ijknm} \times LEQ_{knm}] + [(Z_1 + (Z_3 \times TD_k)) \times (\frac{FAM_{ijkn} - LAM_{ijkn}}{0.01})]$$

$$X_{ijknm} = \{0, 1\} \quad (3.20)$$

The objective function of this problem is minimizing the overall fuel consumption cost (Equation 3.14). Equations (3.15–3.17) ensure that each flight is assigned to one track, on flight level, and one Mach number in the OTS assignment. Equations (3.18–3.19) satisfy the time separation constraints for flights using eastbound and westbound OTS tracks considering the Mach number differences between the leading and following aircraft. Equation 3.20 shows the binary constraint for the decision variable [47].

3.7 Solution Methodology

Optimization problems can be solved by exact or approximation methods (see Figure 3.12). Exact methods obtain optimal solutions and guarantee their optimality. Approximate methods generate high-quality solutions in reasonable computational time, but there is no guarantee of finding a global optimal solution [51]. In the class of exact methods, the following algorithms can be found: dynamic programming, branch and X family of algorithms (branch and bound, branch and cut, branch and price), constraint programming, and A^* family of search algorithms (A^*, IDA^*-Iterative Deepening Algorithms). All the methods in this class contain tree search algorithms. They are based on a divide and conquer strategy to partition the solution space into sub-problems and optimize each sub-problem separately.

In the class of approximate methods, two sub-classes of algorithms are available: approximation algorithms and heuristic algorithms. In approximation algorithms, there is a guarantee on the bound of the obtained solution from the global optimum. Heuristics do not have an approximation guarantee on the obtained solutions. Heuristics find acceptable solutions for large-size problems at reasonable computational costs. Heuristics are classified into two categories: specific heuristics

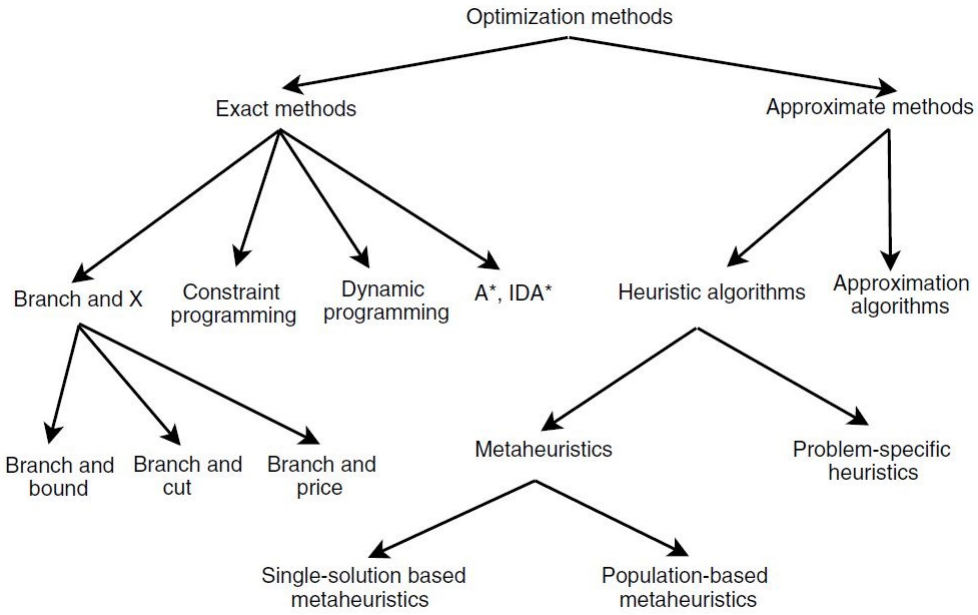

Figure 3.12: Optimization methods.

and metaheuristics. Specific heuristics are tailored and designed to solve a specific problem. Metaheuristics are general-purpose algorithms that can be applied to solve a wide range of optimization problems.

The first step in solving an optimization problem is analyzing its complexity. If a polynomial-time algorithm exists for solving a problem, exact optimization methods can be used. Even if a polynomial-time algorithm does not exist (i.e., NP-hard problems), exact optimization methods can be employed to solve the small-size problems. Besides complexity, the required search time to solve the problem is an important factor. Even for polynomial problems, the power of the polynomial complexity function may be large enough that the real-life problems cannot be solved in a reasonable computational time.

As the first step, the complexity of this problem is examined to see if it belongs to the class of polynomial or non-polynomial problems. Time complexity functions define the amount of time taken by programs regarding the input size. In computer science, big O notation is used to classify algorithms based on the increase in running time or space requirements as the input size grows.

The assignment of oceanic flights to the organized Tracks system (OTS) which is formulated in the previous section is a combinatorial problem, and the growth rate of this problem is exponential.

Exponential time complexity ($O(c^n), c > 1$) indicates an algorithm whose growth rate is exponential with respect to the size of the input. In this problem, the value of c is the number of tracks multiplied by the number of flight levels (e.g., 8×10=80). The size of this problem (n) could be large in real-world operations. According to the NavCanada data related to the flights assigned to OTS tracks on (September 15, 2014) in peak traffic period, 73 flights were assigned to the eastbound OTS tracks between 1:00 AM to 2:00 AM (see Figure 3.13).

Note that oceanic air traffic controllers are the ultimate users of solutions for this assignment problem. Regarding the nature of air traffic controllers' tasks, it is crucial for them to have good-quality solutions in a reasonable time. Given the exponential time complexity, the large size of the problem in real practice, and computational time constraints for oceanic air traffic controllers, metaheuristic optimization algorithms for solving the real-scale assignment problem is proposed.

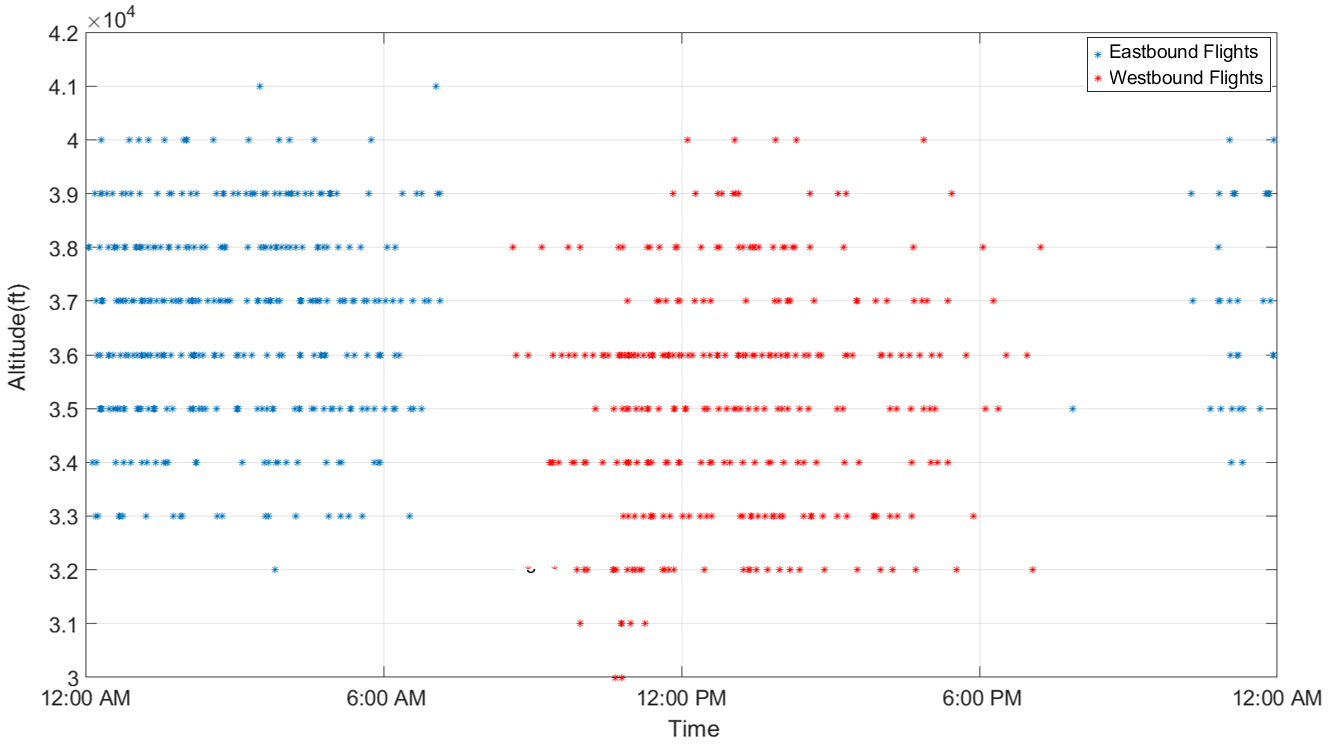

Figure 3.13: Flights assigned to OTS tracks (Sep 15, 2014), source: NAV Canada.

3.7.1 Metaheuristics Optimization Algorithms

Metaheuristics are satisfactory algorithms for finding high-quality solutions for combinatorial problems that cannot be solved with exact optimization algorithms. There are many metaheuristic algorithms inspired by natural processes: simulated annealing from physics; genetic algorithms and artificial immune system from biology; ant colony, bee colony, and particle swarm optimization from species social sciences [51]. Metaheuristic algorithms can be classified into the following categories:

- Population-based search versus single-solution based search

  Single-solution based algorithms (e.g., simulated annealing) manipulate and transform a single solution during the search while in population-based algorithms (e.g., particle swarm optimization) a whole population of solutions is evolved.

- Memory usage versus memoryless methods

  Some metaheuristic algorithms are memoryless. It means, no information extracted during the search process. Some representatives of this class are local search and simulated annealing. While other metaheuristics use a memory that contains some information extracted during the searching. For example, the tabu search algorithm uses short-term and long-term memories.

- Deterministic versus stochastic

  A deterministic metaheuristic solves an optimization problem by making deterministic decisions (e.g., tabu search). In stochastic metaheuristics, some random rules are applied during the search (e.g., simulated annealing, evolutionary algorithms). In deterministic algorithms, starting the searching process with the same initial solution leads to the same final solution, whereas in stochastic metaheuristics, different final solutions can be achieved from the same initial solution.

Two criteria should be considered in using a metaheuristic algorithm: exploitation of the best-found solutions (intensification) and exploration of the search space (diversification). In intensification, the determined promising regions are explored more thoroughly to find better solutions. In diversification, unexplored solution regions are visited to reduce the probability of trapping in local optimal. Single-solution based metaheuristics are exploitation oriented. They have the power to

intensify the search in promising regions. Population-based metaheuristics are exploration oriented and they allow a better diversification in the entire solution space. Metaheuristic algorithm studied widely for air traffic flow problems such as Aircraft departure sequencing [5], Aircraft arrival sequencing [7], Conflict prevention and resolution [9], Optimization of airway network design [14], Route optimization for Unmanned Air Systems (UAS) [27], Optimization of airline cargo operations [8].

The proposed algorithm for solving the OTS assignment problem is a single-solution based optimization algorithm. The main reason for selecting this class of metaheuristics is having a good initial solution to start the searching process. The initial solution is derived from the requested tracks and flight levels determined from the cost matrix analysis. As a strong Single-Solution based metaheuristics algorithm, Simulated Annealing (SA) is selected to provide solutions for the OTS assignment problem.

Simulated Annealing

The work of S. Kirkpatrick et al. introduced the Simulated annealing (SA) algorithm and applied this technique to optimization problems [29]. SA is based on the principles of statistical mechanics. The annealing process requires heating and then slowly cooling a substance to obtain a strong crystalline structure. If the initial temperature is not high enough or a quick cooling is applied, imperfections (i.e., metastable states) are obtained. Strong crystals are created from slow cooling. The SA algorithm simulates the energy changes in a system subjected to a cooling process until it converges to an equilibrium state (i.e., frozen steady states). In a given optimization problem, the objective function is equivalent to the energy state of the system. A solution corresponds to a system state. The decision variables associated with a solution are analogous to the molecular positions. The local minima imply that a metastable state has been reached. The global optimum corresponds to the frozen steady state of the system.

SA is a stochastic algorithm that enables accepting worse solutions under specific conditions to escape from local optima. SA uses a control parameter, called temperature (T), to determine the

probability of accepting non-improving solutions. SA proceeds in several iterations starting from the initial solution with initial temperature (T). At each iteration, SA generates a random neighbor solution by an operator that performs a small perturbation to the solution of the previous iteration. Solutions that improve the objective function are always accepted. Otherwise, the solution is selected with a given probability that depends on the current temperature and the amount of degradation ΔE of the objective function. ΔE represents the difference in the objective value between the current solution and the generated neighboring solution. Higher temperatures lead to higher probabilities of accepting worse moves. As the algorithm progresses, the probability that non-improving moves are accepted decreases based on the Boltzmann distribution shown in equation (3.21):

$$P(\Delta E, T) = e^{-\frac{f(s')-f(s)}{T}} \tag{3.21}$$

3.8 Solution Method Validation

Figure 3.14 illustrates the flowchart of the proposed optimization algorithm for solving the group assignment of flight to the OTS. The algorithm is implemented inside the OTS track assignment module in the Global oceanic model. Before the simulation starts, the model created flight plans based on the optimal track and flight level for all the flights. During the simulation, when flights entered the predetermined entry area, they will be considered in the group OTS assignment procedure. The initial solution is the optimal track and flight level assignment derived from the cost matrix for each flight in the selected group.

The algorithm checks the initial solution for the assignment constraints (e.g., separation minima, feasibility, and accessibility of requested tracks and flights). if the initial solution is a conflict-free assignment for all the flights, the algorithm considers the initial solution as the best solution. if the solution is conflict-free, the model assigns the optimal track and flight levels to all the flights. If all the constraints are not fulfilled, the model activates the proposed optimization algorithm to find

the best conflict-free solution for assigning the flights in the selected group to the OTS tracks and flight levels. The algorithm explores the solution space by changing the flight levels and tracks.

If the new solution is better than the previous solution, it got accepted. Otherwise, the algorithm decides about accepting non-improving solutions based on the current temperature and differences in objective functions of the new solution and previous solution. This cycle continues until reaching the stopping criteria. The stopping rule for this problem is reaching the minimum temperature (T_{min}) or achieving a predetermined number of iterations with no improvement in the best solution.

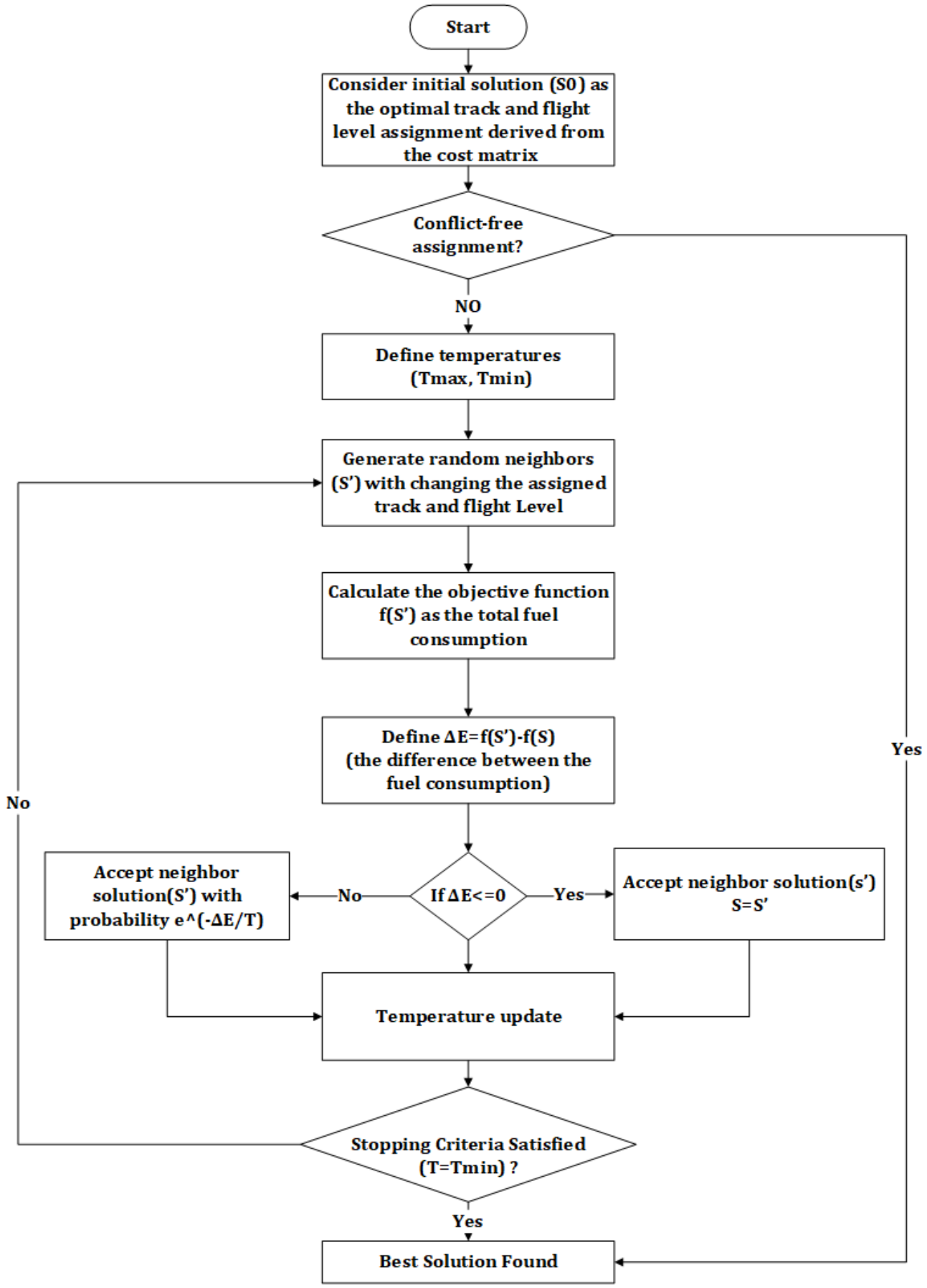

Figure 3.14: Flowchart of the proposed metaheuristics algorithm.

The publicly accessible flight planning website (`https://skyvector.com/`) provides the configuration of North Atlantic tracks. The entry areas for considering the flights in the group assignments are identified based on critical oceanic points in eastbound and westbound tracks. The entry area for eastbound flights is defined by contours between 6 to 10 degrees of eastbound OTS tracks, and the westbound entry area is defined by contours between 3 to 6 degrees of the westbound OTS tracks (see Figure 3.15).

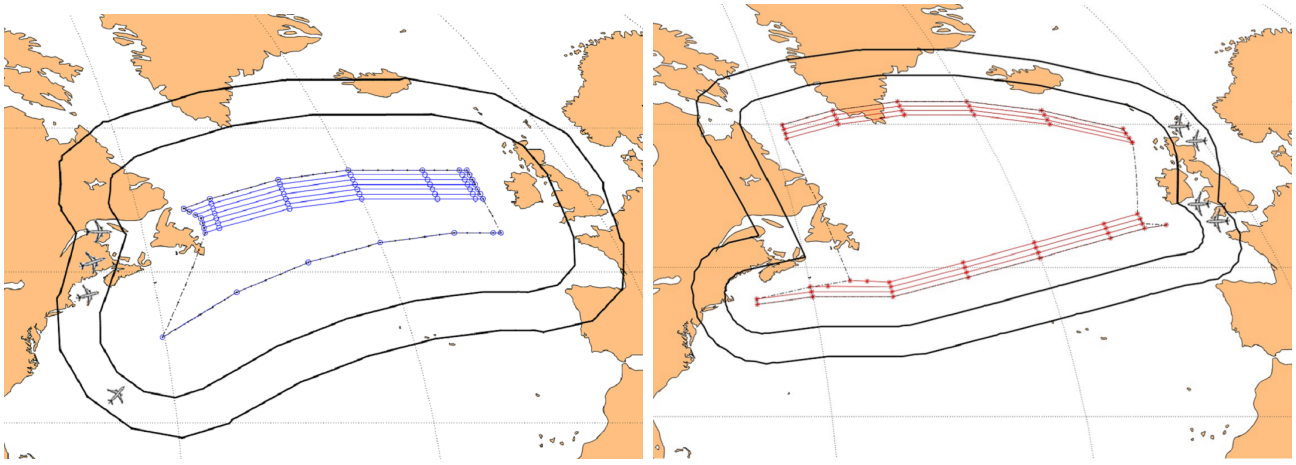

(a) Entry area for eastbound flights. (b) Entry area for westbound flights.

Figure 3.15: Entry area for OTS flights.

To validate the proposed metaheuristics algorithm, a small size problem is used to test the algorithm's ability to find the global optimal. For this test, the algorithm is set to start with a completely random assignment. Then, the algorithm is run to see if it can find the global optimal assignment which is the optimal track and flight level for all the flights. Table 3.1 shows the five selected eastbound flights inside the simulation with the requested track and flight level. Figure 3.16a shows the random solution (iteration 1) with which the proposed algorithm initiates the searching process. Figure 3.16b shows the final solution in which the proposed algorithm reaches to stopping criteria (T_{min}). Figure 3.17 shows the best solution in each iteration and how the algorithm improves the solution until reaching the global optimal. Given this result of this small-size problem, the proposed algorithm is validated to be used for large-scale problems.

Table 3.1: Selected sample of flights for validation.

No.	Flight ID	Origin	Destination	Optimal Track	Optimal Flight Level
1	'GTI8514'	KPSM	EDFH	Track X	FL 370
2	'UAL57'	KEWR	LFPG	Track Y	FL 380
3	'AZA603'	KJFK	LIRF	Track Y	FL 370
4	'TCX723'	KBOS	EGCC	Track V	FL 380
5	'UAL70'	KEWR	EHAM	Track W	FL 380

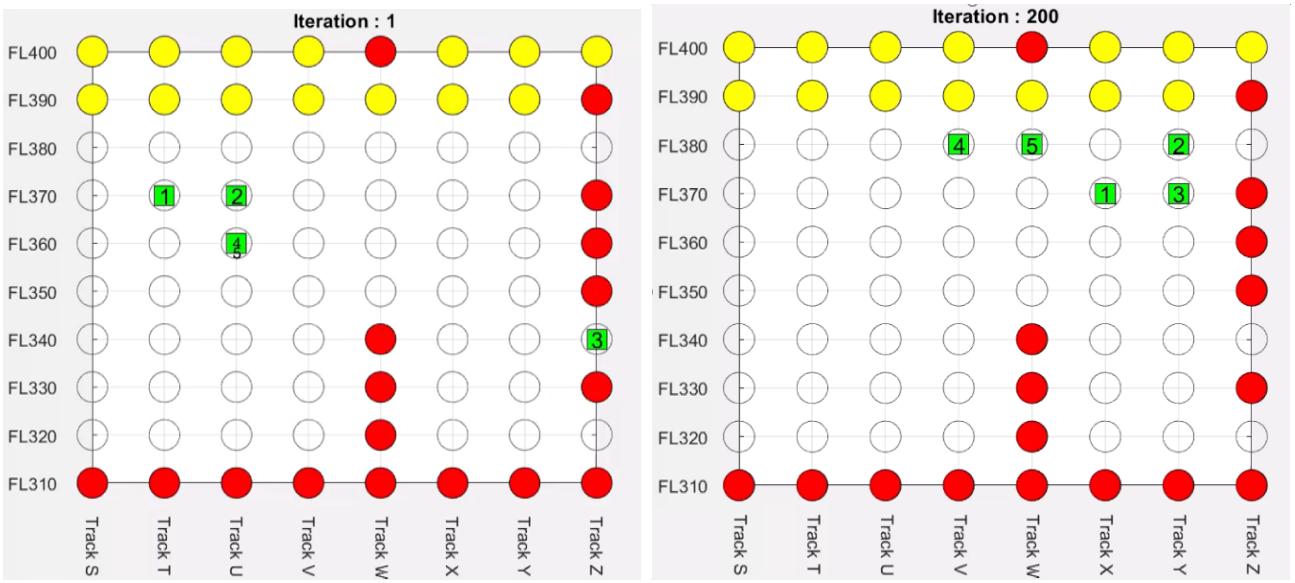

(a) Initial solution (iteration 1). (b) Final solution (iteration 200).

Figure 3.16: Initial and final solutions in the optimization algorithm.

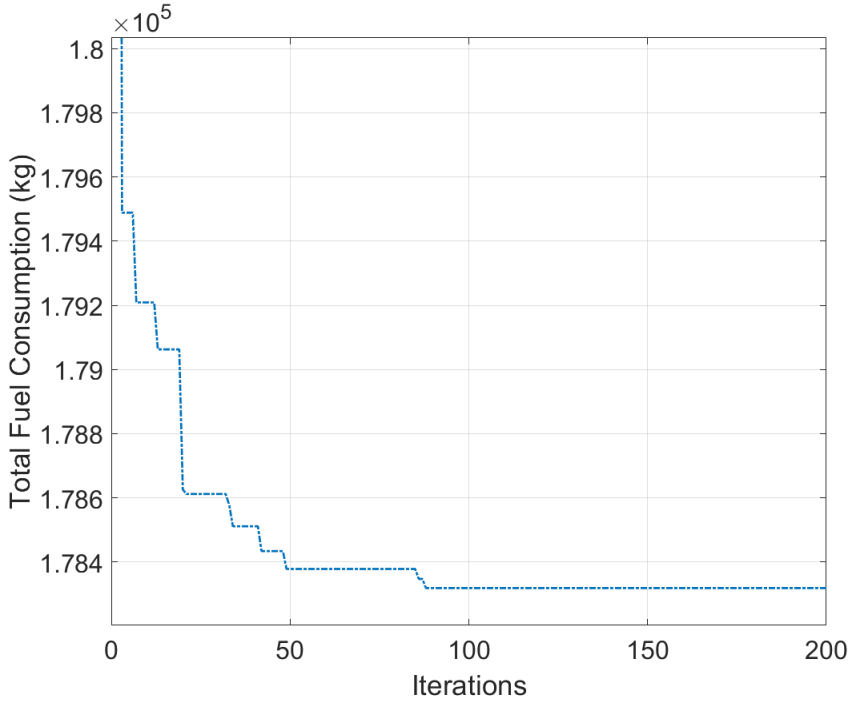

Figure 3.17: Objective function convergence diagram.

3.9 Simulation Scenarios

Table 3.2 shows the list of scenarios for OTS assignment logic. Scenario 1 represents the current logic used by oceanic air traffic controllers. Based on the heuristics algorithm, changing flight levels is their first preference rather than changing tracks. when a flight cannot be assigned to its optimal track and flight level, ATC checks the feasibility of up to three flight levels lower than the requested flight level. If none of these assignments are conflict-free, they check the other assignment alternatives within changing tracks. Scenario 2 represents the ideal procedure of individual assignment. The assumption is this scenario is air traffic controllers have access to the list of assignment priorities derived from the cost matrix for each flight. In this case, if the ideal track and flight level is not available, the ATC check the next best alternative based on the assignment priorities. The proposed algorithm (Scenario 3) has two main advantages. First, the algorithm is a group assignment procedure and it aims to find the best assignments for entire flights inside the group. Second, the proposed method uses a metaheuristics optimization algorithm to find a high-quality solution in reasonable computational time.

Table 3.2: OTS assignment scenarios.

Scenario	**OTS Assignment Approaches**
1	Individual Assignment (Heuristics)
2	Individual Assignment (Full Cost Matrix)
3	Group Assignment (Metaheuristics Optimization)

This study uses the GO Model as a fast-time simulation tool to evaluate the operational benefits of proposed OTS assignment methods. The main inputs for the GO Model are the traffic data set, OTS configuration, Separation standards, and wind data. The FAA provided ATSL with Traffic Flow Management System (TFMS) dataset for the traffic of three consecutive days in June 2016 (24-25-26). This demand set is used to solve the flight assignments to the North Atlantic organized track system (see Figure 3.18).

The wind data used for modeling is collected from the National Center for Atmospheric Research

(NCAR) Reanalysis model. The reanalysis model was developed by the Earth System Research Laboratory Physical Science Division. The data provides the magnitude and direction of the wind every 2.5 degrees latitude and longitude at 17 geopotential heights. For eastbound flights, the wind over the North Atlantic is generally tailwind dominantly because the jetstream flows from the United States to Europe. North Atlantic westbound flights normally experience headwinds which are opposite to the direction of flight. Therefore, tracks are configured to maximize the effect of tailwinds for eastbound flights and minimize headwinds for westbound tracks. Figure 3.19 illustrates the wind vectors over the North Atlantic on June 25, 2016 [32]. Nav Canada, the air navigation system provider in Canada, provided the daily OTS track configurations. The data records include dates, directions, track alphabetic names, entry and exit waypoints, and geographical coordinates.

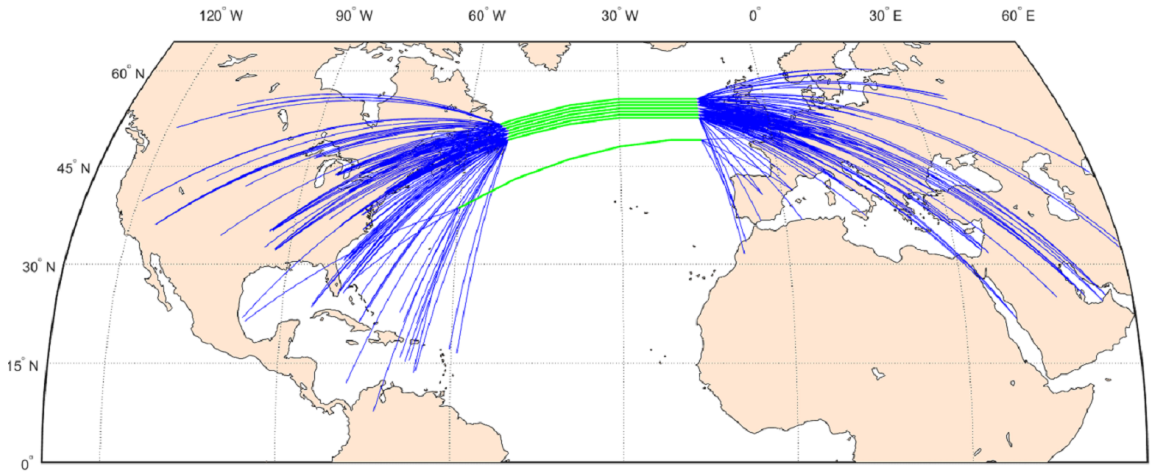

(a) Eastbound OTS traffic (1463 flights).

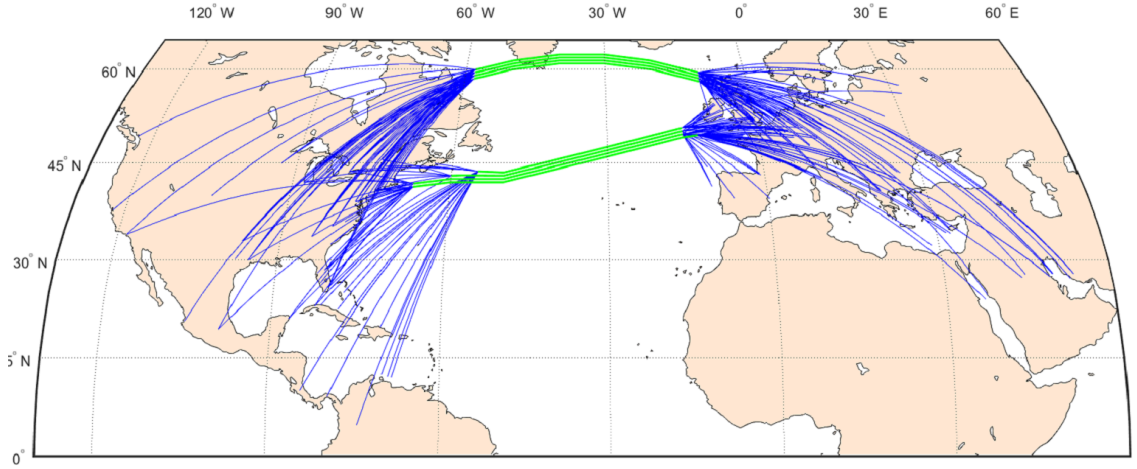

(b) Westbound OTS traffic (841 flights).

Figure 3.18: Simulated OTS flight traffic.

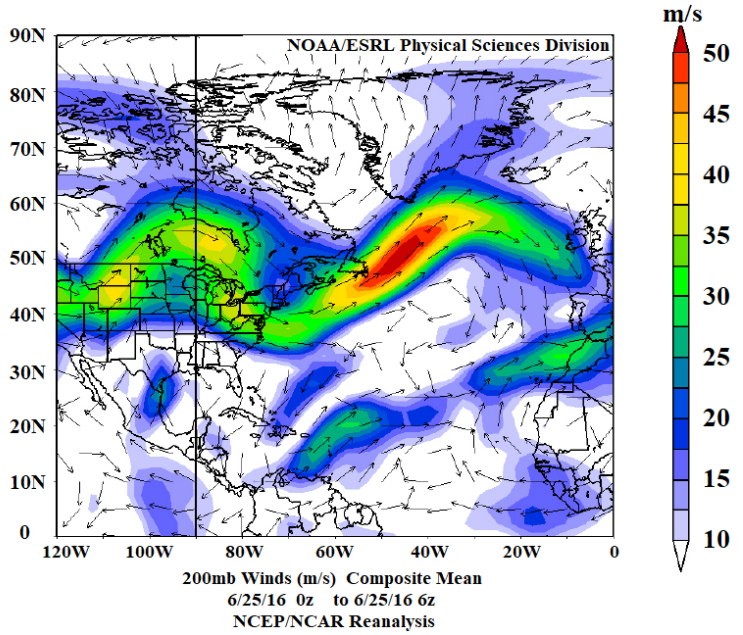

Figure 3.19: Wind vector at 200 mb (39,000 feet), June 25, 2016, source: NOAA/ESRL

3.10 Results and Discussion

The proposed metaheuristic optimization algorithm for group OTS assignment is validated and implemented inside the OTS Assignment module of the GO Model. Then, the GO Model is used to simulate the real-scale traffic to evaluate the potential benefits of different OTS assignment methods in terms of efficiency, level of service, and airline equity.

3.10.1 Fuel Efficiency

Table 3.3 shows the average fuel consumption, travel distance, and travel time for eastbound and westbound flights among scenarios. Figure 3.20 shows the average fuel consumption comparison among scenarios. The results indicate that the least fuel consumption is related to the scenario with the group assignment procedure using the metaheuristic optimization algorithm. The estimated annual fuel consumption savings is 26.5 million kilograms and 15.5 million dollars using the group assignment (metaheuristic) method compared to the existing assignment approach (heuristics), assuming 320 operational days per year, and $1.82 per gallon as the average jet fuel price (2019).

Table 3.3: Average fuel consumption, travel distance, and travel time statistics.

Scenarios		Average Fuel Consumption (kg)	Average Travel Distance (nm)	Average Travel Time (min)
Group Assignment (Metaheuristics)	Eastbound	51,307	3830.1	507.3
	Westbound	44,461	3698.3	431.9
Individual Assignment (Full Cost Matrix)	Eastbound	51,344	3829.8	507.7
	Westbound	44,492	3700.0	432.1
Individual Assignment (Heuristics)	Eastbound	51,421	3829.7	507.2
	Westbound	44,562	3698.5	431.9

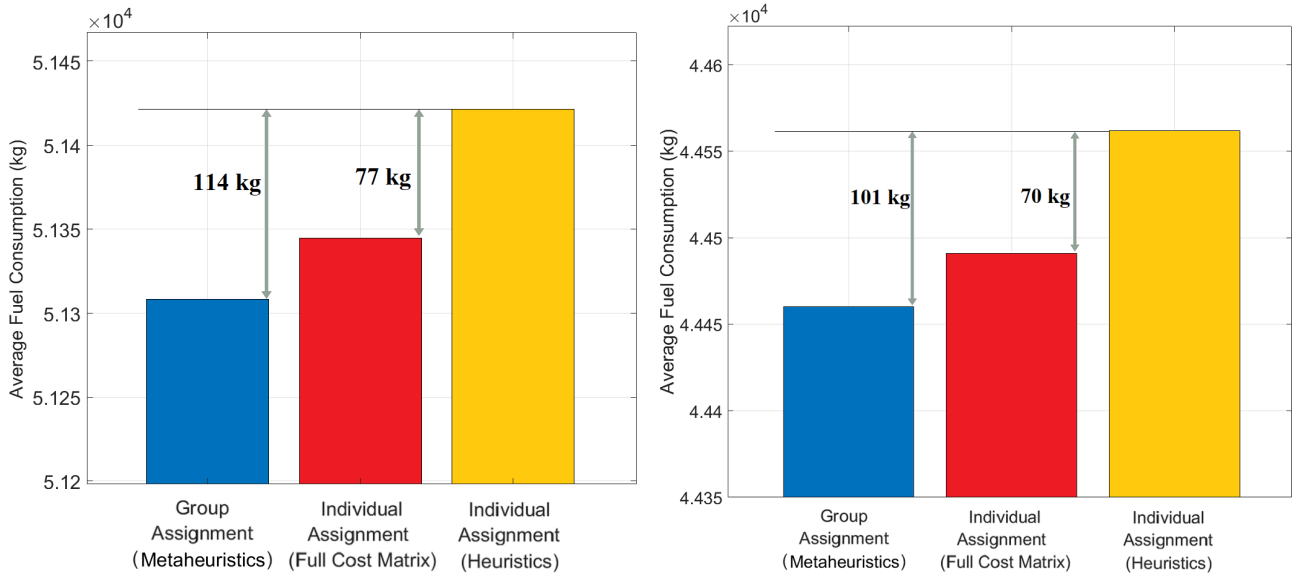

(a) Eastbound fuel consumption comparison. (b) Westbound fuel consumption Comparison.

Figure 3.20: Average fuel consumption comparison.

Figure 3.21 demonstrates the processed computational time for solving the OTS assignment problem using the proposed metaheuristics algorithm. The cumulative distribution diagram shows that the required computational time for 90% of the group assignment problems took less than 5 minutes. The stopping criteria for this problem are reaching the minimum temperature (T_{min}=0) or 200 iterations with no decreases in the total fuel consumption. The hardware configuration used for solving this problem is a desktop computer with 4 cores (8 logical processors), Intel(R) Core(TM) i7-6700 CPU @ 3.40 GHz, with 32 GB physical memory (RAM).

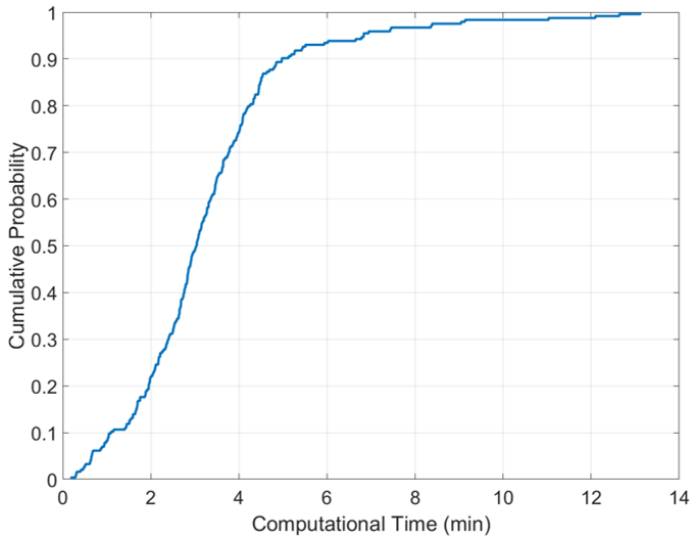

Figure 3.21: Cumulative distribution function of computational time.

3.10.2 Level of Service

The level of service in the flights using the OTS track is defined as the percent of flights that achieve their optimal (requested) track and flight level. As explained in Section 3.4.1, flights request to fly at the ideal track and flight level derived from the cost matrix. Inside the simulation, the ATC routine investigates all the requests considering the required separations at the entry point of tracks, differences in leading-following aircraft's Mach numbers (i.e., closing cases, and opening cases), and the feasibility of flights to reach their ideal flight levels. If the ATC routine detects any violations, it will assign flights to other conflict-free tracks and flight levels according to the corresponding OTS assignment method. Comparing the distributions of ideal track and flight level before simulation (after cost matrix), and assigned track and flight level distributions (after simulation) provides insight into the level of service for each scenario. Figure 3.22 shows the distribution of track and flight levels before and after simulations for all the westbound flights in the middle day of simulation (275 flights). Figure 3.22a illustrates the distribution of requested tracks and flight levels derived from the cost matrices (before simulation). Figures 3.22b–3.22c–3.22d demonstrate the distribution of assigned tracks and flight levels after simulation using the group assignment (metaheuristics), individual assignment (full cost matrix), and individual assignment (heuristics) procedures, respectively.

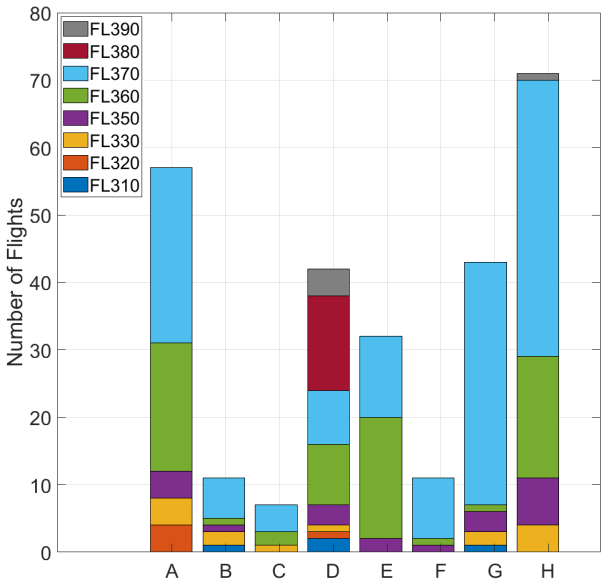

(a) Optimal tracks and flight level distribution (before simulation).

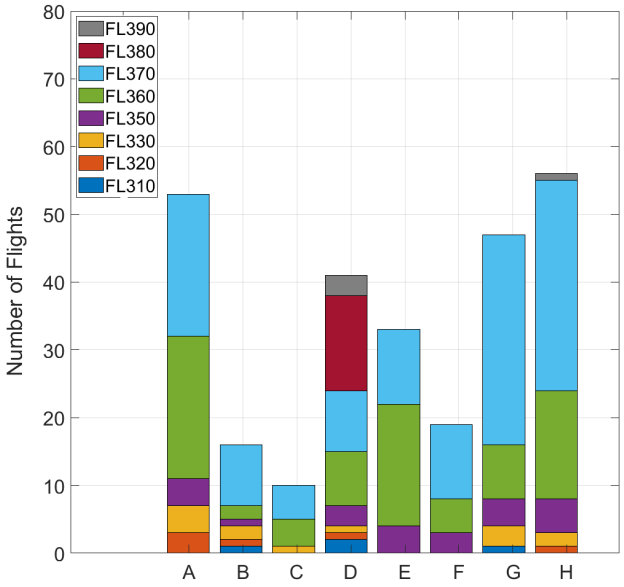

(b) Simulated tracks and flight level distribution (metaheuristics).

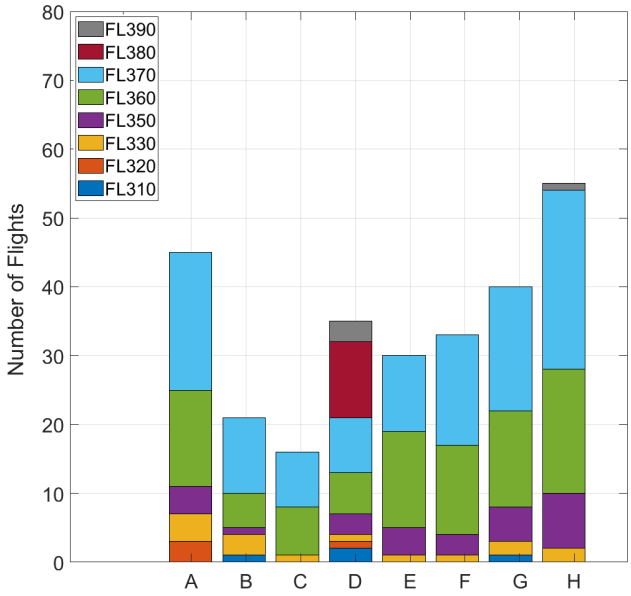

(c) Simulated tracks and flight level distribution (full cost matrix).

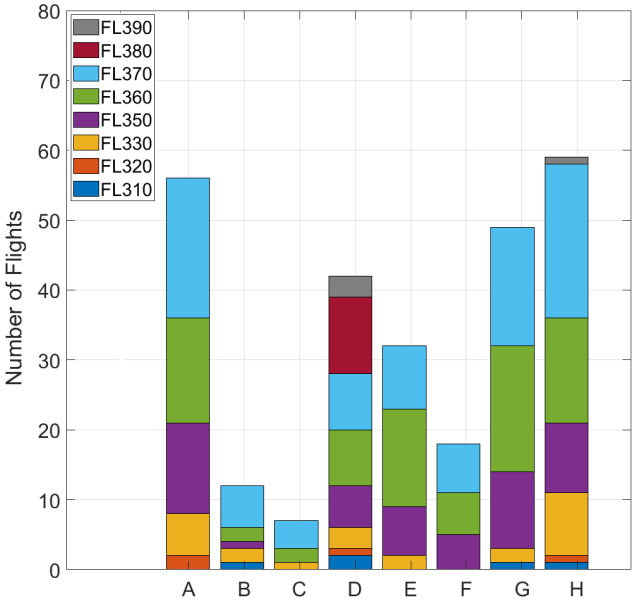

(d) Simulated tracks and flight level distribution (heuristics).

Figure 3.22: Westbound track and flight level distribution.

Figure 3.23 shows the distribution of tracks and flight levels before and after simulations for all the eastbound flights in the middle day of simulation (494 flights). Figure 3.23a illustrates the distribution of requested tracks and flight levels derived from cost matrices (before simulation). Figures 3.23b–3.23c–3.23d demonstrate the distribution of assigned tracks and flight levels for flights

after simulation using three assignment methods.

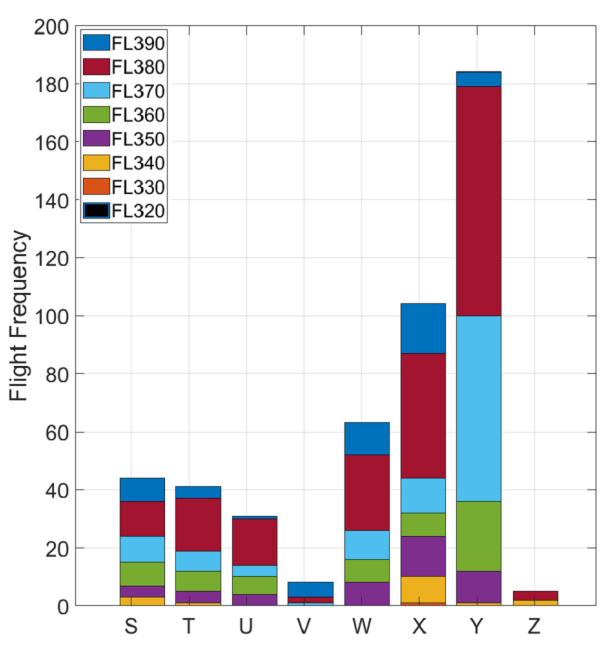

(a) Optimal tracks and flight level distribution (before simulation).

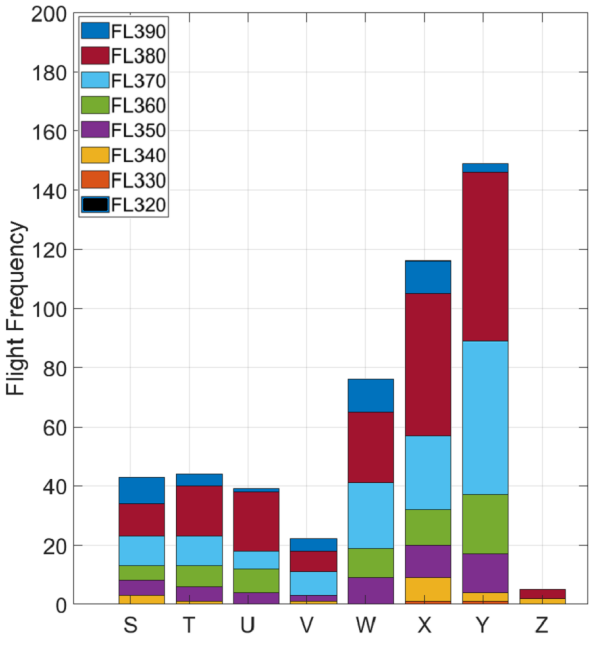

(b) Simulated tracks and flight level distribution (metaheuristics).

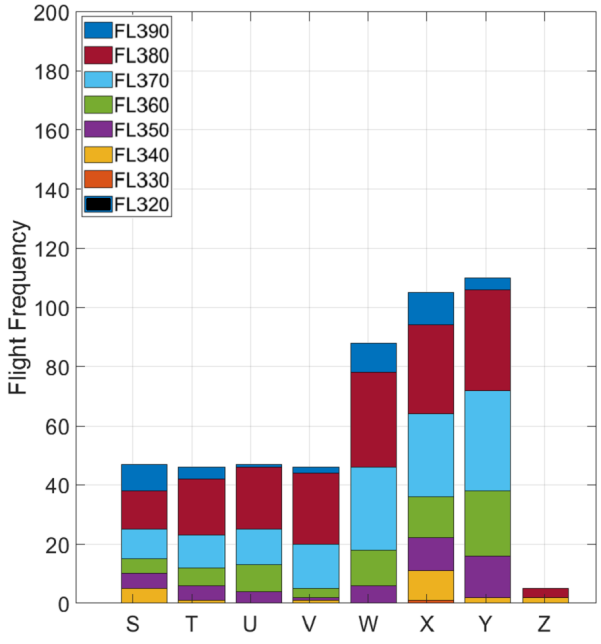

(c) Simulated tracks and flight level distribution (full cost matrix).

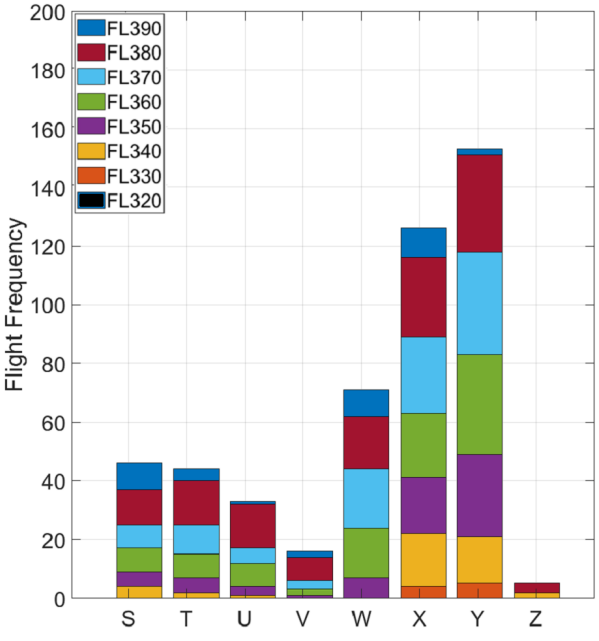

(d) Simulated tracks and flight level distribution (heuristics).

Figure 3.23: Eastbound track and flight level distribution.

Figure 3.24 indicates the statistics of the flight assigned to the organized tracks system. The blue bars show the percentage of flights assigned to their optimal(requested) tracks and optimal flight levels. This measure shows the level of service of air navigation service providers controlling Gander FIR (i.e, eastbound flights) and Shanwick FIR (i.e, westbound flights). The results demonstrate that there is a 15% increase in the level of service for both ANSPs using the group assignment (metaheuristic) method compared to the existing individual assignment (heuristic) method. Note that oceanic air traffic controllers tend to assign flights to (optimal track, non-optimal flight level) alternatives when the ideal assignment is not available since this procedure creates less workload for them.

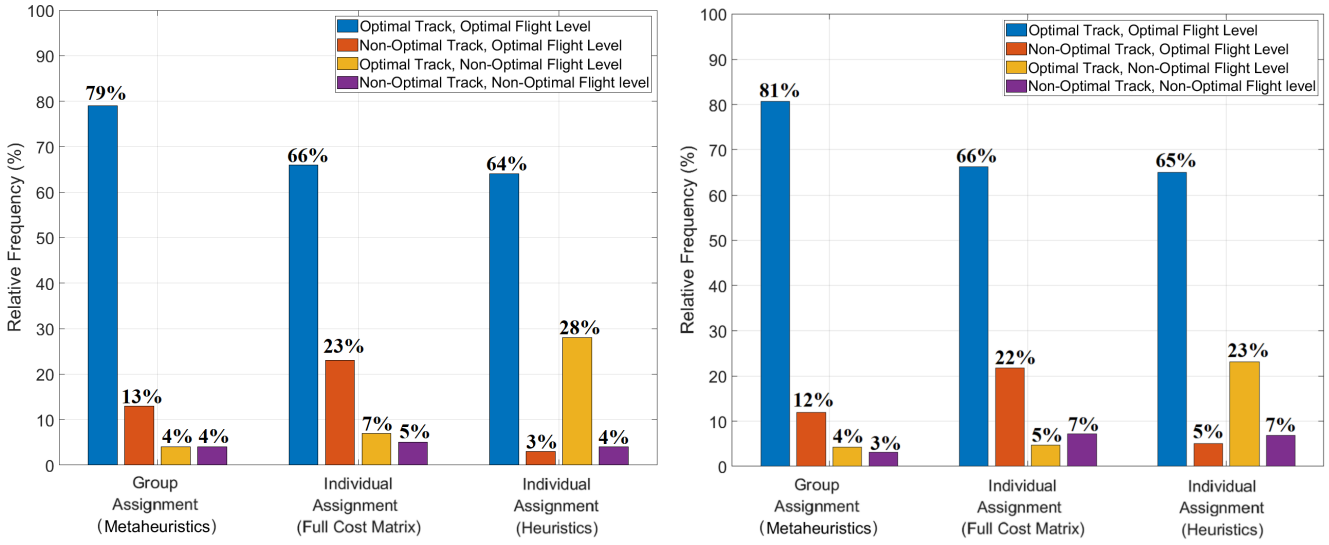

(a) Eastbound flights. (b) Westbound flights.

Figure 3.24: Distribution of track and flight level assignment.

3.10.3 Airline Equity Analysis

Currently, oceanic air traffic controllers use the heuristics algorithm which is a based ”first come, first served” strategy. Systematically, this viewpoint is not able to provide equity of access to the organized track system for airlines. The proposed optimization model for group-based assignment of flights to the OTS tracks can address this issue since the objective function is minimizing the total fuel consumption of flights inside the groups. The percent of flights assigned to optimal tracks

and flight levels to the number of flight operations related to each airline is a realistic measure for evaluating the access equity of airlines to their optimal routes. Figure 3.25 shows the distribution of airlines using the North Atlantic organized tracks system based on the TFMS data.

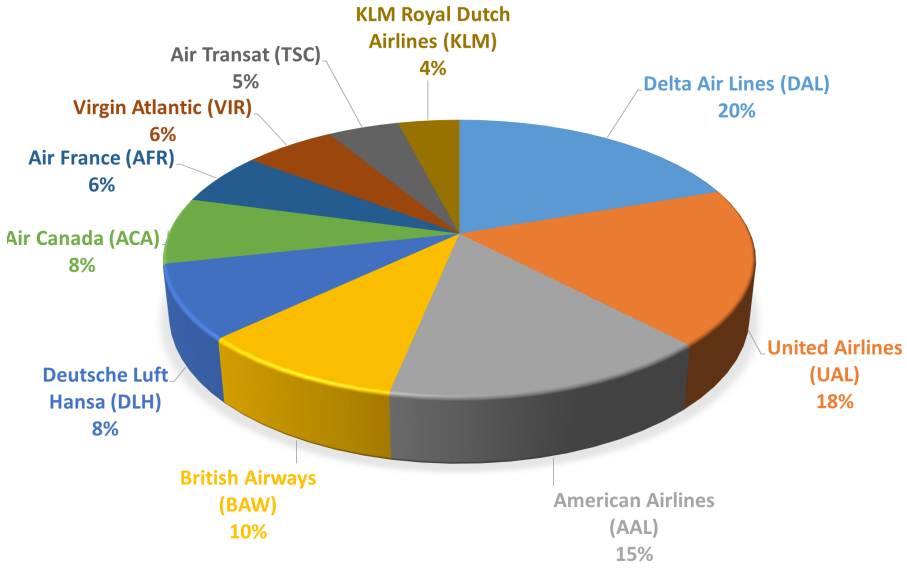

Figure 3.25: Distribution of airlines using the North Atlantic OTS tracks.

Figure 3.26 and Figure 3.27 show the percentage of flights assigned to their requested tracks and flight levels regarding the eastbound and westbound operations for selected airlines, respectively.

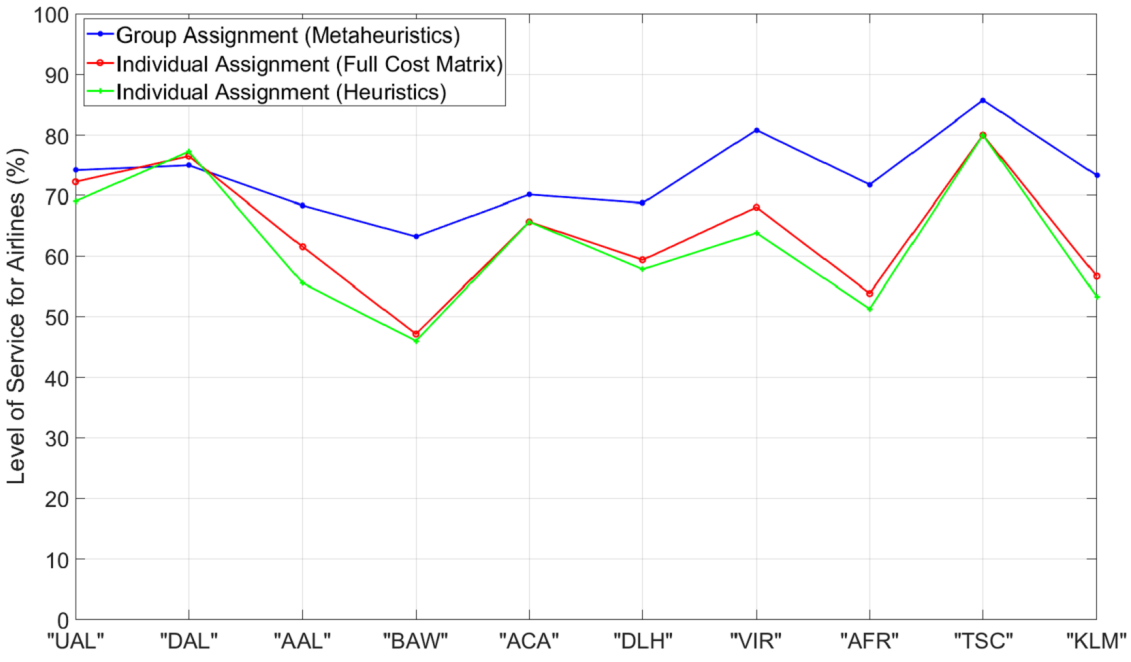

Figure 3.26: Distribution of level of service for airlines (eastbound operations).

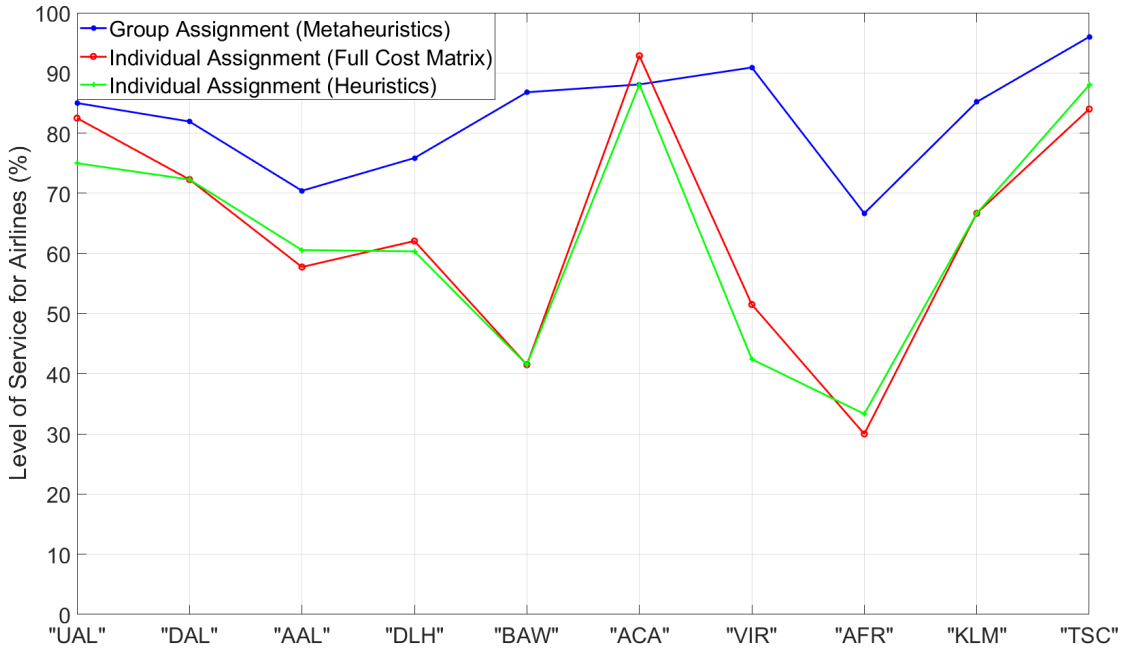

Figure 3.27: Distribution of level of service for airlines (westbound operations).

The results show that the standard deviation of level of service for the selected airlines had 9.6% and 5.8% reductions in the group assignment procedure (metaheuristics) compared to the individual assignment method (heuristics) for eastbound and westbound flights, respectively (see Figure 3.28)

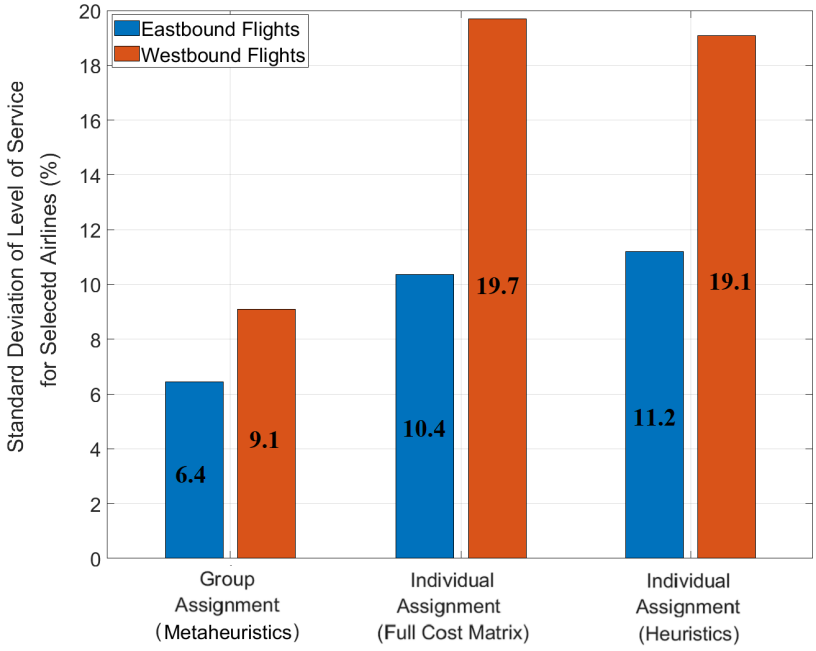

Figure 3.28: Standard deviation of level of service for selected airlines.

The results show that group assignment procedure assigns flights to more optimal routes and higher flight levels at the entry of eastbound and westbound tracks. Note that being assigned to more efficient tracks and flight levels at the track entry points allow flights to have more and earlier step-climbs to higher flight levels in the middle of tracks. Figures 3.29–3.30 illustrate two sample flights in the group assignment procedure (metaheuristics) and individual assignment (full cost matrix).

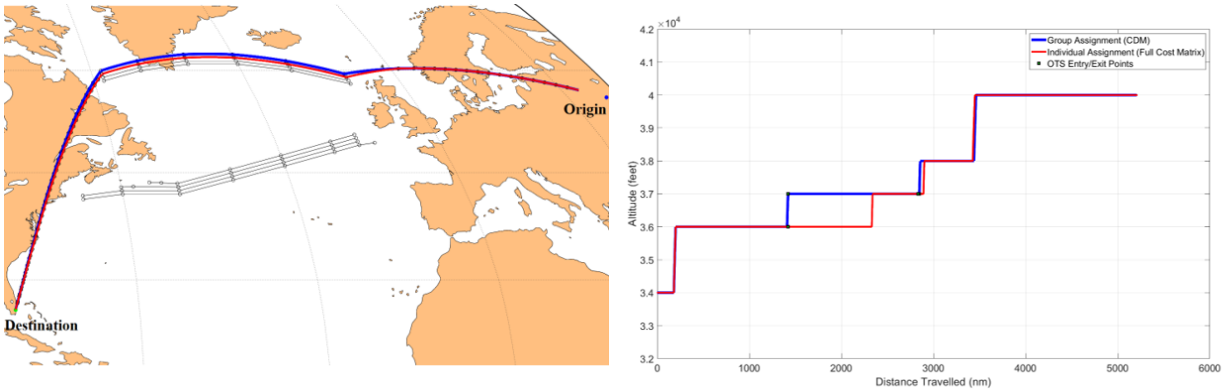

(a) Flight trajectory (aircraft: Airbus 330-200). (b) Altitude profile.

Figure 3.29: A westbound flight sample with 374 kilograms fuel savings.

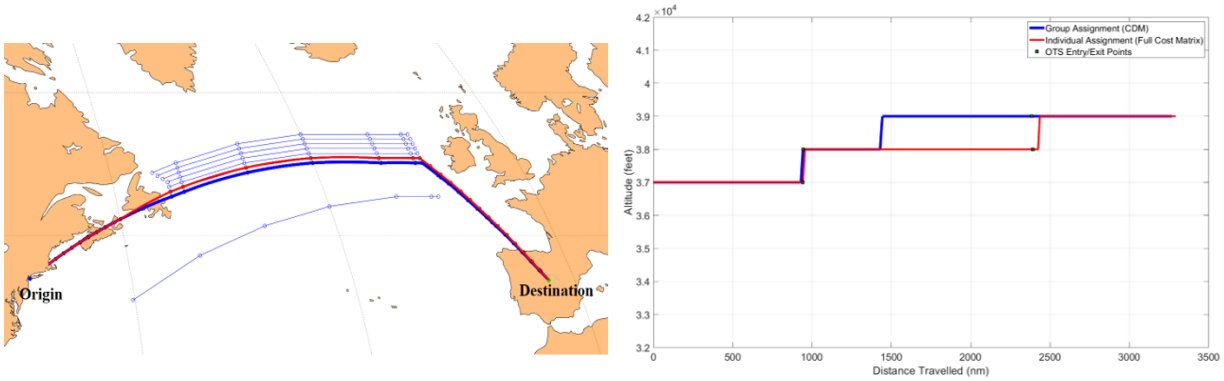

(a) Flight trajectory (aircraft: Airbus 330-200). (b) Altitude profile.

Figure 3.30: An eastbound flight sample with 213 kilograms fuel savings.

Figure 3.31 shows the distribution of communication messages in three OTS assignment scenarios. The result shows that 99% of the flights are assigned to the OTS tracks through the first ten assignment priorities derived from the cost matrix. Given the communication costs between oceanic flights and ANSPs, it is suggested that airlines disclose the first ten OTS assignment alternatives with ANSPs before flight departures.

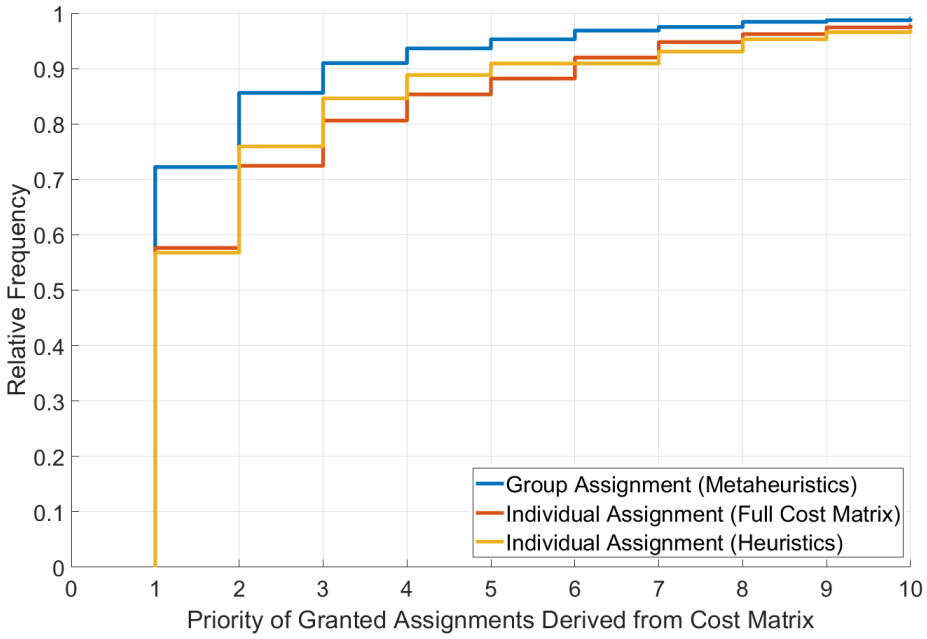

Figure 3.31: Distribution of granted assignment priorities.

3.11 Conclusions

This chapter studies the operational benefits of a novel method for assigning flights to the Organized Track System (OTS) in the North Atlantic airspace. The FAA publishes the OTS configurations as the optimal routes based on weather and wind conditions on a daily basis. Flights intended to use the OTS send their requests with their preferred tracks and flight levels, and oceanic air traffic controllers assign OTS flights to conflict-free tracks and flight levels based on the traffic condition. This study evaluates three methods of flight assignments to the OTS tracks. The first method is a heuristic algorithm used by oceanic ATC as the current procedure. This approach is based on a greedy algorithm as a ”first request, first assign” method. If the requested assignment (i.e., track and flight level) is not conflict-free, the oceanic controllers check the feasibility of other assignments considering the requested track and lower flight levels up to 3000 feet and higher flight levels up to 1000 feet. If these alternatives are not feasible, controllers start checking assignment alternatives in other tracks.

The second approach is an individual assignment algorithm based on using cost matrices which show

the fuel consumption for all combinations of tracks and flight levels. In this method, controllers check the assignment alternatives based on their priorities derived from the cost matrices. The third approach is the group base assignment method using a metaheuristics optimization algorithm to minimize the total fuel consumption for the flights in an entry zone before the OTS tracks. This method is based on the collaborative decision-making concept that encourages airlines to share the required information (e.g., OTS assignment priorities) with air navigation service providers.

In this study, a mathematical model for the group assignment procedure is provided and a metaheuristics optimization algorithm is proposed for the solution methodology for the following reason: First, the time complexity analysis proves that the order of growth for this optimization problem is exponential. Second, the historical data provided by "NAV Canada" shows that the size of this problem is large in congested traffic periods. Third, oceanic air traffic controllers as the ultimate decision-maker need to have high-quality solutions in a reasonable computational time. Considering all these aspects, Simulated Annealing (SA) as one of the single-solution metaheuristics optimization algorithms is selected for solving the group assignment procedure. The reason for choosing a single-solution algorithm is the availability of a good initial solution as the requested tracks and flight levels derived from cost matrices.

The proposed algorithm is validated with a small size problem verifying it can find the global optimal in reasonable computational time. Then, the validated optimization algorithm is implemented inside the Global Oceanic Model which is a fast-time flight simulation tool. This study used the real-scale flight traffic related to three consecutive days on June 24-25-26, 2016. The other inputs are the eastbound and westbound OTS configuration, and the wind data sets for the selected dates. This study simulated the flight traffic in three scenarios with the mentioned OTS assignment logic. The simulation results show the operational benefits of the proposed group assignment procedure in terms of efficiency, level of service, and airline equity.

First, the results show 108 kilograms of average fuel consumption savings and 341 kilograms of average greenhouse gas emission savings using the group assignment (metaheuristics) method compared to the existing track assignment (heuristics) method. The estimated annual fuel consumption savings could reach 26.5 million kilograms and 15.5 million dollars assuming 320 operational days

per year and $1.82 per gallon as the average jet fuel price (2019). Second, the results demonstrate that there is a 15% increase in the level of service among the current system and the proposed procedure. This study defined the level of service as the percent of flights that achieve their optimal (requested) track and flight level. Third, standard deviations of the level of service for selected airlines in the advanced scenario show 9.6% and 5.8% reductions compared to the existing procedure for eastbound and westbound flights, respectively. This study provides insight into the number of assignment priorities which are required to be shared with air navigation service providers for implementing the group assignment procedure. This study shows that 99% of flights are assigned to the organized track system within the first ten assignment priorities derived from cost matrices.

Chapter 4

In-Trail Procedure for Improved Oceanic Air Traffic Operations

The main content of this chapter is from the following papers. Arman Izadi is the first author of the papers and the research is done during his enrollment at Virginia Tech.

- Izadi, A., Hinze, N., Trani, A., and Post, J. A., "In-Trail Procedure for Improved Oceanic Air Traffic Operations," AIAA Aviation 2019 Forum, 2019, p. 2829.

  doi:https://doi.org/10.2514/6.2019-2829.

- Izadi, A., Hinze, N., and Trani, A. A., "Validating Simulations of Oceanic Flights Using Data Link Communication Messages," 2019 Integrated Communications, Navigation and Surveillance Conference (ICNS), IEEE, 2019, pp. 1–12,
   doi:https://doi.org/10.1109/ICNSURV.2019.8735264.

4.1 Introduction

The adoption of reduced oceanic separation standards using technologies such as Automatic Dependent Surveillance-Broadcast (ADS-B) promises to save fuel, reduce emissions, and cut costs for aircraft operators. For several years, the FAA has been evaluating the benefits of reduced oceanic separations using computer simulation models to support infrastructure and avionics investment decisions. Reduced oceanic separation could be particularly relevant to the United States because of the vast oceanic areas controlled by Oakland, New York, and Anchorage Air Route Traffic Control

Centers (ARTCC) [26]. The FAA is developing some airborne ADS-B applications that are expected to provide benefits to operators who choose to equip their aircraft with appropriate avionics including “ADS-B In” (i.e., the ability to receive, process, and display ADS-B data from surrounding aircraft). One such airborne ADS-B application is ADS-B In-Trail Procedures (ITP). ITP is an advanced ”ADS-B In” application that leverages the benefits of ADS-B and allows ITP-equipped aircraft to fly more often at optimal or less turbulent flight levels during oceanic flights [1].

4.2 In-Trail Procedure

Maintaining optimal cruise altitudes for oceanic flights requires many altitude changes since saving fuel consumption is related to flying at optimal flight levels considering wind conditions and turbulence. Aircraft operating in oceanic airspace may end up flying at non-optimal flight levels due to conflicting traffic either at the desired flight level or at flight levels between the current flight level and the optimal flight level. The ADS-B ITP is an application for airborne traffic situational awareness providing more efficient altitude change procedures.

ITP-equipped aircraft and trained flight crews can request ITP maneuvers to their preferred flight level instead of being ”trapped” at a fixed flight level by other aircraft flying in the vicinity. Flight crews flying ITP-equipped aircraft can determine if a safe climb or descent can be performed under ITP criteria and air traffic controllers which has the total traffic picture authorize the ITP requests [40]. In the ITP operation, the maneuvering aircraft (ITP aircraft) obtains the flight identification, altitude, position, and ground speed transmitted by nearby equipped non-maneuvering aircraft (reference aircraft). Based on the precise ADS-B data from the reference aircraft, pilots can make an ITP flight level change request when the separation with potentially blocking aircraft is less than the standard separation minima and greater than the ITP separation criteria (15 nautical miles). If the air traffic controllers determine that standard separation minima will be met with all aircraft except the ITP and reference aircraft, clearance for the climb or descent can be granted. Then, the ITP aircraft can vertically go through the altitude of the reference aircraft [13]. Figure 4.1 shows the terminology of the ITP operation.

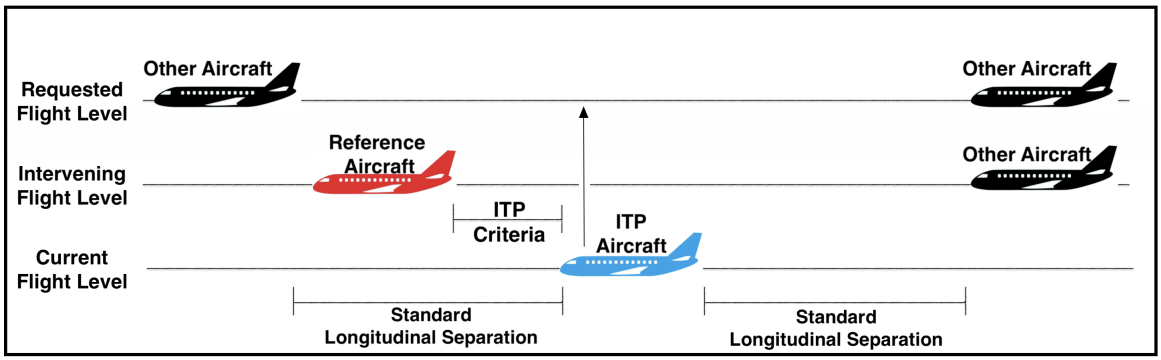

Figure 4.1: ITP terminology.

ADS-B ITP includes of a set of six flight level change geometries which each geometry dictated by whether the ITP aircraft desires to climb or descend and its proximate relationship with the other aircraft. Figure 4.2 shows all the combinations of ITP geometries [13]. The "ITP aircraft" is the blue aircraft with the arrow indicating climb or descend and the red aircraft are "reference aircraft."

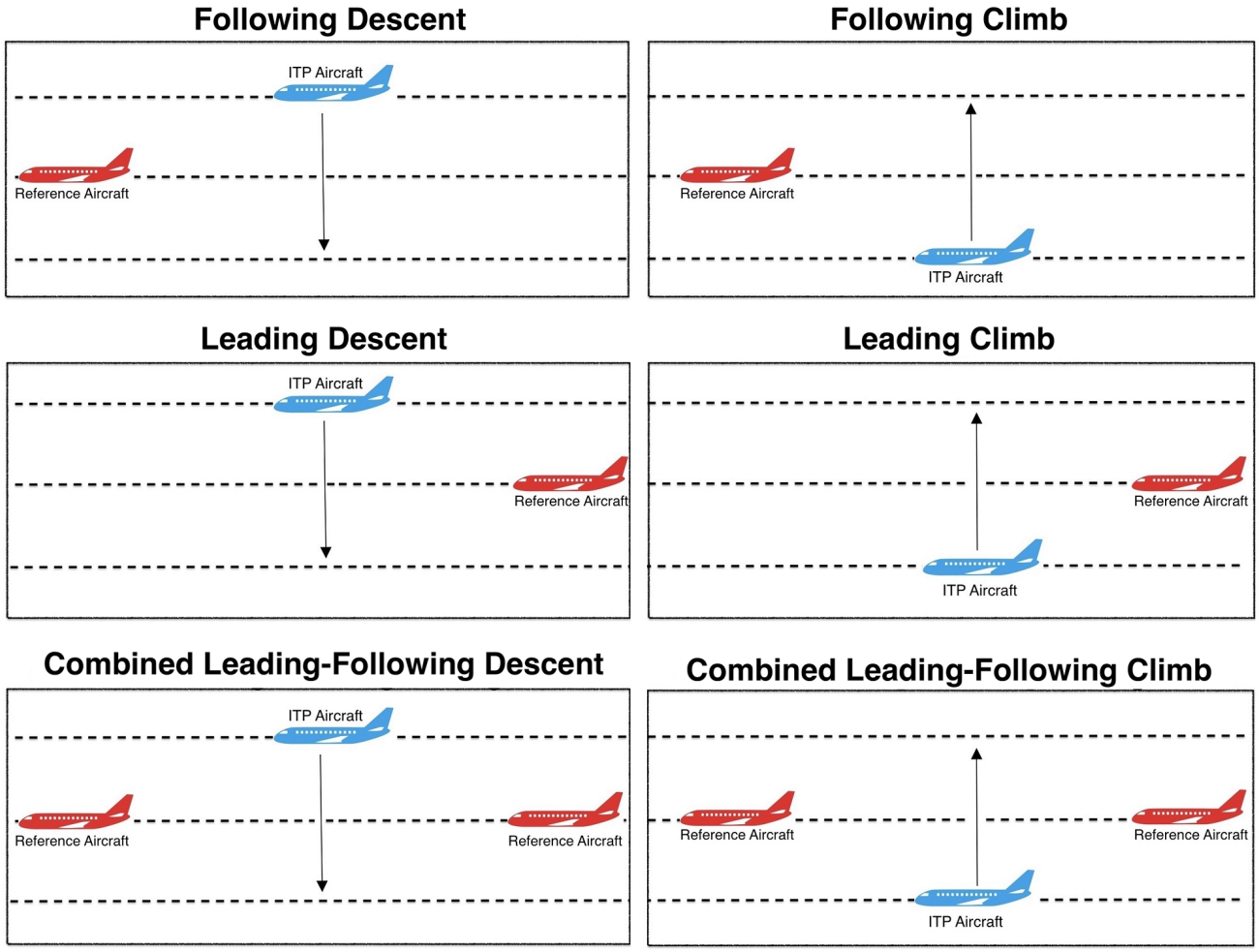

Figure 4.2: ITP geometries.

While there is no limit of the total climbs authorized in the ITP flight level changes, the other aircraft cannot be more than 2,000 feet above or below the ITP aircraft. In the ITP operation, the maneuvering aircraft (ITP aircraft) obtains the flight identification, altitude, position, and ground speed transmitted by proximate ADS-B equipped non-maneuvering aircraft (reference aircraft). Based on the precise ADS-B data from the reference aircraft, pilots can make an ITP altitude change request to air traffic controllers. If the controllers determine that standard separation minima will be met with all aircraft other than the ITP and reference aircraft, clearance for the climb or descent can be granted. Then, the ITP aircraft can vertically go through the altitude of the reference aircraft [13].

The FAA is implementing software changes to the Advanced Technologies and Oceanic Procedures (ATOP) system at the Oakland, New York and Anchorage facilities to take advantage of ITP capability. ITP procedures have been tested in oceanic trials by United Airlines with promising results. According to the FAA operational trials with Boeing 747-400 aircraft in the Pacific oceanic airspace, ADS-B-In/ITP-equipped aircraft saved an average of 573 pounds (260 kilograms) of fuel per flight [1].

Air Transportation Systems Laboratory at Virginia Tech expanded the scope of the GO Model to include all the U.S. oceanic airspace (e.g., Atlantic and Pacific). To address the task of simulating diverse Flight Information Regions (FIRs) with distinct separation standards, the GO Model was modified to include multi-region simulation capabilities with multiple separation standards and various aircraft equipage levels. For accommodating ITP operations, the GO Model is enhanced with a module checking all the requirements for a cleared ITP operation based on the updated air traffic organization policy (ORDER JO 7110.65X) [38].

A summary of the ITP criteria in the GO Model is as follows :

1. The ITP climb or descent shall be requested by the pilot.
2. The altitude difference between the ITP aircraft and any reference aircraft shall be 2000 ft or less.
3. The maximum reference aircraft is two and they can be any combination of ahead or behind

the ITP aircraft.

4. The reported ITP distance between the ITP aircraft and any reference aircraft is 15 NM or more.
5. The maximum closing speed between the ITP aircraft and each reference aircraft shall be Mach 0.06.
6. Both the ITP aircraft and reference aircraft are on the Same tracks or any turn shall be limited to less than 45 degrees.
7. No speed or route change clearance shall be issued to the ITP aircraft until the ITP climb or descent is completed.
8. No instruction to amend speed, altitude or route shall be issued to any reference aircraft until the ITP climb or descent is completed.
9. The ITP aircraft shall not be a reference aircraft in another ITP clearance.

4.2.1 Estimating ITP Distances and ITP Headings

Figure 4.3 shows the approach for calculating the ITP distance based on the angular difference between ITP and reference flight tracks [12]. In the GO Model, we implemented a user-defined parameter as "ITP Projection Length" to check the trajectory projections of both ITP and reference aircraft in the specified time interval. The default value for the ITP projection length is 10 minutes (∼80 nm). The GO Model checks for intersection points in the next 10 minutes of the trajectory projections. If there is no intersection point available, the model picks the Closest Point of Approach (CPA) among ITP and reference aircraft as the ITP distance.

The GO Model is developed to have the capability of multi-region, multi-separation, and multi-equipage modeling. In this study, the model is enhanced to assign user-defined equipage levels to ITP and reference aircraft in each FIR. Note that the GO Model can accept unlimited equipage levels and each equipage level can have its separations standard in each oceanic FIR.

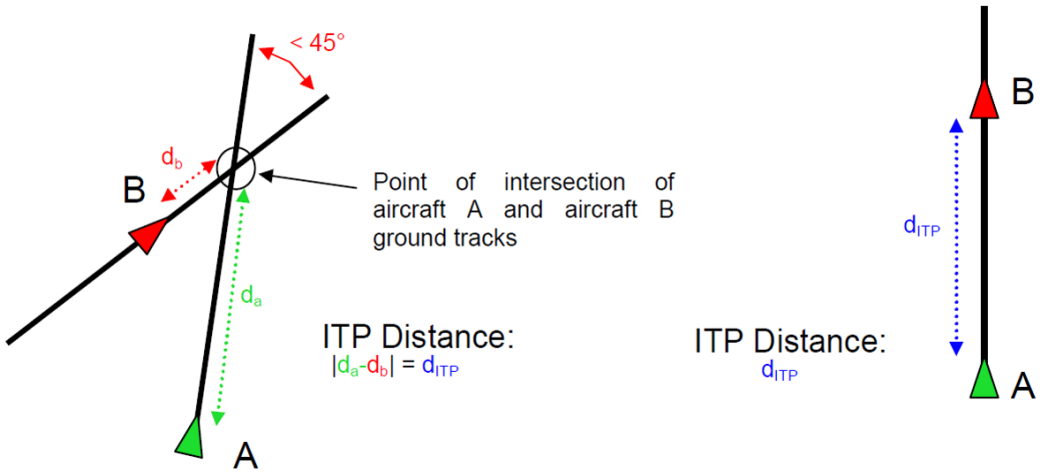

Figure 4.3: ITP distance calculation.

4.2.2 BADA 4.0 for Aircraft Performance Modeling

The GO Model is developed with a hybrid performance model including BADA 3.13 and BADA 4.0. The main aerodynamic model is BADA 3.13. In this study, we improved the GO Model to include a comprehensive list of jets and turboprops for 192 aircraft types. Also, Virginia Tech Air Transportation Systems Laboratory in collaboration with MIT Air Transportation Center developed optimized cost index tables in the aircraft performance model. We developed the GO Model with a variable Mach number optimization routine derived from the BADA 4.0 model for 24 aircraft types. This functionality enables the GO Model to find and assign the optimal Mach number to a given aircraft type for a variety of mass, altitude, and wind speeds during the simulation [44].

In practice, pilots are aware of aircraft weight restrictions and cost index conditions associated with climbs. Improvements to the GO Model substituted the time-set approach controlled by the user with a state-variable algorithm that makes decisions more intelligently and only when climbs are feasible. In the GO Model, the pilot's decisions to pursue climbs are determined by improvements in the Specific Ground Range (SGR) values in the cost tables. A pilot may not attempt a climb if improvements to SGR are not possible even if it is operationally feasible to climb based on aircraft mass constraints. For aircraft types lacking optimized cost tables, the model calculates the fuel consumption to the exit point of the oceanic boundary and decide about climb alternatives based

on fuel consumption.

4.3 Modeling Scenarios

For this study, six scenarios are considered based on three traffic demand sets related to both Pacific and North Atlantic oceanic airspace. The FAA provided Virginia Tech Air Transportation Systems Laboratory with a list of scenarios associated with the Advanced Surveillance Enhanced Procedural Separation (ASEPS) program for the Pacific and North Atlantic regions. The GO Model uses three consecutive days of traffic to load the airspace network and simulate the traffic realistically [23]. The results reported in this study are those associated with flights in the middle day of the simulation. The seed days of Traffic Flow Management System (TFMS) data used in this analysis are:

1. Pacific Demand Set: November 18, 2014
2. Pacific Demand Set: December 27, 2015
3. North Atlantic Demand Set: June 25, 2016

Table 4.1 shows the proposed scenarios with lateral and longitudinal separations for both equipped and not-equipped aircraft pairs.

Table 4.1: Modeling scenarios.

	Scenarios					
Metrics	**1**	**2**	**3**	**4**	**5**	**6**
Oceanic Airspace	Pacific	Pacific	Pacific	Atlantic	Atlantic	Atlantic
Traffic Year	2014	2015	2015	2016	2016	2016
Average Equipage Level	77 %	78 %	100 %	100 %	100 %	100 %
Daily Number of Free Flights	586	667	667	1439	2211	1439
Lat/Lon minima for Equipped Pairs (nm)	30/30	30/30	30/30	30/30	30/30	15/15
Lat/Lon minima for Non-Equipped Pairs (nm)	50/50	50/50				

The FAA published regulations that mandated all aircraft operating in designated airspace should be equipped with "ADS-B Out" by January 1, 2020. Based on the in-progress initiatives in the U.S. airspace, this study assumes all the airlines will equip their aircraft with advanced avionics (e.g., Future Air Navigation System (FANS 1/A) and controller-pilot datalink technology) in the

Pacific and North Atlantic airspace by 2020 [11]. Figure 4.4 demonstrates the simulation boundary for both the Pacific and North Atlantic oceanic regions. Pacific airspace has one FIR (Oakland), and North Atlantic airspace includes eight FIRs including New York West, New York East, Gander, Shanwick, Santa Maria, Reykjavik, Sondrestrom and Bodo.

Other GO Model assumptions considered in the simulation of the traffic for this analysis are:

- The simulation time-step for evaluating aircraft states (distance traveled, mass, and altitude) is ten seconds.
- The traffic in all the scenarios is projected to the year 2020.
- The horizon time interval for air traffic controllers detecting potential conflicts is five minutes.
- A rectangular separation envelope is considered in conflict detection and resolution algorithm.
- NCAR Reanalysis 2 wind model developed by National Oceanic and Atmospheric Administration (NOAA) is used.
- The flight plan generator module is employed to generate wind-optimal flight plans for flights in North Atlantic scenarios.
- BADA aircraft performance model 3.13 and 4.0 with 192 aircraft types are employed in the simulation.

According to the hemispherical rules, eastbound flights should cruise at odd flight levels, and westbound flights should cruise at even flight levels. A visit to New York and Oakland oceanic centers provided insight on the use of hemispherical rules in oceanic regions. In the Pacific Ocean, many long-distance flights do not follow hemispherical rules. In the Atlantic Ocean, hemispherical rules are used more often. In this study, four cases are simulated for each scenario to measure the operational benefits of ITP maneuvers. We simulated two cases with and without hemispherical rules and two cases with enabling and disabling ITP operations. In this analysis, the GO Model considers the ITP operations related to climbs. Figure 4.5 shows the fleet mix of traffic in the middle day of the simulation (December 27, 2015) with a forecast to the year 2020. According to the TFMS data, most of the aircraft operating in Pacific Oceanic airspace are wide-body twinjets.

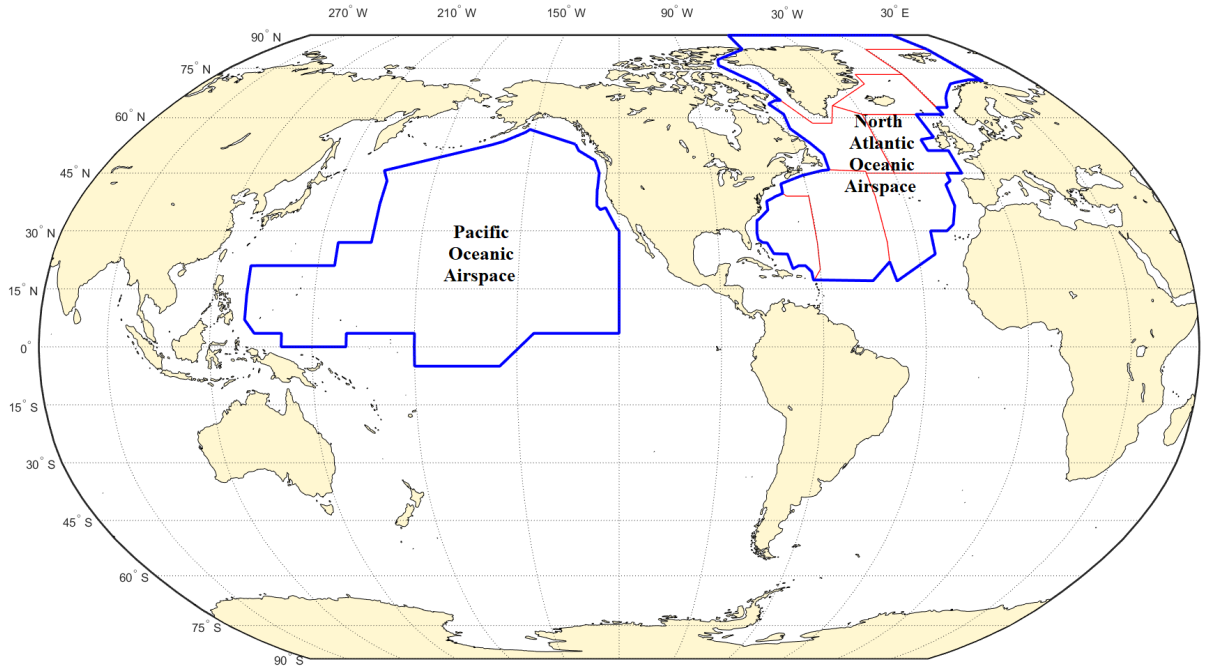

Figure 4.4: Simulation domain.

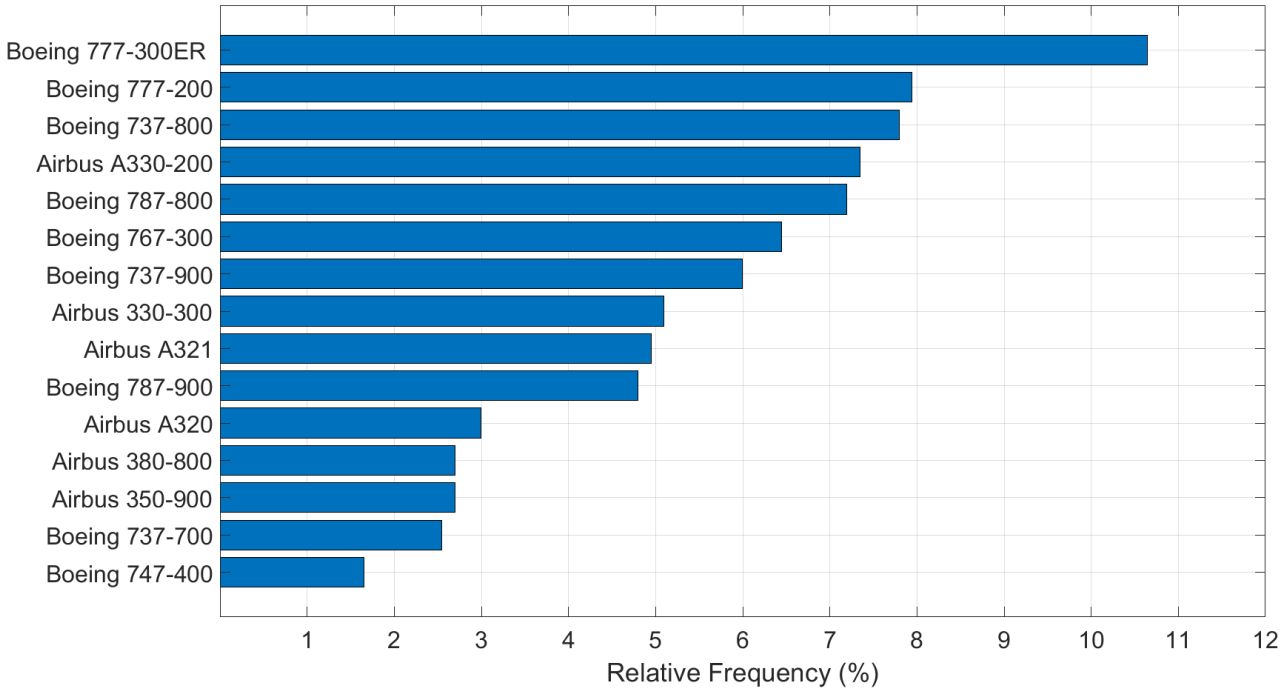

Figure 4.5: Fleet mix of 667 flights on December 27, 2015, in the Pacific oceanic airspace.

4.4 Modeling Results

The GO Model uses a numerical step size of ten seconds to update the flight state variables including altitude, distance, and aircraft mass. Flights were allowed to climb inside and outside the oceanic areas to evaluate the operational benefits for the entire flight trajectories. Table 4.2 shows the number of ITP operations and average fuel consumption savings for the ITP aircraft and affected aircraft with and without considering hemispherical rules. The flights either executed ITP maneuvers or got impacted by ITP maneuvers of other flights are considered as affected flights.

Table 4.2: Scenario results summary.

		Scenarios					
Measures		**1**	**2**	**3**	**4**	**5**	**6**
Number of ITP Operations Not Considering Hemispherical Rules	Granted ITP	4	8	9	18	62	2
	Requested ITP	8	13	11	70	487	4
Average Fuel Consumption Benefit Not Considering Hemispherical Rules (kg)	ITP Flights	161	137	132	166	230	58
	Affected Flights	122	96	104	76	111	58
Number of ITP Operations Considering Hemispherical Rules	Granted ITP	3	5	3	14	57	1
	Requested ITP	16	24	11	84	595	2
Average Fuel Consumption Benefit Considering Hemispherical Rules (kg)	ITP Flights	415	305	336	292	462	670
	Affected Flights	190	68	336	145	237	670
Average Fuel Consumption Benefit of ITP Flights (kg)		288	221	234	229	346	364
Average Number of Climbs		551	773	800	1131	1707	1131
ITP Climbs Percentage		**0.6%**	**0.8%**	**0.8%**	**1.5%**	**3.5%**	**0.1%**
ITP Operations Percentage		**0.8%**	**1.3%**	**0.9%**	**1.1%**	**2.7%**	**0.1%**

In scenarios 4 and 6, 772 flights used the Organized Track System (OTS) in the North Atlantic airspace. OTS flights are not simulated in these scenarios. In Scenario 5, OTS flights are included in the simulation and modeled as User-Preferred Route (UPR) flights. We assume an equal chance of using hemispherical rules in the oceanic airspace. The average fuel consumption benefits of ITP flights in scenarios with and without hemispherical rules determine the "Average Fuel Consumption Benefit of ITP Flights". As an example, the average of 137 kilograms and 305 kilograms is 221

kilograms reported as the average fuel consumption benefits of ITP flights in Scenario 2.

"ITP Climb Percentage" is defined as the average number of granted ITP climbs divided by the total number of climbs. In Scenario 2, there are 5 and 8 granted ITP climbs in cases with and without hemispherical rules, and 773 is the average number of climbs. So, "ITP Climb Percentage" is calculated as $((8+5) \div 2) \div 773 = 0.8\%$. In the simulated scenarios, all the flights which executed ITP maneuvers had one ITP climb in their flight path. "ITP Operations Percentage" shows the ratio of the average number of flights executed ITP maneuvers to the number of equipped flights. The number of equipped flights is defined based on the total number of flights and the average equipage level. In Scenario 2, the number of eligible flights for ITP maneuvers is ($0.78 \times 667 = 520$ flights), and the "ITP Operations Percentage" is defined as $((8 + 5) \div 2) \div 520 = 1.3\%$.

Note that flights can request the ITP operation only when the lateral and longitudinal separations with other aircraft are less than the standard separation minima and greater than the ITP separation criteria (15 nautical miles). This is the main reason for the small probability of executing ITP operations. The results of scenarios with different daily traffic volumes show that the number of granted ITP operations grows nonlinearly with increasing the traffic. Comparing the North Atlantic traffic scenarios (Scenario 4 and Scenario 5), the percentage of ITP operations and ITP climbs grow 145% and 133% with increasing the demand by 53%. Also, comparing the results of the Pacific 2014 and 2015 demand sets (Scenario 1 and Scenario 2) shows that 63% and 33% increase in ITP operations and ITP climbs percentages derived from 14% traffic growth in the Oakland oceanic airspace.

Our results show that with equipping aircraft with ADS-B technology and reducing the separation minima to 15/15 nautical miles in the North Atlantic airspace in 2020, the ITP operation maneuvers will be reduced to 0.1% since most of the flights will execute climbs regarding the reduced standard separation minima. Figure 4.6 shows that 137 kilograms are the mean fuel consumption savings for ITP flights in Scenario 2 without considering the hemispherical rules. The number of ITP maneuver requests is 13. The ATC routine in the model accepted 8 of the ITP requests and rejected 5 of them due to traffic. Note that all the results are related to the middle day of the three-day simulation.

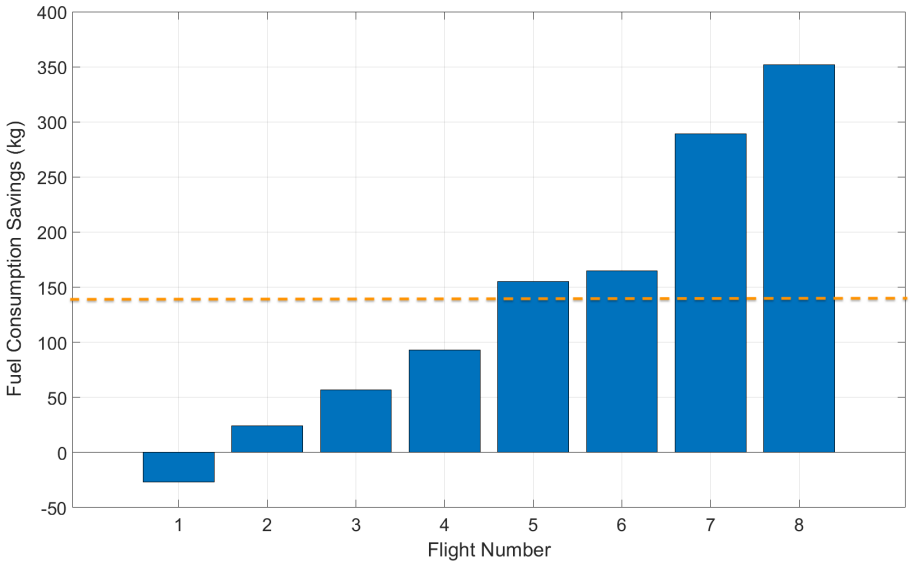

Figure 4.6: Fuel consumption saving for ITP flights (no hemispherical rules).

The results of the simulation can identify the affected flights by comparing the fuel consumption of all the flights in two cases with and without ITP operations. Figure 4.7 shows that 96 kilograms are the mean fuel consumption savings for affected flights in Scenario 2 which executed ITP maneuvers or got impacted by ITP maneuvers of other flights.

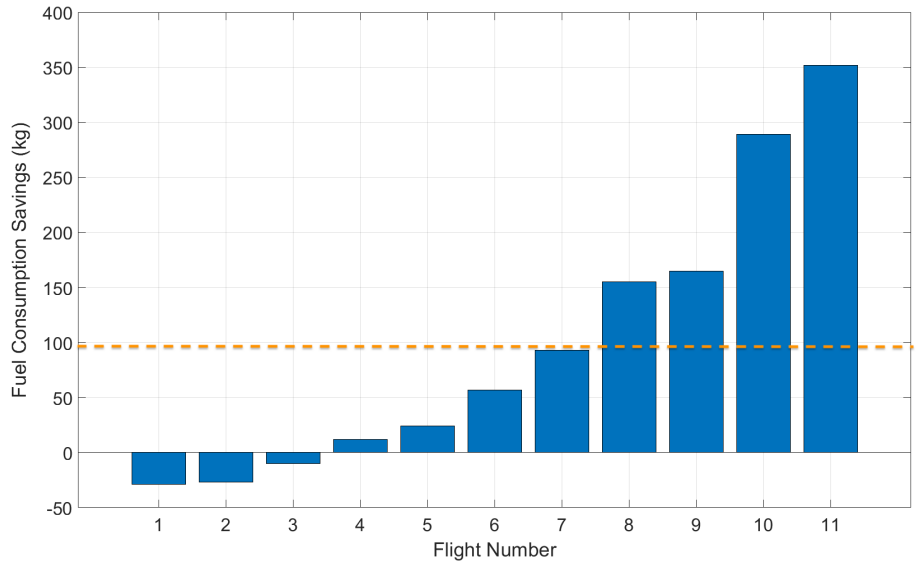

Figure 4.7: Fuel consumption saving for affected flights (no hemispherical rules).

Figures 4.8–4.9 show two examples of flights which executed ITP operations in the Pacific oceanic airspace. The main reason for fuel consumption savings in flights performed ITP climbs is that

they find the chance to have earlier step-climbs and burn less fuel at higher flight levels.

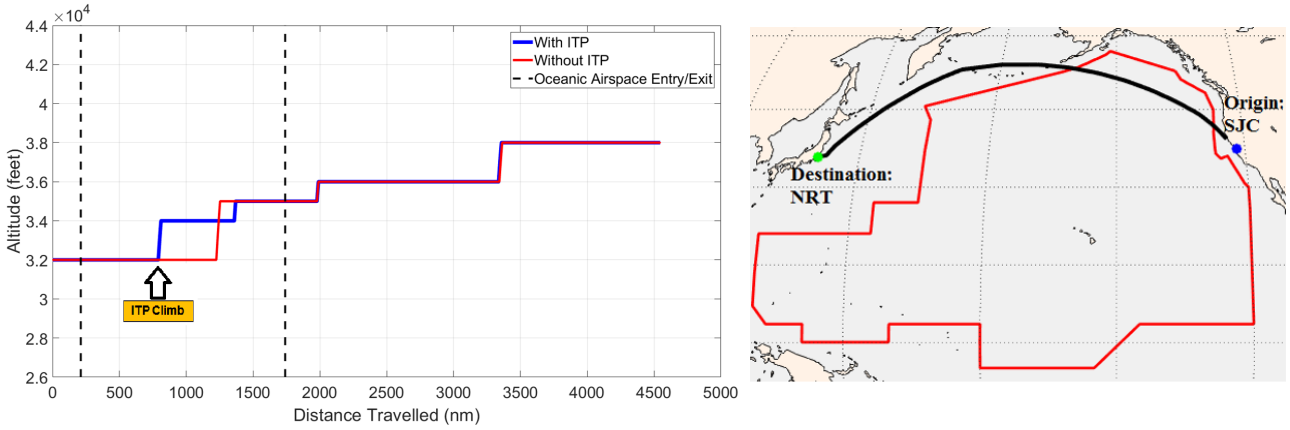

(a) Altitude profile. (b) Aircraft type: Boeing 787-900.

Figure 4.8: A sample flight with 155 kilograms fuel consumption benefit.

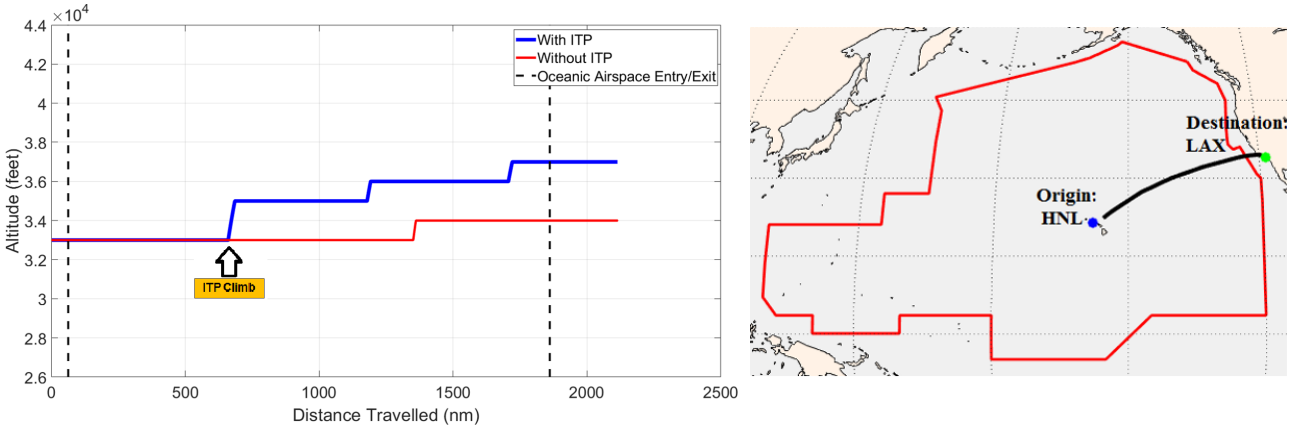

(a) Altitude profile. (b) Aircraft type: Airbus Airbus 321-200.

Figure 4.9: A sample flight with 350 kilograms fuel consumption benefit.

4.5 Validation

A critical phase in developing computer simulation models is validation. In this study, we used the communication messages between pilots and air traffic controllers from the Advanced Technology Oceanic Procedure (ATOP) system to validate the results of simulating ITP operations. For this purpose, forty-five days of Controller-Pilot Data Link Communication (CPDLC) messages related to the year 2014 in the Pacific Ocean are analyzed [24].

In this study, we employed a message dataset from the Advanced Technology Oceanic Procedure (ATOP) system. The data span 45 successive days (July 20 - August 3) in 2014 associated with Pacific airspace (Oakland Oceanic Center). The ATOP dataset contains two types of messages: Controller-Pilot Data Link Communication (CPDLC) and Automatic Dependent Surveillance-Addressable (ADS-A). CPDLC is a data link application allowing direct exchanges of text-based messages between air traffic controllers and pilots. Exchanging the messages among ground stations and aircraft significantly improves the communication capabilities compared to traditional voice communication. CPDLC communications reduce air traffic controllers' workloads. CPDLC messages contain pilots' requests for changing flight levels, performing lateral deviations due to traffic or weather events, and the air traffic controllers' responses to pilot requests. ADS-A messages are automatic aircraft position reports sent to the air navigation service provider showing aircraft position, altitude, time, temperature, wind speed, and ground speed.

As the first step, the CPDLC and ADS-A messages are parsed and sorted based on their received time. Then, four-dimensional (4-D) flight trajectories (i.e., latitude, longitude, altitude, time) are created using the messages. We defined the oceanic boundary for the traffic simulation in the Pacific Ocean consistent with the ATOP controlled area. Figure 4.10 shows the proposed six sectors (red lines) creating the Pacific oceanic boundary (black line). The blue points show the reconstructed flight trajectories based on the coordinates reported in the ATOP messages.

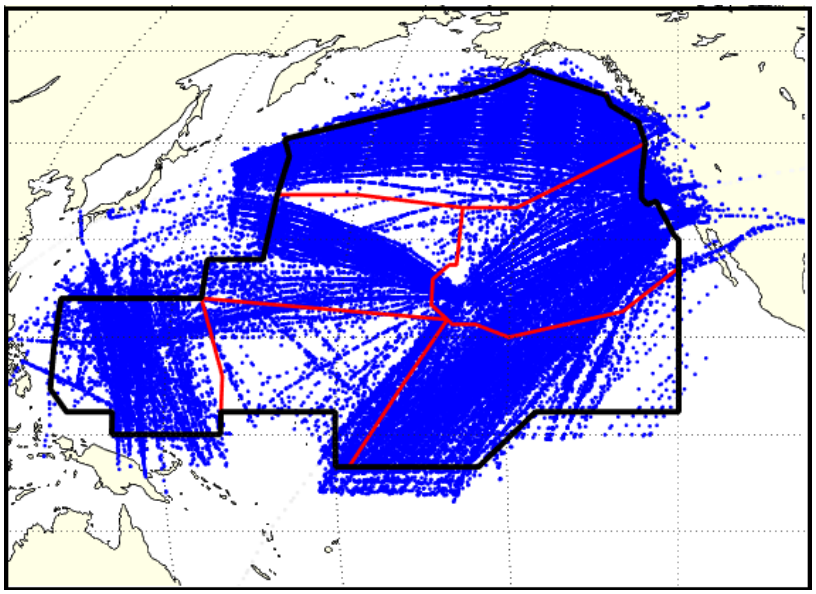

Figure 4.10: ATOP controlled airspace in the Pacific ocean.

To validate the aircraft's climb frequency, ATOP messages are used to reconstruct the altitude profiles. Figure 4.11 illustrates a flight example from Los Angles to Brisbane with a Boeing 777-300 ER. This figure demonstrates three step-climbs in Oakland Oceanic airspace. The red points show the reported altitude based on ADS-A messages. We analyzed 26,807 flight in 45 successive days in 2014 and calculated the number of step-climbs for each flight based on reconstructed altitude profile. Figure 4.12 shows the average number of step-climbs for the flights in the analysis period. The result shows 1.45 as the average number of step-climbs per flight in this period.

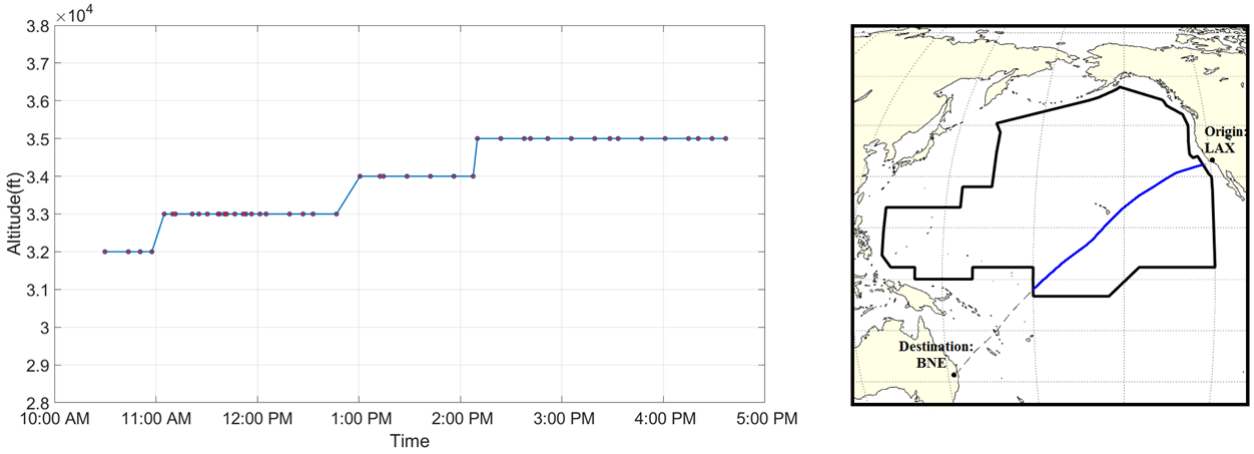

Figure 4.11: Example of a 4-dimensional flight trajectory.

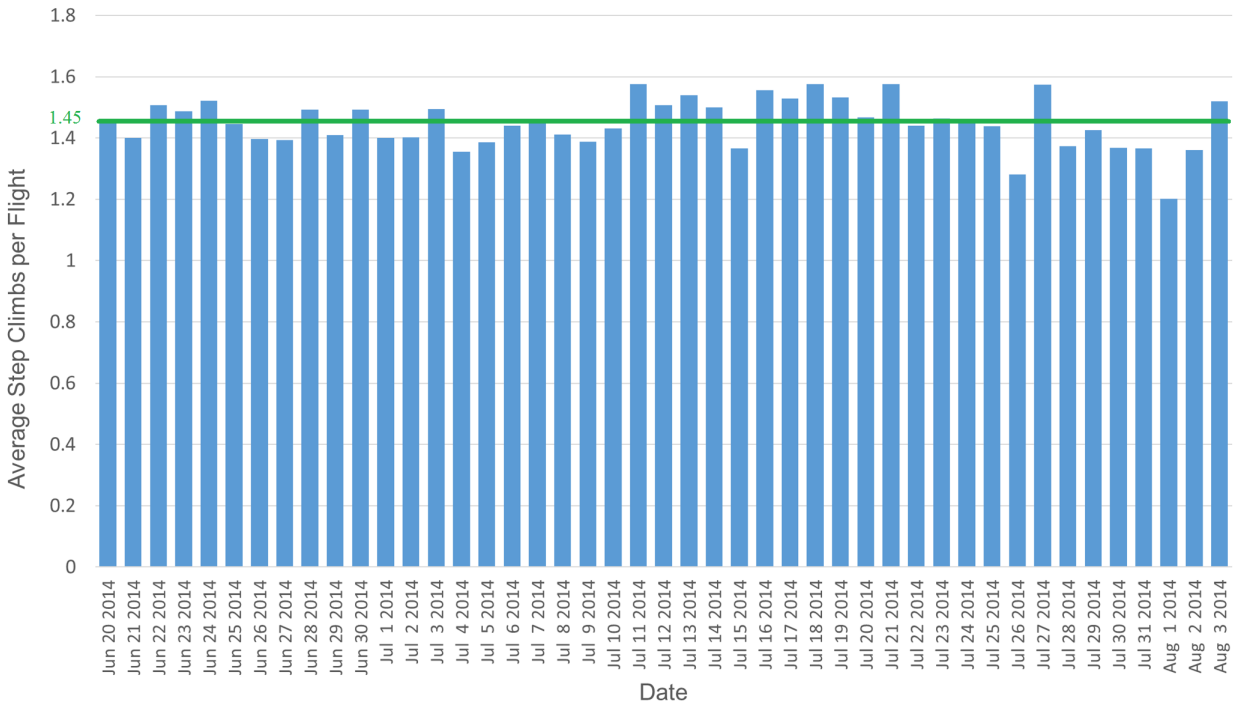

Figure 4.12: Distribution of average step climbs.

We examined the pilots' messages sent the ITP requests and analyzed ITP separations between ITP aircraft and reference aircraft in the CPDLC messages. Table 4.3 shows an example of messages exchanged between a pilot and an air traffic controller for an ITP operation clearance. The FAA

Table 4.3: Example of CPDLC messages.

Date	Time	Flight ID	CPDLC Message	Sender
July 12, 2014	9:40:07 AM	UAL838	REQUEST CLIMB TO F360	Pilot
July 12, 2014	9:40:07 AM	UAL838	ITP 19 NM BEHIND DAL284	Pilot
July 12, 2014	9:47:14 AM	UAL838	REPORT LEVEL F360	ATC
July 12, 2014	9:47:14 AM	UAL838	CLIMB TO AND MAINTAIN F360	ATC
July 12, 2014	9:47:55 AM	UAL838	WILCO	Pilot
July 12, 2014	9:50:32 AM	UAL838	LEVEL F360	Pilot

has implemented infrastructure changes to the ATOP system at the Oakland, New York, and Anchorage facilities to take advantage of ITP capability. United Airlines participated in evaluating the operational benefits of ITP operations in the Pacific oceanic airspace. Figure 4.13 shows the distribution of ITP separation in the Pacific traffic simulation and CPDLC messages. The minimum of ITP separation in both simulation results and CPDLC messages are 15 nautical miles. This is consistent with the ITP requirement in the air traffic organization policy.

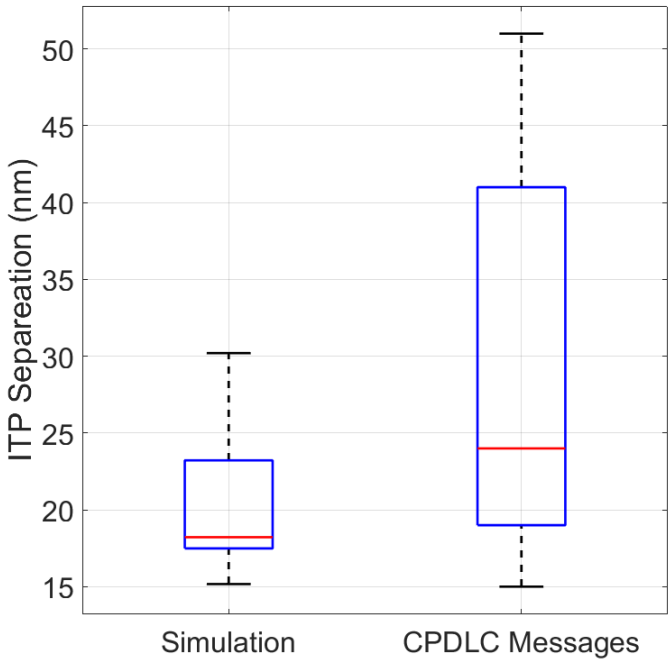

Figure 4.13: ITP separation comparison.

The ITP requests analyzed in CPDLC messages are associated with ITP operation trials by United Airlines using “Boeing 747-700” in the Pacific Ocean. The reason for the higher standard deviation of ITP separations in the CPDLC messages is that pilots requesting ITP procedures used conservative buffers above the minimum ITP separation in the trial operations.

4.6 Conclusions

One of the key technologies in modernizing the National Airspace System (NAS) and enhancing situational awareness is Automatic Dependent Surveillance-Broadcast (ADS-B). This study aims to quantify the operational benefits of the In-Trail Procedure (ITP) as one of the advanced surveillance procedures using the Global Oceanic Model- a fast-time computer simulation tool. This procedure allows ITP aircraft (equipped with ”ADS-B In” technology) to have reduced lateral and longitudinal separations with reference aircraft (equipped with ”ADS-B Out” technology) while climbing or descending to requested flight levels.

According to the FAA evaluations, the percentage of performed ITP maneuvers compared to ITP capable flights in the Pacific Ocean between August 2011 and June 2014 is 1.01%. Based on the simulation results, the ratio of the average granted ITP operations compared to equipped flights is 0.8% and 1.1% for 2014 and 2015 Pacific traffic demand. The results of simulating the ITP maneuvers for North Atlantic demand set (2016) show that the number of granted ITP operations grows nonlinearly with increasing the traffic. Based on the results, the ITP operations percentage and ITP climb percentage grow 145% and 133% with increasing the demand by 53%, respectively. Also, comparing the results of the Pacific 2014 and 2015 demand sets, 63% and 33% increase in ITP operations percentage and ITP climbs percentage derived from 14% traffic growth in the Oakland oceanic airspace.

Based on the FAA’s operational trials with Boeing 747-400 in the Pacific Ocean, ITP-equipped aircraft saved an average of 260 kilograms of fuel per flight. The results of simulating the 2014 and 2015 traffic in the Pacific Ocean show that 248 kilograms are the average fuel consumption saving when the traffic either following or not following the hemispherical rules with the same probability.

This study employed the text-based communication messages between pilots and air traffic controllers to validate the results of traffic simulations in the Pacific Ocean. The messages dataset is derived from the Advanced Technology Oceanic Procedure (ATOP) system containing Controller-Pilot Data Link Communication (CPDLC) and Automatic Dependent Surveillance-Addressable (ADS-A) messages in the Oakland Oceanic Center.

Acknowledgments

This project was executed as part of the National Center of Excellence for Aviation Operations Research (NEXTOR II) consortium. Special thanks to Joseph Post from the Federal Aviation Administration Office of NAS systems Engineering and Integration for the technical and financial support of this work. Any opinions, findings, and conclusions presented herein do not necessarily reflect the views of the FAA

Chapter 5

Summary

5.1 Summary of Results

As this dissertation comes to close, it is important to review its contributions. This dissertation focused on improving flight operations in the oceanic and remote airspace. All the research effort done in this work has been implemented and tested inside a fast-time simulation tool (i.e., Global Oceanic model), developed by Air Transportation Systems Laboratory at Virginia Tech.

The first research study was associated with the benefit analysis of a novel weather application providing near real-time, satellite-based meteorological information to flights in remote and oceanic regions. This project is sponsored by the Federal Aviation Administration (FAA) Weather Technology in the Cockpit (WTIC) program. This effort is called the Remote Oceanic Meteorology Information Operational (ROMIO) demonstration. This study quantified the operational benefits of the ROMIO demonstrations using two approaches: 1) statistical flight analysis, and 2) simulation-based analysis. In the first approach, 18,326 historical flights crossing Inter-Tropical Convergence (ITCZ) are studied. The statistical analysis shows the benefits of ROMIO-aided strategic decision making and having earlier deviation maneuvers for convective weather avoidance. The statistical t-tests with a 95% confidence level prove that 1) the deviation maneuvers in the Post-ROMIO period have lower deviation angles in comparison to the Pre-ROMIO period, 2) the average lateral deviation in the Post-ROMIO period is less than the Pre-ROMIO period.

In the second approach, the Global Oceanic (GO) model which is a fast-time simulation tool is employed to simulate real-scale traffic exposing convective weather in the oceanic airspace. The simulation results show that providing satellite-based meteorological information using the ROMIO

demonstration gives the oceanic flights more strategic decision-making advantages for avoiding convective weather events. In terms of efficiency, flights in ROMIO-enabled Scenario executed fewer deviation maneuvers with lower average deviation angles and lateral deviations. Comparing the ROMIO-enabled Scenario with 30-minute look-ahead horizon and the onboard radar with 20-minute look-ahead horizon shows the following average benefits: 115 kilograms fuel consumption savings, 14 nautical miles travel distance savings, 1.8 minutes average travel time savings, and 363 kilograms greenhouse gas emissions savings. The annual fuel consumption savings for three participating airlines (i.e., DAL, UAL, AAL) could reach 15.3 million kilograms of fuel consumption and 8.97 million dollars, considering $1.82 per gallon as the jet fuel price in 2019. The annual saving of carbon dioxide is 48.3 million kilograms, and the social cost of carbon could reach 2.4 million dollars.

In terms of safety, flights in the ROMIO-enabled Scenario generated less potential workload for air traffic controllers, and flights had less exposure to convective weather areas.

The second research effort provides an optimization technique for improving the current system of flight assignments to Organized Track System (OTS) in the North Atlantic airspace. Due to the size and complexity of this problem, and the restriction of computational time for oceanic air traffic controllers, a metaheuristics optimization algorithm is used for solving the group assignment procedure. The proposed algorithm shows the operational benefits in terms of fuel consumption savings, growth in the level of services, and more airline equity collaborations. The simulation results show 108 kilograms of average fuel consumption savings and 341 kilograms of average greenhouse gas emission savings using the group assignment (metaheuristics) method compared to the existing track assignment approach. The estimated annual fuel consumption savings is 26.5 million kilograms and 15.5 million dollars assuming 320 operational days per year, and $1.82 per gallon as the average jet fuel price (2019). Second, the results demonstrate that there is a 15% increase in the level of service among the baseline and the advanced scenario. This study defined the level of service as the percent of flights that achieve their optimal (requested) track and flight level. Third, standard deviations of the level of services for airlines in the advanced scenario show 9.6% and 5.8% reductions compared to the baseline scenario for eastbound and westbound flights, respectively

The third research area studies the potential benefits of a novel surveillance operation, In-Trail Procedure (ITP). ITP is an advanced ADS-B In application that allows flights to fly more often at optimal or less turbulent flight levels. This procedure allows ITP aircraft (equipped with "ADS-B In" technology) to have reduced separations with reference aircraft (equipped with "ADS-B Out" technology) while climbing or descending to requested flight levels. The results of simulation using the GO Model were consistent with the FAA evaluations derived from the operational trials of United Airlines using Boeing 747-400 aircraft in the Pacific Ocean. The results of simulating the 2014 and 2015 traffic in the Pacific Ocean show approximately 1% of the flight can benefit the ITP operations and save on average 248 kilograms fuel consumption. Also, the results of traffic simulation in the North Atlantic airspace show that the percentage of ITP operations grows nonlinearly with increasing the traffic.

5.2 Recommendations for Future Research

1. The ROMIO demonstration is a now-casting weather application. The results show that the ROMIO-enabled scenario with 10 minutes additional look-ahead horizon beyond the onboard radar scenario provides the best operational benefits. The recommendation for improving the ROMIO application is adding the forecast capability enabling the flight to take advantage of forecasted weather data on convective weather alerting. Some suggestions to enhance the ROMIO demonstration are improving the fidelity of CDO and CTH contours, displaying the aircraft position on the ROMIO application, and adding wind vectors (i.e., speed and direction of winds) to CDO and CTH contours.

2. It is recommended that oceanic air traffic controllers implement and test the proposed group assignment procedure using the metaheuristic optimization algorithm in the real-world. The proposed algorithm is computationally fast and can provide high-quality assignment solutions is a reasonable time. The objective function of the proposed algorithm is the minimization of total fuel consumption. Other alternatives for the objective function of the group assignment procedure are minimizing total travel time and total time-related operational cost, and

maximizing airline equity collaborations.

3. In this study, we evaluate the operational benefits of ITP climb procedures for better fuel efficiency. It is recommended to improve the GO Model to study the safety benefit of ITP descends for avoiding turbulent altitudes. According to the Advisory Circular for thunderstorms (AC-0024C), clear air turbulence can occur beneath the anvil of a large cumulonimbus. Cloud Top Height (CTH) is one of the ROMIO weather products displaying cloud top contours at flight altitudes of FL320, FL340, FL360, FL380, and FL400. Future researches can investigate ITP operations using the CTH contours to avoid anvil clouds, thunderstorms, and turbulent altitudes.

   The GO Model has been enhanced to simulate flights with an unlimited number of equipage levels. Each equipage level can have specific lateral and longitudinal separations, maximum operational altitudes, and parameters related to the step-climbs. In future studies, it is suggested to consider multiple equipage levels related to different communication, navigation, and surveillance technologies.

Bibliography

[1] ADS-B, In Trail Procedures (ITP). <https://www.faa.gov/nextgen/programs/adsb/pilot/itp/>. [Page last modified: October 27, 2016 10:20:29 AM EDT].

[2] FAA Advisory Circular, AC 00-24C (Thunderstorms). <https://www.faa.gov/documentlibrary/media/advisory_circular/ac%2000-24c.pdf>, 2013.

[3] What is the ITCZ and why does it matter? <http://www.oceannavigator.com/November-December-2017/ITCZ-and-why-it-matters/>, 2017.

[4] ROMIO Application Viewer. <https://wtic-romio.bcisse.com/romio/>, 2019.

[5] Fu Ali, Lei Xiujuan, and Xiao Xiao. The Aircraft Departure Scheduling Based on Particle Swarm Optimization Combined with Simulated Annealing Algorithm. In *Evolutionary Computation, 2008. CEC 2008.(IEEE World Congress on Computational Intelligence). IEEE Congress on*, pages 1393–1398. IEEE, 2008.

[6] Michael O Ball, Robert Hoffman, D Lovell, and Avijit Mukherjee. Response Mechanisms for Dynamic Air Traffic Flow Management. In *Proceedings of the 6th Europe-USA ATM Seminar. Baltimore. US*, 2005.

[7] Dong Bing and Du Wen. Scheduling Arrival Aircraft on Multi-Runway Based on an Improved Artificial Fish Swarm Algorithm. In *2010 International Conference on Computational and Information Sciences*, pages 499–502. IEEE, 2010.

[8] Eric Bonabeau and Christopher Meyer. Swarm Intelligence: A Whole New Way to Think About Business. *Harvard business review*, 79(5):106–115, 2001.

[9] Ivan Y Burdun and Oleg M Parfentyev. AI knowledge Model for Self-Organizing Conflict Prevention/Resolution in Close Free-Flight Air Space. In *Aerospace Conference, 1999. Proceedings. 1999 IEEE*, volume 2, pages 409–428. IEEE, 1999.

[10] EA Bustamante, CK Fallon, JP Bliss, WR Bailey III, and BL Anderson. Pilots' Workload, Situation Awareness, and Trust During Weather Events as a Function of Time Pressure, Role Assignment, Pilots' Rank, Weather Display, and Weather System. *International Journal of Applied Aviation Studies*, 5(2):347–367, 2005.

[11] Norma Campos, Thea Graham, Roy Grimes, and Kimberly Joyce. North Atlantic Data Link Mandate: Cost Impact to US Commercial Operators. In *TRB 92nd Annual Meeting, Washington, DC*, 2013.

[12] Ryan C Chartrand, Frank J Bussink, Thomas J Graff, and Kenneth M Jones. Operational Improvements From Using the In-Trail Procedure in the North Atlantic Organized Track System. 2009.

[13] Ryan C Chartrand, Katrin P Hewitt, Peter B Sweeney, Thomas J Graff, and Kenneth M Jones. In-Trail Procedure Air Traffic Control Procedures Validation Simulation Study. 2012.

[14] Cai-long Chen and Wen-bo Du. A Multi-Objective Crossing Waypoints Location Optimization in Air Route Network. In *Intelligent Systems and Applications (ISA), 2011 3rd International Workshop on*, pages 1–4. IEEE, 2011.

[15] Stephanie Chung, KImberly Noonan, and Joseph Post. NATSIM: A Systems Dynamics Model of North Atlantic Air Traffic. In *The 26th Congress of ICAS and 8th AIAA ATIO*, page 8912.

[16] Todd C Farley, R John Hansman, Mica R Endsley, Keith Amonlirdviman, and Laurence Vigeant-Langlois. The Effect of Shared Information on Pilot/Controller Situation Awareness and Re-route Negotiation. 1998.

[17] Eldridge Frazier, Cathy Kessinger, Tenny Lindholm, Bob Barron, Gary Blackburn, Jim Olivo, Bill Watts, Rocky Stone, Desmond Keany, Matt DeRis, et al. The Remote Oceanic Meteorology Information Operational Demonstration. In *2018 Integrated Communications, Navigation, Surveillance Conference (ICNS)*, pages 5A2–1. IEEE, 2018.

[18] Christine M Gerhardt-Falk, EA Elsayed, Dale Livingston, and Brian Colamosca. Simulation of the North Atlantic Air Traffic and Separation Scenarios-Communication Effects. Technical

report, Federal Aviation Administration Atlantic City NJ Airport and Aircraft Safety Research and Development, 2000.

[19] Thomas Grasse, Christina Schilke, and Jens Schiefele. Symbology Evaluation for Strategic Weather Information on the Flight Deck. In *Digital Avionics Systems Conference, 2008. DASC 2008. IEEE/AIAA 27th*, pages 4–B. IEEE, 2008.

[20] Aswin Gunnam, Antonio Trani, Tao Li, Thea Graham, and Norma Campos. Computer Simulation Model to Measure Benefits of North Atlantic Data link Mandates and Reduced Separation Minima. 14th AIAA Aviation Technology. In *Integration, and Operations Conference, American Institute of Aeronautics and Astronautics*, 2014.

[21] R John Hansman. The Effect of Shared Information on Pilot/Controller and Controller/Controller Interactions. In *New concepts and methods in air traffic management*, pages 143–159. Springer, 2001.

[22] Peter H Howard and Derek Sylvan. The Economic Climate: Establishing Expert Consensus on the Economics of Climate Change. *Institute for Policy Integrity*, pages 438–441, 2015.

[23] Arman Izadi, Nicolas Hinze, Antonio Trani, and Aswin K Gunnam. Measuring Fuel and Travel Time Benefits for the Caribbean Oceanic Flights Through Computer Simulations. In *2018 Aviation Technology, Integration, and Operations Conference*, page 4236, 2018.

[24] Arman Izadi, Nicolas Hinze, and Antonio Trani. Validating Simulations of Oceanic Flights Using Data Link Communication Messages. In *2019 Integrated Communications, Navigation and Surveillance Conference (ICNS)*, pages 1–12. IEEE, 2019.

[25] Arman Izadi, Nicolas Hinze, and Antonio Trani. Evaluating Air Traffic Controllers' Workload Through Computer Simulations. In *2019 Winter Simulation Conference (WSC)*, pages 3172–3183. IEEE, 2019.

[26] Arman Izadi, Nicolas Hinze, Antonio Trani, and Joseph A Post. In-Trail Procedure for Improved Oceanic Air Traffic Operations. In *AIAA Aviation 2019 Forum*, page 2829, 2019.

[27] Aleksandar Jevtić, Diego Andina, Aldo Jaimes, Jose Gomez, and Mo Jamshidi. Unmanned Aerial Vehicle Route Optimization Using Ant System Algorithm. In *System of Systems Engineering (SoSE), 2010 5th International Conference on*, pages 1–6. IEEE, 2010.

[28] Cathy Kessinger, Michael Donovan, Richard Bankert, Earle Williams, Jeffrey Hawkins, Huaqing Cai, Nancy Rehak, Daniel Megenhardt, and Matthias Steiner. Convection Diagnosis and Nowcasting for Oceanic Aviation Applications. In *Remote Sensing Applications for Aviation Weather Hazard Detection and Decision Support*, volume 7088, page 708808. International Society for Optics and Photonics, 2008.

[29] Scott Kirkpatrick, C Daniel Gelatt, and Mario P Vecchi. Optimization by Simulated Annealing. *science*, 220(4598):671–680, 1983.

[30] Alexander Klein, Sadegh Kavoussi, Robert Lee, and Chad Craun. Estimating Avoidable Costs due to Convective Weather Forecast Inaccuracy. In *11th AIAA Aviation Technology, Integration, and Operations (ATIO) Conference, including the AIAA Balloon Systems Conference and 19th AIAA Lighter-Than*, page 6811, 2011.

[31] Tao Li. *General Aviation Demand Forecasting Models and a Microscopic North Atlantic Air Traffic Simulation Model*. PhD thesis, Virginia Tech, 2015.

[32] Yanqi Liang. *Improvements to the Global Oceanic Model and Performance Assessment of the North Atlantic Organized Track System*. PhD thesis, Virginia Tech, 2017.

[33] Yanqi Liang, Arman Izadi, Nicolas Hinze, and Antonio Trani. Performance Assessment of the North Atlantic Organized Track System Using the Global Oceanic Model. In *2018 Aviation Technology, Integration, and Operations Conference*, page 3351, 2018.

[34] DA Livingston. Application of Composite Separation to the North Pacific Track System. *FAA/CT-TN83/34*, 1984.

[35] Alberto Lupidi, Christian Moscardini, Andrea Garzelli, Fabrizio Berizzi, Fabrizio Cuccoli, and Marcello Bernabò. Polarimetry Applied to Avionic Weather Radar: Improvement on Meteorological Phenomena Detection and Classification. In *2011 Tyrrhenian International Workshop*

on Digital Communications-Enhanced Surveillance of Aircraft and Vehicles, pages 73–77. IEEE, 2011.

[36] Michael V McCrea, Hanif D Sherali, and Antonio Trani. A Probabilistic Framework for Weather-based Rerouting and Delay Estimations within an Airspace Planning Model. *Transportation Research Part C: Emerging Technologies*, 16(4):410–431, 2008.

[37] A Nuic. User Manual for the Base of Aircraft Data (BADA) Revision 3.10. *Atmosphere*, 2010: 001, 2010.

[38] U.S. Department of Transportation (Federal Aviation Administration). Air Traffic Organization Policy, Order JO 7110.65X. 2017.

[39] Oliver Ohneiser. The Effect of Weather State-Change Notifications on General Aviation Pilots' Behavior, Cognitive Engagement, and Weather Situation Awareness. 2015.

[40] International Civil Aviation Organization, editor. *The Twenty-First Meeting of the APANPIRG ATM/AIS/SAR Sub-Group*, ATM/AIS/SAR/SG/21, 2011.

[41] Chuanwen Quan, Antonio Trani, and Sale Srinivas. Modeling the Economic Impact of Adverse Weather into En Route Flights. *Transportation research record*, 1788(1):76–82, 2002.

[42] Olga Rodionova, Daniel Delahaye, Mohamed Sbihi, and Marcel Mongeau. Trajectory Prediction in North Atlantic Oceanic Airspace by Wind Networking. In *Digital Avionics Systems Conference (DASC), 2014 IEEE/AIAA 33rd*, pages 7A3–1. IEEE, 2014.

[43] Olga Rodionova, Mohamed Sbihi, Daniel Delahaye, and Marcel Mongeau. North Atlantic Aircraft Trajectory Optimization. *IEEE Transactions on Intelligent Transportation Systems*, 15(5):2202–2212, 2014.

[44] Folse Sarah, Henry Tran, Luke Jensen, and John Hansman. Cruise Altitude and Speed Optimization Implemented in a Pilot Decision Support Tool. In *16th AIAA Aviation Technology, Integration, and Operations Conference*, page 4211, 2016.

[45] Manuela Sauer, Matthias Steiner, Robert D Sharman, James O Pinto, and Wiebke K Deierling. Tradeoffs for Routing Flights in View of Multiple Weather Hazards. *Journal of Air Transportation*, 27(2):70–80, 2019.

[46] Christina Schilke and Peter Hecker. Dynamic Route Optimization based on Adverse Weather Data. *Fourth SESAR Innovation Days*, 2014.

[47] Hanif D Sherali, Raymond W Staats, and Antonio Trani. An Airspace Planning and Collaborative Decision-Making Model: Part I—Probabilistic Conflicts, Workload, and Equity Considerations. *Transportation Science*, 37(4):434–456, 2003.

[48] Hanif D Sherali, Raymond W Staats, and Antonio Trani. An Airspace-Planning and Collaborative Decision-Making Model: Part II—Cost Model, Data Considerations, and Computations. *Transportation Science*, 40(2):147–164, 2006.

[49] Sathya S Silva, Luke Jensen, and R John Hansman. Pilot Perception and Use of ADS-B In Traffic and Weather Services (TIS-B and FIS-B). In *15th AIAA Aviation Technology, Integration, and Operations Conference*, page 2849, 2015.

[50] Thomas Louis Spencer. *Enhanced Air Transportation Modeling Techniques for Capacity Problems*. PhD thesis, Virginia Tech, 2016.

[51] El-Ghazali Talbi. *Metaheuristics: from Design to Implementation*, volume 74. John Wiley & Sons, 2009.

[52] Nikolaos Tsikas. *Performance Assessment of Operations in the North Atlantic Organized Track System and Chicago O'Hare International Airport Noise Study*. PhD thesis, Virginia Tech, 2016.

[53] Jeffrey C Tu. Cockpit Weather Information (CWIN) System. In *Proceedings of the IEEE 1996 National Aerospace and Electronics Conference NAECON 1996*, volume 1, pages 29–32. IEEE, 1996.

[54] Thomas WM Vossen. Fair Allocation Methods in Air Traffic Management. 2004.

[55] Thomas WM Vossen, Robert Hoffman, and Avijit Mukherjee. Air Traffic Flow Management. In *Quantitative Problem Solving Methods in the Airline Industry*, pages 385–453. Springer, 2012.

[56] Michael Wambsganss. Collaborative Decision Making through Dynamic Information Transfer. *Air Traffic Control Quarterly*, 4(2):109–125, 1996.

[57] John Werth. Airborne Weather Radar Limitations. *The Front*, 2014.

[58] Almira Williams and Israel Greenfeld. Benefits Assessment of Reduced Separations in North Atlantic Organized Track System. In *6th AIAA Aviation Technology, Integration and Operations Conference (ATIO)*, page 7816, 2006.

[59] Almira Williams, Stephane Mondoloni, Richard Western, Tamara Karakis, and Kenneth Jones. Beneficial Applications of Airborne Separation Assurance Systems (ASAS) in the Southern Pacific Airspace. In *AIAA 5th ATIO and16th Lighter-Than-Air Sys Tech. and Balloon Systems Conferences*, page 7337.

[60] Almira Williams, Stephane Mondoloni, Richard Western, Tamara Karakis, and Kenneth Jones. Application of Airborne Systems for Improving North Atlantic Organized Track System Operations. In *AIAA 5th ATIO and 16th Lighter-Than-Air Sys Tech. and Balloon Systems Conferences*, page 7338, 2005.

[61] Shu-Chieh Wu, Joel Lachter, Walter W. Johnson, and Vernol Battiste. Assessment of the Use of Electronic Flight Bags for Displaying Enhanced Traffic and Weather Information on the Flight Deck. volume 5, pages 3537 – 3542, 2010.